

INVESTIGATING THE EFFECTS OF LIGHTWEIGHT RECYCLED BUMPER AND  
CHASSIS SYSTEM ON VEHICLE CRASHWORTHINESS

BATUHAN GÜRER

AUGUST 2016

INVESTIGATING THE EFFECTS OF LIGHTWEIGHT RECYCLED BUMPER AND  
CHASSIS SYSTEM ON VEHICLE CRASHWORTHINESS

A THESIS SUBMITTED TO  
THE BOARD OF GRADUATE PROGRAMS  
OF  
MIDDLE EAST TECHNICAL UNIVERSITY, NORTHERN CYPRUS CAMPUS

BY

BATUHAN GÜRER

IN PARTIAL FULFILLMENT OF THE REQUIREMENTS FOR  
THE  
DEGREE OF MASTER OF SCIENCE IN  
THE  
SUSTAINABLE ENVIRONMENT AND ENERGY SYSTEMS PROGRAM

AUGUST 2016

Approval of the Board of Graduate Programs

\_\_\_\_\_  
Prof. Dr. M. Tanju Mehmetođlu  
Chairperson

I certify that this thesis satisfies all the requirements as a thesis for the degree of Master of Science

\_\_\_\_\_  
Assoc. Prof. Dr. Ali Muhtarogđlu  
Program Coordinator

This is to certify that we have read this thesis and that in our opinion it is fully adequate, in scope and quality, as a thesis for degree of Master of Science.

\_\_\_\_\_  
Assoc. Prof. Dr. Volkan Esat  
Supervisor

Examining Committee Members

Assoc. Prof. Dr. Volkan Esat	Mechanical Engineering Prog. METU NCC	_____
Assist. Prof. Dr. Behzat B. Kentel	Mechanical Engineering Prog. METU NCC	_____
Assoc. Prof. Dr. Muhammad Sabieh Anwar	Physics Dept. LUMS, Pakistan	_____
Assist. Prof. Dr. Ceren İnce	Civil Engineering Prog. METU NCC	_____
Assist. Prof. Dr. Dizem Arifler	Physics METU NCC	_____

**I hereby declare that all information in this document has been obtained and presented in accordance with academic rules and ethical conduct. I also declare that, as required by these rules and conduct, I have fully cited and referenced all material and results that are not original to this work.**

Name, Last name: Batuhan GÜRER

Signature :

## **ABSTRACT**

### **INVESTIGATING THE EFFECTS OF LIGHTWEIGHT RECYCLED BUMPER AND CHASSIS SYSTEM ON VEHICLE CRASHWORTHINESS**

Gürer, Batuhan

MSc, Sustainable Environment and Energy Systems Program

Supervisor: Assoc. Prof. Dr. Volkan Esat

August 2016, 108 pages

Accidents are one of the main reasons of death for people across the globe, among which automobile accidents are a major portion resulting in fatalities and various injuries. Crashworthiness is an engineering concept that is used to analyse the ability of vehicle structure to cover and protect passengers in the case of an accident or impact. Crashworthiness aims to affect the design of the structure of the vehicle so that it absorbs as much energy as it can which is sustained from an impact by plastically deforming in a controllable behaviour. The remaining amount of the impact energy can then be handled by the restraint system to protect the occupants from the consequences of the secondary impact in the vehicle. The current trend in automobile design and manufacturing is to increase the number of lightweight and recycled components that forms the vehicle. In this way, an effort towards sustainable manufacturing and reducing carbon footprint is made. However, using unconventional materials might affect the strength and energy absorption capabilities of the automobile chassis and body that may induce a change in the crashworthiness of the vehicle. This study aims to bring insight into the effects of lightweight and recycled bumper beam system in vehicle crashworthiness through computational modelling. In addition, investigations of crashworthiness of different modifications that are made on the system geometry

are carried out. Various finite element models embodying lightweight and recycled bumper beam systems are generated and simulated to evaluate several design choices and modifications.

Keywords: Recycled material, lightweight material, geometrical modifications, finite element analysis, crush force efficiency, specific energy absorption.

## ÖZ

### HAFIF GERİ DÖNÜŞTÜRÜLEBİLİR MALZEME İLE ÜRETİLMİŞ ÖN TAMPON VE ŞASI SİSTEMİNİN ARAÇ KAZA DAYANIMI ÜZERİNDEKİ ETKİLERİNİN İNCELENMESİ

Gürer, Batuhan

Yüksek Lisans, Sürdürülebilir Çevre ve Enerji Sistemleri

Tez Yöneticisi: Doç. Dr. Volkan Esat

Ağustos 2016, 108 sayfa

Tüm dünyada kazalar birçok insanın hayatını kaybetmelerinin en büyük sebeplerinden biridir. Bu kazaların içinde de en çok can kaybına ve yaralanmaya sebebiyet veren bölüm trafik kazalarına aittir. Araç kaza dayanımı, araç yapısının herhangi bir kaza ya da çarpışma durumunda yolcuları ne kadar ve nasıl koruduğunu inceler. Aslında bu kavram, araç yapısının tasarımını tamamiyle etkileyen bir faktördür. Çünkü burada asıl amaç kaza enerjisinin mümkün olabildiğince çok emilmesini sağlamaktır. Bu da kontrollü plastik şekil değiştirme davranışıyla mümkün olabilir. Bunların dışında, özel sistemler kullanılarak kalan kaza enerjisinin tümü emilebilir ve bu sayede ikincil çarpışmanın etkilerinden yolcuların korunması sağlanabilir. Günümüz otomobil endüstrisinin ele aldığı yeni bir eğilim sayesinde daha hafif ve geri dönüştürülebilir malzemeden üretilen otomobil parçalarının sayısında artış görülmektedir. Bu yönelim sayesinde sürdürülebilir üretim geliştirilebilecek ve karbon ayakizi oranlarında düşüş sağlanılabilecektir. Fakat bu hafif ve geri dönüştürülebilir malzemelerin araç ve şasi gövdesinde kullanımı; mukavemet ve çarpışma enerjisinin emilimi bakımından güçsüzleşmeye neden olabilir. Böylece araç kaza dayanımının da ciddi düşüşler gözlemlenebilir. Bu çalışmanın asıl amacı; daha hafif ve geri dönüştürülebilir malzemeler ile oluşturulan aracın sonlu eleman modelinin çarpışmalara karşı dayanımını incelemektir. Bunlara

ek olarak, çeşitli geometrik değişikliklerin araç kaza dayanımı üzerindeki etkileri de incelenmiştir. Çalışmada, hafif ve geri dönüştürülebilir malzemedен oluşturulmuş birçok sonlu elemanlar modeli bilgisayar ortamında yaratılmış ve simüle edilmiştir. Alınan sonuçlara göre, birçok tasarım ihtimali ve geometrik değişiklik değerlendirilmiştir.

Anahtar Kelimeler: Geri dönüştürülebilir malzeme, hafif malzeme, geometrik değişiklikler, sonlu elemanlar analizi, kaza kuvveti verimliliği, özgün absorpsiyon enerjisi.

## **ACKNOWLEDGMENTS**

I believe that certain events and moments change our life and certain people accompany us at these moments. Masters studies are an important event that affect my future life. In this section, I would like to express my deepest gratitude's to those special people who always support and help me overcome problems when completing my master thesis.

First of all; I would like to thank my thesis advisor, Assoc. Prof. Dr. Volkan Esat, who always help me overcome problems with his excellent knowledge, guidance, and patience. I become a professional user on Marc Mentat 2013™ with his extended knowledge. Besides, I would like to thank all of my committee members for their precious suggestions and ideas.

I would like to thank all METU NCC Mechanical Engineering Program instructors, and technicians. I would like to specially thank my classmate and colleague, Kemal Maşera, who always supports me with his wise ideas.

I would like to specially thank my parents Serap and Levent Gürer and my precious grandparents Sumru Dumanlı, Ülker and Kemal Gürer who had supported me both morally and materially since I was born. I believe that a few words are not enough to thank those special people. Whenever I need any help, they stay with me to overcome problems and give their best wishes to me.

In those three years, I would like to thank Nazlıcan Kılıç for her best wishes, and support. She encourages me to survive the hardship and stay with me in both good and bad times.

Finally, I would like to thank my friends who provide full support during the whole period of thesis completion.

## TABLE OF CONTENTS

ABSTRACT .....	iii
ÖZ .....	v
ACKNOWLEDGMENTS .....	vii
TABLE OF CONTENTS.....	viii
LIST OF FIGURES .....	xi
LIST OF TABLES .....	xv
1. INTRODUCTION .....	1
1.1 Aim and Motivation of Thesis.....	1
1.2 Organization of the Thesis.....	4
2. LITERATURE REVIEW .....	5
2.1 Material Selection .....	5
2.2 Modelling and Finite Element Analysis .....	10
2.2.1 Modelling.....	11
2.2.2 Finite Element Analysis and Tests .....	14
2.3 Manufacturing Methods and Effects.....	21
2.4 Joining Methods .....	22
3. MODEL GENERATION .....	24
3.1 Toyota Yaris Modelling .....	24
3.2 Modelling of the Simplified Bumper and Chassis System .....	27
3.3 Quasi-Static Analysis.....	29
3.4 Dynamic Transient Analysis.....	30
3.5 Solution Parameters .....	32
3.6 Sensitivity Analysis.....	35

3.7 Material Properties .....	36
3.7.1 Mild Steel.....	37
3.7.2 Dual Phase Steel .....	38
3.7.3 AA 5182 Aluminium Alloy.....	40
3.7.4 Recycled AA-7175 Chips .....	41
3.7.5 Aluminium with Carbon Nanotube Reinforcement .....	42
3.7.5 Titanium Matrix Composite with Carbon Nanotube Reinforcement.....	43
3.8 Profile Thickness Effect.....	44
3.9 Velocity Analysis .....	46
3.10 Geometry Modifications .....	47
3.10.1 Removing Rectangular Parts from Bumper Beam .....	47
3.10.2 Removing Rectangular Parts from Rails .....	48
3.10.3 Crash Zone Generation.....	49
3.10.4 Hexagonal Cross-Section .....	51
3.10.5 Runner .....	52
3.10.6 Range Hood .....	53
3.11 Hybrid Bumper and Chassis System .....	55
3.11.1 Hybrid Bumper and Chassis System with Different Material Combination	55
3.11.2 Hybrid Bumper and Chassis System with Different Geometrical Modifications.....	56
4. RESULTS AND DISCUSSION.....	58
4.1 Sensitivity and Error Analysis .....	58
4.1.1 Sensitivity Analysis .....	58
4.1.2 Error Analysis.....	60
4.2 Quasi-static Analysis vs Dynamic Transient Analysis .....	61

4.3 Profile Thickness Effect.....	62
4.4 Velocity Analysis .....	70
4.5 Geometrical Modifications .....	73
4.6 Material Analysis .....	81
4.7 Hybrid Bumper and Chassis System .....	88
5. CONCLUSION .....	94
REFERENCES .....	97
APPENDIX .....	100
Part A: Profile Thickness Effect.....	100
Part B: Velocity Analysis .....	102
Part C: Geometrical Modifications .....	103
Part D: Material Analysis .....	105
Part E: Hybrid Bumper Beam and Chassis System .....	107

## LIST OF FIGURES

Figure 1 Number of deaths in traffic accidents around the world (World Health Organization 2016).....	1
Figure 2 Global Fossil Fuel Carbon Dioxide Emissions (WHOI 2006) .....	3
Figure 3 Different bumper beam models and their total weight (Kim et al. 2015).....	7
Figure 4 Trend line of both CNT addition and without CNT are given in the graph of peak alternating stress vs their fatigue life (Grimmer & Dharan 2008) .....	10
Figure 5 Schematic configuration of the desired bumper (Moghaddam & Ahmadian 2011) .....	12
Figure 6 Impact layout (Hosseinzadeh et al. 2005).....	13
Figure 7 FE model of simplified bumper beam (Belingardi et al. 2013) .....	13
Figure 8 Finite element model of the commercial vehicle (Qi et al. 2006) .....	14
Figure 9 The tube impacted with a rigid wall (Acar et al. 2011).....	15
Figure 10 Front impact of vehicle in both FEA environment and real life (Qi et al. 2006) .....	15
Figure 11 Simulation and real life crash tests are compared in acceleration graph (Qi et al. 2006) .....	16
Figure 12 GMT and SMC deflections (Hosseinzadeh et al. 2005) .....	17
Figure 13 (a) Tensile modulus and (b) tensile strength of both materials (Davoodi et al. 2010).....	18
Figure 14 (a) Impact property and (b) density of both materials (Davoodi et al. 2010) .....	18
Figure 15 Bumper beam profiles considered (Besant et al. 2001) .....	19
Figure 16 For 120 kJ drop energy; force graph of a carbon skin-honeycomb core sandwich for both real life test and predicted (Besant et al. 2001) .....	20
Figure 17 Detailed fixation method (Davoodi et al. 2008) .....	22
Figure 18 Meshed Toyota Yaris 2010 model (The George Washington 2015).....	25
Figure 19 Front of the vehicle model.....	25
Figure 20 Classified element groups .....	26
Figure 21 Simplified model (on the left) and Toyota Yaris model (on the right).....	28

Figure 22 Quasi-static analysis: top view of the FE model .....	29
Figure 23 Element number changing areas .....	36
Figure 24 Flow curve of mild steel (Zein et al. 2013) .....	38
Figure 25 Dual Phase Steel microstructural representation (Steel Market Development 2015a).....	39
Figure 26 Flow curve of DP-500 steel (Steel Market Development 2015b) .....	39
Figure 27 Flow curve of AA 5182 (Smerd et al. 2005) .....	41
Figure 28 Flow curve of AA 7175 recycled chips (Pantke et al. 2013) .....	42
Figure 29 Flow curve of Al-CNT (Esawi & El Borady 2008) .....	43
Figure 30 Flow curve of Titanium with MWCNT (Kondoh et al. 2009).....	44
Figure 31 Modified bumper beam .....	48
Figure 32 Removed parts from rails.....	49
Figure 33 Bumper beam system with crush zone.....	50
Figure 34 Detailed view of crash zone model .....	50
Figure 35 Bumper beam system with hexagonal cross-section .....	51
Figure 36 Bumper beam system with runner .....	52
Figure 37 Detailed view of runner model .....	53
Figure 38 Bumper beam system with range hood.....	54
Figure 39 Detailed view of range hood model.....	54
Figure 40 Hybrid bumper and chassis system.....	56
Figure 41 Maximum strain energy vs number of elements.....	59
Figure 42 Computational time vs number of elements.....	60
Figure 43 Computational time vs number of elements.....	60
Figure 44 Crush force vs displacement graph for both quasi-static and dynamic transient analysis .....	61
Figure 45 Total strain energy vs time graph for both quasi-static and dynamic transient analysis .....	62
Figure 46 Deformed auxiliary view of quasi-static analysis.....	62
Figure 47 Crush force vs displacement graph for different thickness values.....	63
Figure 48 Total strain energy vs crash time graph for different thickness values.....	65

Figure 49 Deformed shape of 4 mm thick profile .....	68
Figure 50 Deformed shape of 5 mm thick profile .....	68
Figure 51 Deformed shape of 6 mm thick profile .....	69
Figure 52 Deformed shape of 7 mm thick profile .....	69
Figure 53 Crush force vs displacement graph for different velocity values .....	71
Figure 54 Total strain energy vs crash time graph for different velocity values .....	71
Figure 55 Deformed shape of 30 kph initial velocity model .....	72
Figure 56 Deformed shape of 40 kph initial velocity model .....	72
Figure 57 Deformed shape of 60 kph initial velocity model .....	73
Figure 58 Deformed auxiliary view of 80 kph initial velocity model .....	73
Figure 59 Crush force vs displacement graph for different geometrical shape .....	74
Figure 60 Total strain energy vs crash time graph for different geometrical shapes .....	74
Figure 61 Deformed shape of range hood model .....	78
Figure 62 Deformed auxiliary view of crash zone model .....	78
Figure 63 Deformed shape of runner model .....	79
Figure 64 Deformed shape of WR (rails) model .....	79
Figure 65 Deformed shape of WR (bumper) model .....	80
Figure 66 Deformed shape of hexagonal cross-section model .....	80
Figure 67 Flow curve of different material types .....	81
Figure 68 Crush force vs displacement graph for different material types .....	82
Figure 69 Total strain energy vs crash time graph for different material types .....	82
Figure 70 Deformed shape of mild steel model .....	85
Figure 71 Deformed shape of DP-500 model .....	85
Figure 72 Deformed shape of AA-5182 model .....	86
Figure 73 Deformed shape of 7175 recycled model .....	86
Figure 74 Deformed shape of Al-CNT model .....	87
Figure 75 Deformed shape of Titanium with MWCNT model .....	87
Figure 76 Crush force vs displacement graph for different material types .....	88
Figure 77 Total strain energy vs crash time graph for different material types .....	89
Figure 78 Deformed shape of H-1 model .....	91

Figure 79 Deformed shape of H-2 model.....	91
Figure 80 Deformed shape of H-3 model.....	92
Figure 81 Deformed shape of H-4 model.....	93
Figure 82 Deformed auxiliary view of 4 mm thick profile .....	100
Figure 83 Deformed auxiliary view of 5 mm thick profile .....	100
Figure 84 Deformed auxiliary view of 6 mm thick profile .....	101
Figure 85 Deformed auxiliary view of 7 mm thick profile .....	101
Figure 86 Deformed auxiliary view of 30 kph initial velocity model .....	102
Figure 87 Deformed auxiliary view of 40 kph initial velocity model .....	102
Figure 88 Deformed auxiliary view of range hood model .....	103
Figure 89 Deformed auxiliary view of runner model.....	103
Figure 90 Deformed auxiliary view of hexagonal model .....	104
Figure 91 Deformed auxiliary view of DP-500 model .....	104
Figure 92 Deformed auxiliary view of AA-5182 model.....	105
Figure 93 Deformed auxiliary view of 7175 recycled model .....	105
Figure 94 Deformed auxiliary view of Al-CNT model.....	106
Figure 95 Deformed auxiliary view of Titanium with MWCNT model.....	106
Figure 96 Deformed auxiliary view of H-1 model .....	107
Figure 97 Deformed auxiliary view of H-2 model .....	107
Figure 98 Deformed auxiliary view of H-3 model .....	108
Figure 99 Deformed auxiliary view of H-4 model .....	108

## LIST OF TABLES

Table 1 Static deflection test results for different laminates (Velmurugan & Balaganesan 2013) .....	21
Table 2 Element groups and their definitions.....	27
Table 3 Different trials and related parameters .....	31
Table 4 Different trials and related parameters (Table 3 continue).....	32
Table 5 Different number of elements of the bumper beam system.....	36
Table 6 Mechanical properties of mild steel (Zein et al. 2013) .....	37
Table 7 Mechanical properties of DP-500 Steel (Steel Market Development 2015b) .....	39
Table 8 Mechanical properties of AA-5182 (Smerd et al. 2005).....	40
Table 9 Mechanical properties of AA 7175 recycled chips (Pantke et al. 2013) .....	42
Table 10 Mechanical properties of Al-CNT (Esawi & El Borady 2008).....	43
Table 11 Mechanical properties of Titanium with MWCNT (Kondoh et al. 2009) ....	44
Table 12 Dimensions of chassis rails for 7 mm thickness shell elements.....	45
Table 13 Dimensions of bumper beam for 7 mm thickness shell elements.....	46
Table 14 Total mass of bumper beam system for all thickness values.....	46
Table 15 Dimensions of three different rectangular areas.....	48
Table 16 Dimensions of four different rectangular areas.....	49
Table 17 Dimensions of new bumper beam system.....	51
Table 18 Dimensions of new bumper beam system.....	52
Table 19 Dimensions of new bumper beam system.....	53
Table 20 Dimensions of new bumper beam system.....	55
Table 21 Three different hybrid model with used materials and related mass values .....	56
Table 22 Dimensions of geometrically hybrid system .....	57
Table 23 Mass values for each thickness .....	63
Table 24 Crush force efficiency for different thickness values .....	66
Table 25 Specific energy absorption for different thickness values .....	67
Table 28 Crush force efficiency for different geometrical shapes.....	76

Table 29 Specific energy absorption for different geometrical shapes.....	77
Table 28 Crush force efficiency for different material types.....	84
Table 29 Specific energy absorption for different material types.....	84
Table 30 Crush force efficiency for hybrid systems .....	90
Table 31 Specific energy absorption for hybrid systems .....	90

# 1. INTRODUCTION

## 1.1 Aim and Motivation of Thesis

Every year around 1.25 million people lost their lives in traffic accidents (Anon n.d.). Careless driving, not obeying rules of traffic, drinking, and speeding causes traffic accidents. According to Figure 1, number of deaths in traffic accidents in developed countries is lower than ones that occurred in developing or undeveloped countries. Developed countries' strict traffic regulations and their applications decrease the number of traffic accidents. Same situation is not observed in undeveloped or developing countries. Engineers seek new type of systems to prevent car crashes or reduce fatalities by modifying chassis of vehicle.

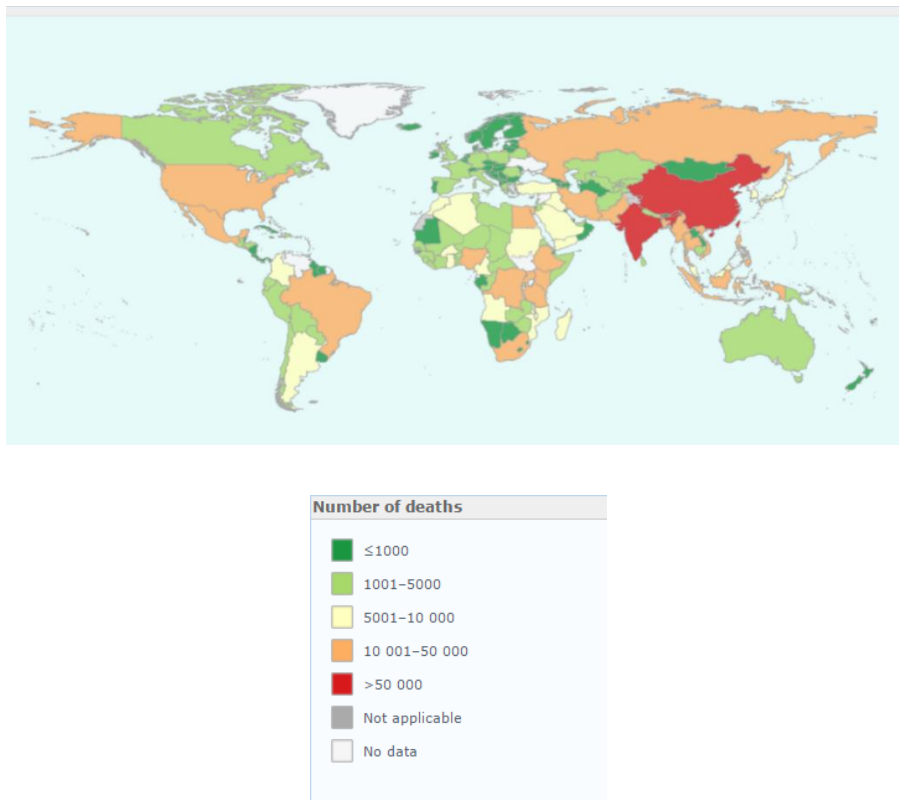


Figure 1 Number of deaths in traffic accidents around the world (World Health Organization 2016)

Nowadays, the term of “global warming” becomes a trend. Societies and governments seek a way to stop this extraordinary phenomenon. Global warming term is related with the increase in the cumulative temperature of the earth. In other words, cumulative temperature of the earth is continuously rising. On earth, every system works in sequence and balance where global warming becomes a threat for the balance of the earth. Seasons and weather conditions are changed. As a result, fertility of crops decreases. Another important problem associated with it is the level of sea waters. Due to the rise of atmospheric temperature, ice caps are melting down and sea water levels rise.

Burning of fossil fuels for many purposes suddenly increased after 1750 when the industrial revolution took place. The main reason of global warming is the carbon emissions. At the end of combustion reaction of fossil fuels, harmful products like carbon dioxide, sulphur dioxide, and carbon monoxide are produced and emitted directly to the atmosphere, causing a greenhouse effect. Annual carbon dioxide emission graph is given in Figure 2. It can be said that carbon emission is directly related with modernisation. Earth’s atmosphere is acting as a semi translucent medium and absorbs light that is coming from the sun. Then, earth surface acts similarly as the atmosphere and reflects some of the coming light beams back to the space. At that point, emitted carbons absorb deflected light beams in the atmosphere, hence temperature is not stabilized and rise dramatically. According to statistics of OICA (2015), approximately 90 million cars around the world are registered in 2015. Almost all of them burn fossil fuels to produce their power. That explains about the rising carbon emission values in Figure 2. Governments seek new ways to reduce this greenhouse gas emission. Main scope of UN FCCC (2015) is to keep global average temperature increase below 1.5°C. If temperature rise is above 2°C, results will be catastrophic and irreversible for earth.

Second important issue is related with the availability of fossil fuel reserves due to their limitation on earth. Increasing demand for fossil fuels is currently observed on earth. Klass model gives a new impulse to calculate depletion time of fossil fuels like

oil, coal, and gas. According to the model of Shafiee & Topal , Earth have oil reserves that cover 35 years, 107 years for coal, and 37 years for gas (2009). Nowadays engineers mainly focus on the issue of alternative and clean energy. Solar, wind, tidal, geothermal, nuclear, and hydro power can be sustainable options for alternative energy.

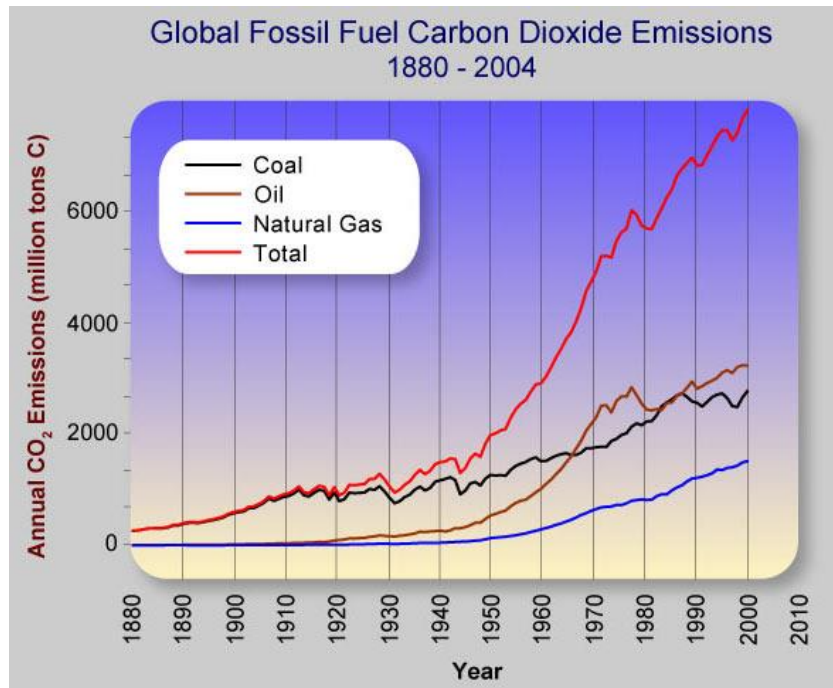


Figure 2 Global Fossil Fuel Carbon Dioxide Emissions (WHOI 2006)

On the other hand, world's reserves of metal and other materials are also limited and many production companies use bulk materials to produce their products. At the end of all production stages, scrap materials usually in the form of chips are created. For sustainability purposes, recyclability of those chips has utmost importance.

This study aims to contribute to the reduction of carbon emissions that are caused by road vehicles. This can be achieved by reducing weight of the vehicle. Because heavy vehicle needs more energy to move and more fuel is used. In order to reduce weight, composite materials can be an alternative. Many composites have a property of low density and high strength. Using recycled materials may be

preferred for sustainability purposes. In this context, full frontal car-to rigid-wall impact is investigated for Toyota Yaris, and then the bumper beam system, which is the vital part to absorb the majority of frontal crash energy, is modified to come up with an optimal solution. The objectives are to increase the absorbed energy and decrease total mass of the car.

## **1.2 Organization of the Thesis**

This thesis has five chapters in total. First chapter introduces research topic, shows motivation and gives an idea about the reason to choose this research topic. Chapter 2 is about the literature review. Previous researches are presented in this chapter. Gaps of those research studies are highlighted. Investigations on different material types, modelling of similar analysis, manufacturing methods to produce bumper beam, and joining effects are given. Chapter 3 gives detailed information about how modelling and finite element analyses are done. It is the development stage of many different parameters like material type, geometric shape, thickness of shell elements, and velocity. Moreover, necessary information about those models are given. Chapter 4, data that are gathered from finite element analysis (FEA) software is tabulated and compared with the base model. Parameters of crush force, absorbed impact energy, crush force efficiency, and specific absorbed energy supplied and comparison was carried by using that information. Last chapter summarizes the whole research, provides the major outcomes and findings, and suggests recommendations for future work.

## **2. LITERATURE REVIEW**

This chapter is composed of literature review on material selection, manufacturing methods and effects, and joining methods. The literature review helps to understand what have been done so far, and state of the art regarding bumper and chassis systems, and select the best alternatives in order to create an optimum model for bumper beam and chassis system.

### **2.1 Material Selection**

Bumper beams are the energy absorbing elements. Energy absorbing elements are used in order to protect occupants of the vehicle. They absorb impact energy by deforming. The most common energy absorber type is the thin-walled tubes. Although there are lots of different cross sectional types of thin-walled tubes, this study focuses on the crashworthiness of tapered type thin-walled tubes in order to increase energy absorption characteristic of vehicle. Energy absorbing characteristic and absorbed crush force are two parameters to design energy absorbers. It is not sufficient to absorb maximum amount of impact energy. Peak crush force is also important to protect occupants. Those two parameters affect the efficiency of the absorber element. Crush force efficiency can be calculated by dividing average crush force to peak value. If weight is important during the design stage, specific energy absorption parameter is taken into consideration. Specific energy absorption can be defined as the ratio of absorbed energy to total mass of the system Acar et al. (2011).

It is important to select a material which is lighter and stronger than those that are used conventionally in today's bumper systems as there is a continuous increase in the world automotive production rate. Predictions show that; car production size will reach 76 million in each year. World has limited petroleum reserves, because of which petroleum prices will considerably increase in the near future. It is possible to mitigate this problem by reducing the mass of the car. It can be saved 250 million barrels of crude oil annually by reducing car weight by 25% Davoodi et al. (2010).

Today many car manufacturers select lighter materials to be used in their cars. Audi A8 is produced by using aluminium material in its space frame chassis which reduces vehicle's mass from 1348 kg to 1121 kg. Ford Motor Company's Lincoln Mark VIII is produced incorporating lighter structural materials by saving 175 kg when compared to its conventional steel models Cole et al. (1995).

This research aims to design a bumper beam that;

- is easy to manufacture
- is economically cheap but relatively strong through the use of material solutions such as composites
- Reduces weight of the car
- Improves impact behaviour
- Reduces carbon footprint during manufacturing and throughout its life span

Similar research was also conducted by Hosseinzadeh et al. (2005), in which glass mat thermoplastic (GMT) is used as bumper beam material. Crash analysis is carried out by using finite element analysis software (LS-DYNA ANSYS 5.7). Authors seek an answer for the effects of ribs that are used as a reinforcement element for GMT type car bumper. In order to see the effect of ribs; ribbed and unribbed crash cases are investigated. Crash scenarios are created for metallic, GMT type and short-fibre composite (SMC) type car bumpers. Impact behaviour of both SMC and GMT type bumper show better performance compared to the conventional ones. On the use of plastic materials, Luda et al. (2003) take polypropylene based car bumpers into consideration. They are recycled materials, whose mechanical properties are adversely affected due to the chemical structure of the material. Research show that mechanical properties can be improved by adding special chemicals like antioxidant systems into the system, as in the work of Kim et al. (2015), who improved the conventional GMT material. Mass reduction is the primary aim of this research. Glass and carbon mat thermoplastic (GCMT) composite is invented in the light of those purposes. Conventional GMT is composed from 28 % unidirectional glass fibre layer and 35 % woven glass fibre layer. Four different GCMT is created in

that research. In case 1; 50 % of unidirectional glass fibre is altered with carbon fibre. In case 2; 100% of unidirectional glass fibre is altered with carbon fibre. In case 3; 50 % glass fibres that are located inside of the woven layer are altered with carbon fibre. In case 4; 100 % glass fibres that are located inside of the woven layer are altered with carbon fibre. Authors found that up to 33 % weight reduction is possible when it is compared to the conventional GMT bumper beam and this weight difference shown in Figure 3.

Belingardi et al. (2015) focus on the production stage of GMT. Pultrusion and die-forming are used as the production methods. High quality production and cost effectiveness make those two production methods good candidates. The two production methods offer many different types of GMT. From die-forming, three different materials are produced Belingardi et al. (2015). Those are GMT, GMTex, and GMT-UD.

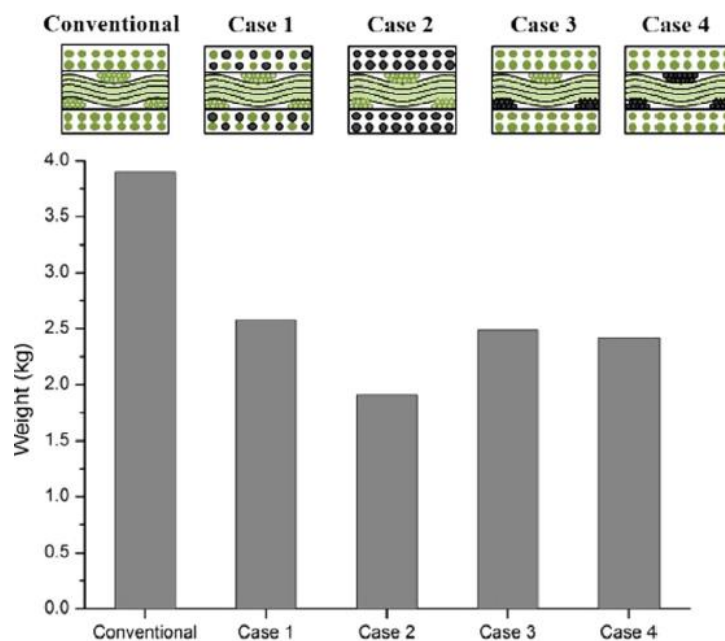


Figure 3 Different bumper beam models and their total weight (Kim et al. 2015)

Due to their high strength and low weight, carbon fibres are widely used materials among all other composites. Today, most racing companies use carbon fibres when they produce parts of the vehicles. Carbon fibres are generally mixed with other

composite materials like Kevlar, aluminium honeycomb structure, and nanocomposite to improve their mechanical properties. In order to produce carbon fibre epoxy material the resin transfer moulding (RTM) is preferred because it completes the production in one step Saidpour (2006). By using RTM; it is possible to produce shapes that are not possible or feasible to produce by using metal structures.

Fibres are widely used as reinforcement elements of a composite material in today's industry due to their lightweight and high strength. Their impact behaviour and mechanical properties have been researched extensively. Metallic glasses are one of the choices to increase strength of a machine part. In fact, they are not tough enough in both tension and compression case. Conner et al. (1998) found a new way to increase strength of metallic glasses by using tungsten or steel fibres. Reinforced material is nearly thousand times stronger than the one that does not have the reinforced fibre Conner et al. (1998).

As a composite material for bumper beam both glass fibre and carbon fibre can be used. Cheon et al. (1995) investigate the crashworthiness of those materials and compare them with conventional steel bumper. Hybrid kenaf and glass reinforced epoxy composites are investigated and compared with GMT by Davoodi et al. (2010). Mechanical properties of natural fibres can be improved by adding both natural and glass fibres. Researchers aim to improve crashworthiness of vehicle's bumper beams which is made from the hybrid of kenaf and glass fibre. Improvement can be possible by applying production method of sheet moulding compound (SMC). As a matrix of hybrid material, epoxy is selected and it is reinforced with the kenaf and synthetic glass fibre. Although fabricated fibres show a good performance in a crash scenario, a new fibre production method name as "pultrusion" improve their mechanical properties. Belingardi et al. (2013) compares the characteristics of E-Glass and epoxy pultruded bumper beam, steel and E-Glass and epoxy fabric composite. Authors' claim that new and promising manufacturing method named as pultrusion makes those materials cost-effective. Generally

straight axis composite profiles are produced with this method. However, curved axis ones are also achieved in recent years. Pultruded composites have more complex impact response and damage mechanisms than the conventional ones, which are dependent on different parameters. Composites such as carbon fibre and epoxy resin absorb impact energy by holding damage rather than yielding because they have a brittle structure. Sometimes this damage can be visible. If damage occurs internally, it will lead a catastrophic fatigue failure.

Another conventional material that is used in vehicle structures is aluminium. It is lighter than steel but heavier than the carbon or glass epoxy composites. Joining and manufacturing methods of aluminium is different from steel. In light of low weight system, aluminium foam honeycomb sandwich panels are taken into consideration. They are preferably used in energy absorption systems in aerospace industry. Besant et al. (2001) modelled composite sandwich panels which are composed of brittle composite skins reinforced by ductile core to improve strength of the fibre composites. They applied an impact test to understand energy absorption behaviour under impact load. Characteristics of sandwich panels under low velocity impact are not much addressed in the literature. However, sufficient amount of research have been conducted in order to predict crashworthiness of carbon, glass and Kevlar monolithic panels in the case of low velocity impact. Those sandwich type panels have good damage-tolerance as their core is able to absorb impact energy by deforming itself and prevent high local bending strains.

Carbon nanotubes are the newest material type in the industry. Velmurugan & Balaganesan (2013), state that composites are mainly researched and improved in the aerospace industry. Since weight reduction due to composite parts can save power and fuel.

In today's automotive industry, metals are arguably the most frequently used material with respect to their high impact energy absorption capacity. Second common material is the polymer composites. However their plastic deformation characteristics are not as good as metals. However, they have higher specific energy

absorption than metals. In recent years, polymers with small portion of strong fillers exhibit higher mechanical properties. According to the experiments nano scale composites show different mechanical properties than their macro ones. The main reasons are dimensions, volume fraction, matrix material, manufacturing process, and interaction between nano filler and its matrix. On the other hand, nano size carbon fibres have higher quasi-static fracture toughness than the micro-filled epoxies. At the same volume percentage, which is 78%, nano particles have better fracture toughness. In another approach by Grimmer & Dharan (2008) multi-walled carbon nanotubes are added inside the matrix of glass fibre polymer composites. This study addressed the improvement in the life cycle of glass fibre by adding multi-walled carbon nanotubes. In Figure 4, number of load cycle difference is clearly shown. Carbon nanotube addition increases the fatigue life cycle of the material as carbon nanotubes stop large crack propagations. Carbon nanotubes have a specification of higher density nucleation areas.

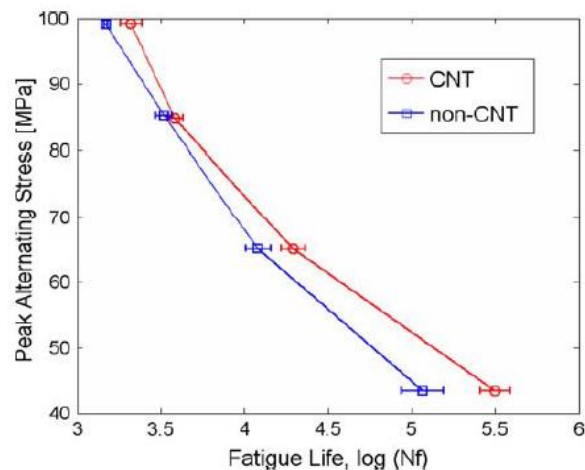


Figure 4 Trend line of both CNT addition and without CNT are given in the graph of peak alternating stress vs their fatigue life (Grimmer & Dharan 2008)

## 2.2 Modelling and Finite Element Analysis

Producing composite test materials and conducting relevant tests are not a highly efficient way of designing car parts due to production cost and its time consuming operation. Computational modelling and, in particular, finite element analysis is a

cost effective and fast way in designing such features. Researchers create different models on virtual environment and create their own test conditions without consuming both time and capital.

### **2.2.1 Modelling**

Frontal bumper beam system is composed from three different components (Figure 5): first one is fascia, which covers the bumper beam and gives an artistic visual to vehicle. It has aerodynamic properties but it has no to very little energy absorption effect in a crash scenario. Second component is the bumper beam whose main purpose is to absorb majority of the impact energy for frontal impacts while preserving other components of the vehicle as much as possible and protecting its occupants from injuries and fatalities. Besides, it is the heaviest component of the bumper due to its metallic structure and protective features. Last component is the absorber or absorber mechanism. It consists of structural beams or dampers and springs to absorb some of the impact energy. According to Moghaddam & Ahmadian (2011) bumper beam can be classified as foam, honeycomb, and mechanical type. The authors of the aforementioned study create a bumper system which covers low-speed impact by using its springs and high-speed impacts by deformations on the beam cells. Bumper beam mechanism is given in Figure 5. Main components of this bumper system are;

- Front rubber tape is manufactured from propylene material and absorb low-speed impacts
- Fascia helps aerodynamic performance of vehicle and acts as a roller for spring system
- Spring system has two different classifications. Vertical ones are in 26 number and absorb kinetic energy of impact as a potential energy of spring. Horizontal ones are 4 in number to create a connection between fascia and bumper beam

- Conics and base plate are the parts that absorb energy in high-velocity impact
- Connecting plastic parts are composed from propylene material and connected to the bumper base plate

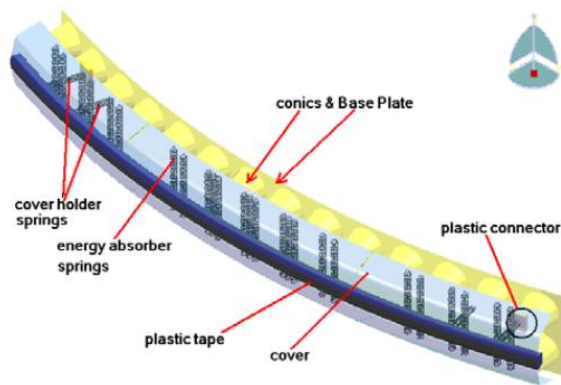


Figure 5 Schematic configuration of the desired bumper (Moghaddam & Ahmadian 2011)

Hosseinzadeh et al. (2005), investigated the ribs effect on bumper system which is produced by using GMT and compared results with other bumper models. Created model was given in Figure 6. Test was conducted by using ANSYS 5.7 software. 3-D drawing and all other properties of car bumper were imported to the software. Then, bumper was assembled with two semi-cubic plastic propylene holders which acted as a shock absorber. Besides, they were believed to protect the car bumper from the excess energy that was created in high velocity impact. Those holders were attached to the chassis of the car by using screws. At the connection points, one fourth of the car mass was also loaded. On the other hand, steel impactor was also modelled.

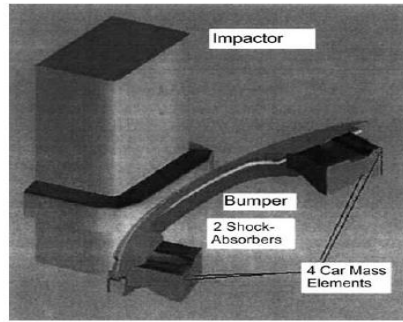


Figure 6 Impact layout (Hosseinzadeh et al. 2005)

Similarly, Belingardi et al. (2013) created a model which has four different parts in the form of two longitudinal crash boxes, one rigid wall and one deformable transverse beam. The model shown in Figure 7 was created with the help of ABAQUS Explicit version 6.10-1 software. The beam was made from pultruded E-Glass fibre-epoxy matrix which was another type of composite material. Mechanical properties of materials were obtained from the literature. The authors claimed that more realistic results can be obtained by modelling whole vehicle's body in the analysis of frontal impact test.

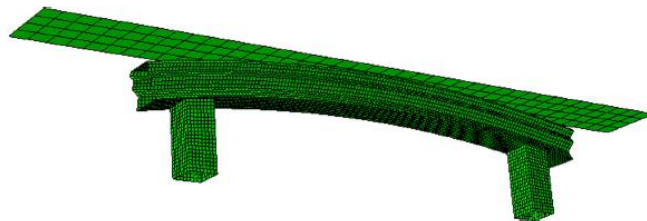


Figure 7 FE model of simplified bumper beam (Belingardi et al. 2013)

Qi et al. (2006) classifies main body under several names which are frame, front inner, front wall, cabin, doors, and bed. Unigraphics and Catia software were used to create 3D model of each sub-group. Then, for meshing of generated parts, all files were imported to the Hypermesh software. However, it is not easy to develop all independent parts of vehicle and meshing them, because there were lots of different joint types, elements that were used for geometrical shapes and many different special conditions for joints that need to be considered. Besides, engine of the vehicle was defined as a rigid part. Figure 8 shows the finite element model of

the vehicle. Dummy passenger was also developed to investigate the forces that act on human body in a frontal impact crash scenario.

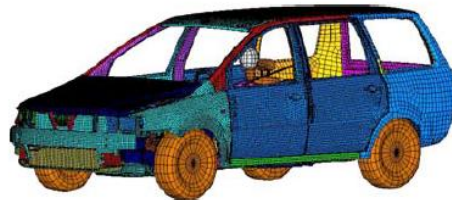


Figure 8 Finite element model of the commercial vehicle (Qi et al. 2006)

### 2.2.2 Finite Element Analysis and Tests

In various studies, after model creation part is accomplished, finite element analysis and or real life tests are conducted. Researchers check their hypothesis whether they are valid or not and discuss their idea about their research by showing results. Generally on crashworthiness of bumper and chassis, researchers simulate impact their bumper model on a rigid wall by using finite element analysis software and results are tabulated and discussed to have a better understanding of the crash situation. Acar et al. (2011) claim that experiments are unpractical due to high application prices and being highly time consuming. They selected finite element method in investigating the crash performance of circular cross-sectional tubes of 150 mm diameter and 180 mm height. Various tubes with and without axisymmetric indentations were developed. In a crash test scenario, a rigid wall of 1500 kg and 9 m/s initial velocity, lead to a 45 kJ initial impact energy (Figure 9). Wall thickness, number of indentations, radius of indentations, and taper angle are the initial parameters that are decided by the researchers. Impact performance of wall is evaluated with respect to the crush force efficiency, specific energy absorption parameters and weight parameter. However, authors claimed that it was not easy to maximize both CFE and SEA so authors define a function  $f$  (Equation 1) to evaluate impact performance of tubes.

$$f = w * \frac{CFE}{CFE_0} + (1 - w) \frac{SEA}{SEA_0} \quad [1]$$

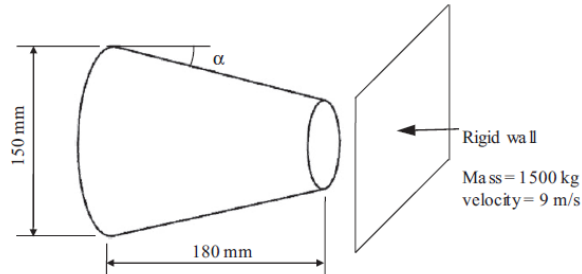


Figure 9 The tube impacted with a rigid wall (Acar et al. 2011)

On the other hand Qi et al. (2006) investigate the performance of the finite element method in their analyses. Authors of this study conducted two different crash scenarios (low and high speed crash) in both real crash test environment and computer medium. Moment of crash is given in Figure 10 and results are presented in Figure 11. Results of both tests were similar and computer model simulates the same test highly realistically. Computer modelling saves both time and money during the research. It is also possible to predict and take precautions against initial stage problems in computer modelling.

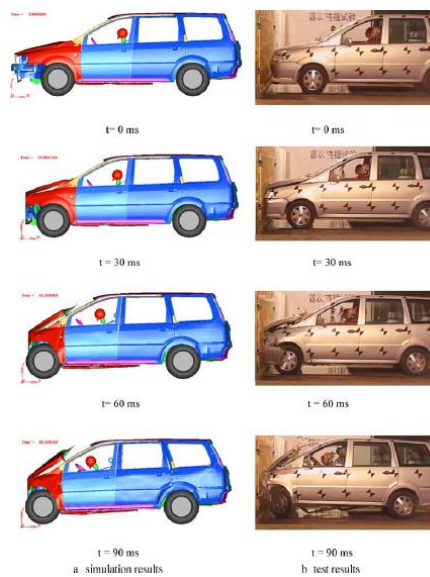


Figure 10 Front impact of vehicle in both FEA environment and real life (Qi et al. 2006)

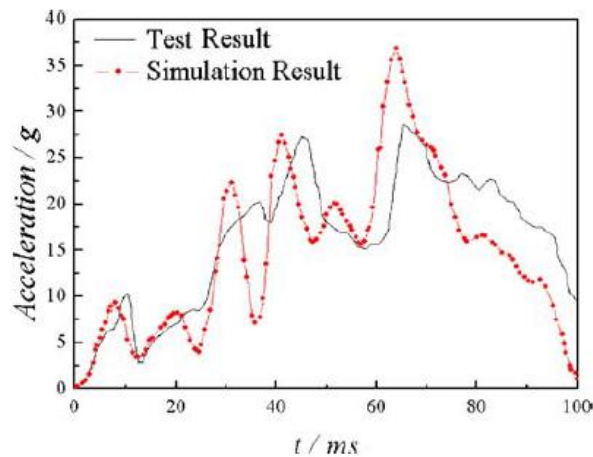


Figure 11 Simulation and real life crash tests are compared in acceleration graph (Qi et al. 2006)

Hosseinzadeh et al. (2005), analysed crashworthiness behaviours of both steel and aluminium materials. Impact occurred at 4 km/h velocity and deflections of the bumper beam, kinetic energy between impactor and bumper beam, and von Mises stress distribution along both horizontal and vertical paths were reported. Stress distribution show unexpected characteristics because of vibrations that occurred during impact. Test results gave an idea about how structural reliability and manufacturing costs are affected from shape. As a result, both metal and aluminium type of bumpers failed for the desired purpose.

Hosseinzadeh et al. (2005), also analysed crashworthiness behaviours of GMT type bumper made of fibreglass composite with short fibres. Size of 12-25 mm long randomly mixed fibres were mixed with thermoplastic resin. In order to investigate bumper beam realistically, it was reinforced with ribs and weight of the passengers were also added to the system. Addition of the ribs to the system had some effects on the crashworthiness performance of bumper beam. In order to understand the rib effect, researchers of this study performed three different crash scenarios. Results show that an early reduction occur in the deflection of ribbed case. However, researchers found a better composite and lightweight material called short fibre composite (SMC), through which the crashworthiness performance is investigated. In SMC; thermoset resin is mixed with short-fibres. Researchers

claimed that there are lots of benefits to use SMC instead of GMT which are listed below:

- Easy to produce
- Ribs are removed for new design, so it is easier to manufacture
- Lighter
- The volume of SMC will decrease by decreasing the thickness.

Comparison of SMC and GMT is given in Figure 12 show that maximum deflection increases by 5% when SMC type of bumper is used.

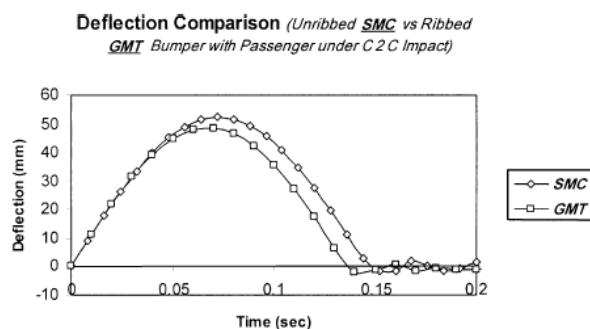


Figure 12 GMT and SMC deflections (Hosseinzadeh et al. 2005)

Similar to this research, Davoodi et al. (2010) created a new hybrid material whose fibre structure is improved. They apply tensile test and Izod impact test on both hybrid material and GMT type bumper and compare them. Figure 13 shows that both tensile strength and Young's modulus of hybrid bumper beam were higher than those of the GMT one. Although impact force of hybrid bumper is lower than that of the GMT one in Figure 14, it can be used as a bumper beam material in automotive industry. Another important aspect is related with their densities. The reason of high density in hybrid material is the density difference between propylene and epoxy.

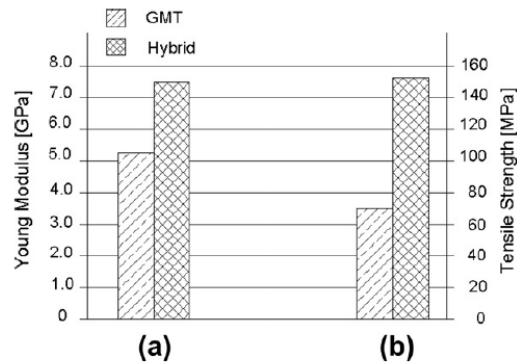


Figure 13 (a) Tensile modulus and (b) tensile strength of both materials (Davoodi et al. 2010)

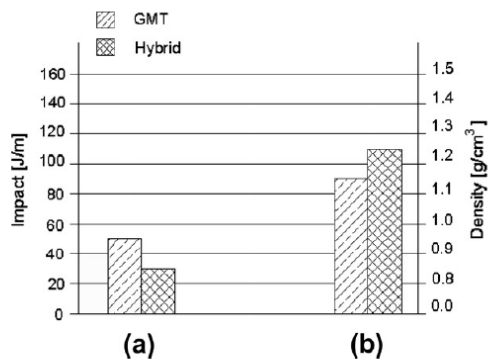


Figure 14 (a) Impact property and (b) density of both materials (Davoodi et al. 2010)

Mechanical properties and impact behaviour of fibres were also investigated by some other researchers. Fibres are widely used in many different industrial areas as a composite material. They are lightweight so it can be expected that their impact absorption characteristics are lower than conventional materials like metals and aluminium. However, previous research shown that this hypothesis is not valid. Cheon et al. (1995) investigated the crashworthiness of composite bumper which is made from both glass and carbon fibres and found out that although weight of the car decreases by 30% with respect to the steel type bumper case, composite bumpers impact behaviour stays still. Belingardi et al. (2013) also investigated the

glass fibres. However, they come up with a new production method called pultrusion. They investigated the mechanical properties of pultruded E-Glass and epoxy and also compared it with fabric E-Glass and epoxy. Like other composite materials E-Glass and epoxy has relatively high stiffness, high strength, high energy absorption capacity, and low-weight. E-Glass and epoxy is generally used as a structural material. Other utilization areas of this material is bumper beam and roadside safety structures. Not only protecting vehicle's occupants but also protecting life of pedestrians during an accident Belingardi et al. (2013). This study claims that pultrusion method increases the specific strength and energy absorption capacity of the material. Model of bumper beam is given in modelling section. Researchers applied crash test by using this model and finite element method. First of all, they tried to find an optimal profile shape for bumper beam among all alternatives which is given in Figure 15.

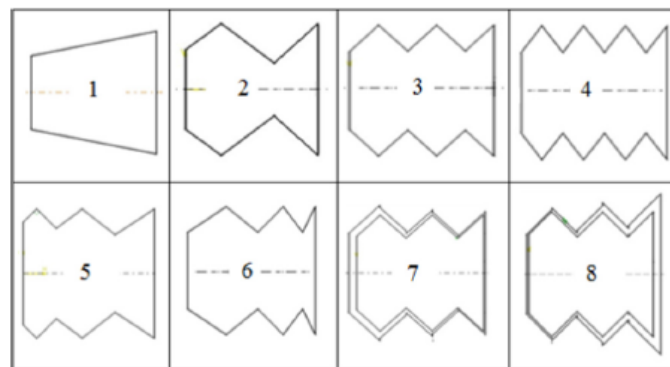


Figure 15 Bumper beam profiles considered (Besant et al. 2001)

Researchers claimed that some parameters like fibre and matrix type, section shape and dimensions, impact velocity, impact angle, shape of striker, target geometry and material affect the impact behaviour of bumper beam. They analysed the bumper system, which hit the wall with 15 km/h by using finite element method. Number of grooves increase in the first row of Figure 15 whereas shape alternatives are given in the second row of same figure. Due to high energy absorption characteristic, best option is profile 7.

Besant et al. (2001) conducted relevant mechanical tests by using finite element analysis software. Non-linearity, and plastic deformations of core and other deformations that occur inside of the material were also taken into consideration by applying dynamic analysis through the finite element model. As a core material, metal honeycomb is used. It is anisotropic, therefore elasto-plastic part of the analysis requires a new approach. Moreover, research compared both experimental and finite element results of the sandwich panels with carbon fibre skins and aluminium honeycomb cores under low velocity impact test. In the impact test 120 J drop energy is applied. 20 mm diameter flat-nosed impactor is used. Impactor has a mass of 5.38 kg and dropped from the height of 2.27 m. According to Figure 16, test results perfectly fit the real life case response. Graph helps understanding the impact behaviour of sandwich panels under related impact loads.

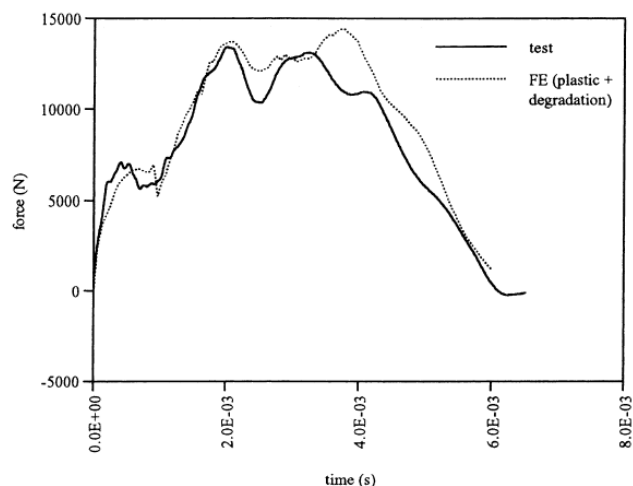


Figure 16 For 120 kJ drop energy; force graph of a carbon skin-honeycomb core sandwich for both real life test and predicted (Besant et al. 2001)

Another choice for light but strong materials is the nano composites. Velmurugan & Balaganesan (2013) classified nano composites with respect to the separation of nano-clay platelets. Those are clustered, intercalated and exfoliated. Quasi-static punch test, impact test, and stiffness and energy absorption in quasistatic test were then conducted. Results that are given in Table 1 show that energy absorption characteristics of nano composites are increasing due to the amount of nano clays that are dispersed inside the composite. Moreover, layer number and layer

orientation affect the energy absorption capacity. It can be concluded that nano clay addition to the model protects fibres and improves energy absorption capacity as they act as a second filler system.

Table 1 Static deflection test results for different laminates (Velmurugan & Balaganesan 2013)

Layer orientation	Item	Percentage of nano clay					
		Without clay	1	2	3	4	5
3 (0) <sub>3</sub>	Stiffness in N/mm	202.53	211.49	216.67	235.89	219.15	221.18
	Energy in J	8.26	8.61	9.32	10.74	11.56	13.32
3 (0/45/0)	Stiffness in N/mm	202.42	212.66	219.35	238.92	224.45	223.51
	Energy in J	9.21	9.47	10.02	11.25	11.86	14.06
5 (0) <sub>5</sub>	Stiffness in N/mm	297.10	336.08	352.47	356.42	328.3	299.74
	Energy in J	17.14	17.84	19.99	20.01	20.56	24.32
5 (0/45/0/45/0)	Stiffness in N/mm	298.01	338.18	355.18	361.23	329.1	301.84
	Energy in J	17.83	18.48	20.18	22.32	23.85	24.93
8 (0) <sub>8</sub>	Stiffness in N/mm	505.1	506.6	519.3	579.2	523.1	521.5
	Energy in J	46.20	48.52	48.99	49.33	49.82	54.21

### 2.3 Manufacturing Methods and Effects

There are various different manufacturing methods used in order to produce composite bumper beams. However, each method has its own advantages and disadvantages. This research seeks to find a manufacturing method that has low cost, easy to manufacture and give higher strength to the product. For the same purpose, Beyene et al. 2014 investigate the effects of pultrusion and die-forming and seek to find new alternatives to both vehicle's frontal and rear bumper which absorb most of the impact energy during low velocity impact. Authors of this paper claim that pultrusion is a fully-automated and low cost production process, which makes it easy to produce composite profiles with constant cross-section. Products that are produced from pultrusion method are relatively stronger than the other composite material production methods. On the other hand, die forming is another technique in producing composite shells with desired shape. Both bumper beam and crash boxes are produced as one integrated component in this method. It helps reduce both the assembly step and the production of two different components. Besides, this process eliminates joining of parts and improves strength of the whole body.

Same manufacturing methods (pultrusion and die-forming) were also investigated by Belingardi et al. (2015). Authors compared the crash performance of both pultruded and die-formed bumper beams with steel and the fabric type in terms of impact energy, peak load, crash resistance, energy absorption, and stiffness. According to this research, best crashworthiness characteristic among all other alternatives under 8 km/hr impact were gathered from bumper beam crash box that was produced by using die forming process. Products that are produced with die forming shows better crashworthiness performance.

## 2.4 Joining Methods

Unlike conventional materials like steel and aluminium, conventional joining methods like welding, bolting, riveting are not easily used to join bumper beam that is produced from composite materials. In this thesis, composite bumper beam is going to be joined with the steel or aluminium monocoque chassis. Nowadays, monocoque chassis is widely used in automotive industry. Davoodi et al. (2008) use fibre reinforced epoxy composite absorbers. Absorbers are placed between the fascia and the reinforcement beam. Moreover, two steel plates are used in order to fix absorbers at that location. Upper plate is fixed to the fascia by using snap fits and lower plate is fixed to the reinforced beam by riveting. Therefore, elliptical shape of absorbers (Figure 17) is also helpful on the crashworthiness issue.

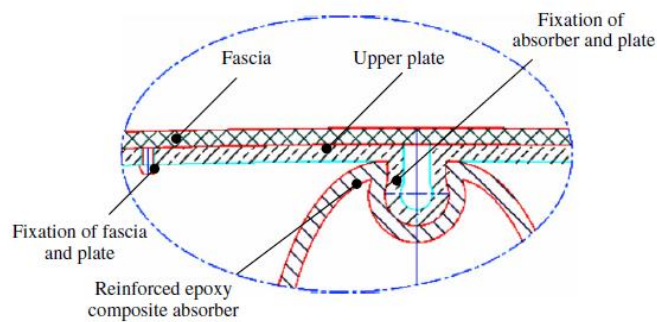


Figure 17 Detailed fixation method (Davoodi et al. 2008)

Another joining method for both glass and carbon fibre reinforced plastics is suggested by Balle et al. (2009). Authors of this study claimed that ultrasonic plastic welding or metal welding can be the solution of this joining problem of dissimilar materials. Ultrasonic welding technology is also available for joining glass and carbon fibre textiles without thermoplastic matrix to metal. Advantages of ultrasonic welding are low energy input, low temperature at the welding zone, and short welding time. Those advantages make this joining technology better than adhesive bonding, brazing, and soldering. Investigations of the welded areas show that metallic surfaces are directly joined with the fibres. Due to the ultrasonic oscillation, fibres which are at the contact area are completely broken.

Detailed research on dissimilar material joining is done by Martinsen et al. (2015). Dissimilar materials can be joined using spark plasma sintering. Joining operation of silicon carbide and graphite is achieved successfully at 2000°C and no cracks are observed at the joining point.

Friction riveting and friction spot welding are other dissimilar material joining techniques. Generally this method is used to join metal to polymers. In friction riveting, metal rivet is rotated at high speeds and pressed into the polymer. Due to poor heat transfer rate of polymer, high temperature has just melted the contact point. On the case of thermoplastic polymer to metal joining injection over-moulding can be used as it is not possible to join those two materials by adopting conventional methods. Polymer is melted and poured into the holes that are located on the metal part. There is a self-locking mechanism when polymer is cooled down.

### **3. MODEL GENERATION**

This section provides information about the generated model that is used for the simulation of the bumper and chassis system in crash tests. Through recent software packages, more realistic crash scenarios can be simulated and investigated, whose results are in good agreement with real life situations. Moreover, software packages help reduces both time and capital that are spent on the project. In this research, Marc Mentat 2013™ finite element method (FEM) modelling software is used in order to analyse crash performance of bumper beam and chassis system. Marc Mentat 2013™ is capable to solve non-linear finite element analysis and gives reliable results. Besides, software is able to analyse many finite element cases from solid mechanics to electromagnetic. In this research, frontal car bumper and chassis system is going to hit the rigid wall with low and high velocities and crash performance of different type of materials for the bumper and chassis beam system is investigated.

#### **3.1 Toyota Yaris Modelling**

First, it is essential to develop 3D model of vehicle and then, meshing is applied on this model. However, it is a difficult and time-consuming process. Therefore, meshed vehicle body is directly taken from and as a courtesy of The George Washington (2015). Brand of meshed car is Toyota Yaris 2010. There are 974,383 elements on the model in Figure 18. Model was created realistically in such a way that all parts of vehicle were created and meshed individually. Dimensions of the vehicle are also same as the real one.

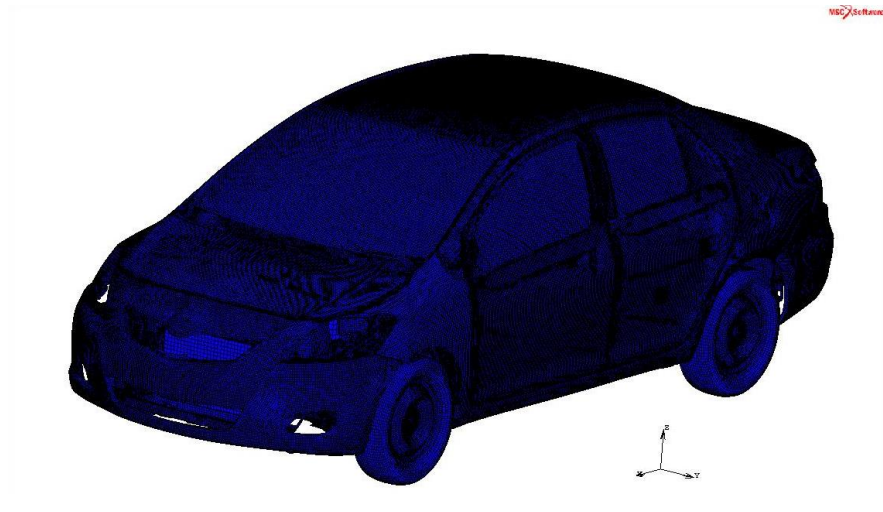


Figure 18 Meshed Toyota Yaris 2010 model (The George Washington 2015)

Another reason to select Toyota Yaris 2010 is the monocoque chassis type. Reason to choose monocoque chassis car is that many car manufacturer companies produce their family size cars by using monocoque chassis. In monocoque chassis, loads on the vehicle are supported by the external skin of the vehicle. Moreover, they are less expensive and stronger with respect to the older techniques.

In this research, the main focus point is not the whole vehicle's crash performance. As a result, the elements from the lower end of windshield to the end of rear bumper are removed (Figure 19).



Figure 19 Front of the vehicle model

In the model five different element classes are used. These can be listed as penta6, hex8, tria3, quad4, and line2 (Figure 20). Selection of those different element classes requires separate assignment of material and geometrical properties. This is due to the complexity of the geometry and the feature of element selection in the Marc Mentat 2013™ finite element (FE) model, which has to be done by selecting elements individually. This requires considerable time. In order to eliminate this problem, all different component of vehicle is grouped. Grouped element regions are given in Table 2. This research focuses on the analyses on the bumper beam integrated with chassis rails. The other sub-groups are neglected.

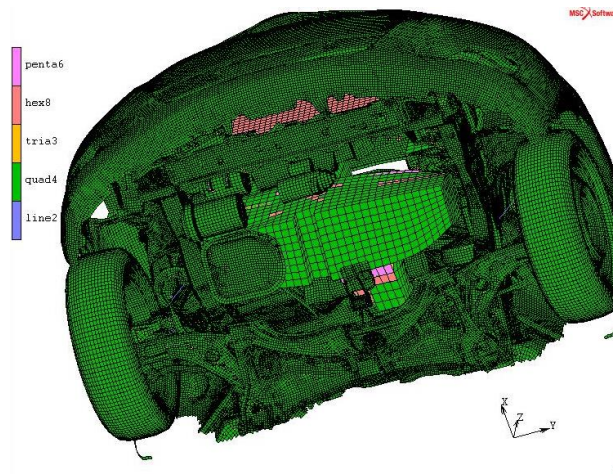


Figure 20 Classified element groups

Table 2 Element groups and their definitions

Group Name	Definition
Bumper	Fascia
Bumper Beam	Connected to the rails of vehicle and absorb front crash energy
Engine	All engine parts inside of hood
Frame	Frame of radiator
Glass	Windshield
Hood	-
Interior	All sheet metal materials except hood
Radiator	-
Rails	Rails work as an energy absorber elements that are connected to the chassis of vehicle
Tire	-
Underframe	All underframe elements

### 3.2 Modelling of the Simplified Bumper and Chassis System

As it is mentioned before, 3-D meshed model of Toyota Yaris was taken from a university database. Although 3-D modelling and meshing are already done, the model is far from being complete for the purposes of this research. Model generation involves overcoming various different problems such as assigning different element types, resolving continuity conditions between the vehicle's parts in the mesh, etc.

This research mainly focuses on the bumper and chassis beam system in 0° frontal crash angle; in other words, in full-frontal impact without any offset. If energy absorption capacity of the bumper beam increases, less energy will be transmitted to the other parts of the vehicle and occupants. In the light of this knowledge, a simplified model was created. This bumper beam and chassis system model has similar dimensions and properties as the real Toyota Yaris bumper beam in Figure 21.

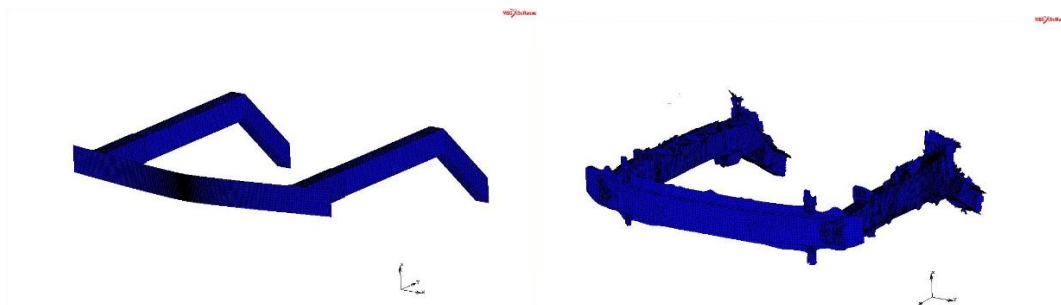


Figure 21 Simplified model (on the left) and Toyota Yaris model (on the right)

In this research, different profile thicknesses, lightweight materials, geometries and hybrid models are utilised in the model and their behaviours under the same crash scenarios are investigated.

After 3-D modelling is completed, model is meshed by using quad (4) type shell elements with a thickness of 7 mm. In order to get a more accurate result, element number is increased as much as possible being in accordance with a sensitivity analysis. Simplified model have 23840 elements. There is no specific connection between the rails and the bumper beam representing a joining method. In other words, model is created as a whole body. On the other hand, Toyota Yaris bumper beam and rails are manufactured separately, and then jointed by using bolts and nuts. However, in this research any joining type is neglected.

In this research, bumper and chassis system was crashed to the rigid wall. For that reason, a rigid wall surface with sufficient length and width was created and located exactly at the opposite of the bumper and chassis system. Location of the surface

on the coordinate system is arranged so that it lies across the mid-point of bumper beam. In other words, distances to the left-right and up-down points of the surface have same magnitude to this mid-point origin.

Both quasi-static and dynamic transient type of analysis is applied for the model that is generated. Crashworthiness of bumper and chassis system potentially behave differently in those two types of analyses. Results reveal the differences.

### 3.3 Quasi-Static Analysis

In quasi-static analysis, bumper and chassis system is fixed at a point but the wall surface is mobile. In fact, it is the same thing as bumper and chassis system hitting the wall, where relative motion is not changed. Motion of the surface is calculated to mimic an impact at a certain velocity. Generally, low speed frontal car crashes' duration are varied between 40 ms to 100 ms that depend on the velocity of car (Jones & Wierzbicki 2010). 0.1 s is decided as crash duration and constant velocity of the surface during the crash is taken as 2500 mm/s. It means that surface is going to deform bumper and chassis system by 250 mm at the end of the crash.

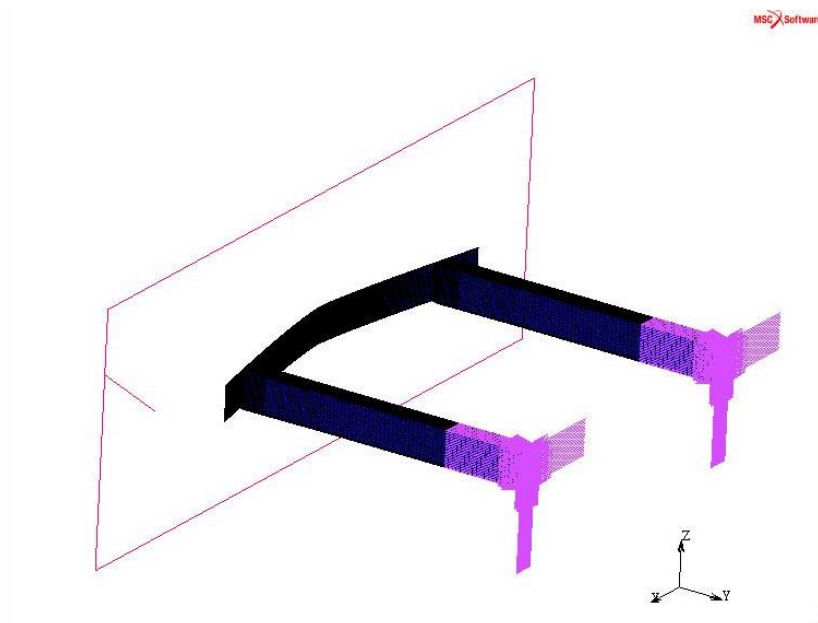


Figure 22 Quasi-static analysis: top view of the FE model

Mobile wall (purple surface), meshed bumper and chassis system, and boundary conditions are visualized in Figure 22. The force applied from the surface contacts the mid-point of the bumper beam first. Tilted parts of the chassis were eliminated during analysis stage to prevent rotation of the whole model.

### **3.4 Dynamic Transient Analysis**

Dynamic analysis potentially gives more realistic results with respect to the quasi-static one. In this type of analysis, bumper and chassis system moves freely and rigid wall is standing still. This way, inertia and buckling effects under dynamic load are also taking into consideration. Another difference of the dynamic analysis is the density of the material to be taken into consideration for the calculations. Instead of constant displacement, initial velocity is used and it is 16667 mm/s (60 km/hr). After bumper hits the wall this value is decreasing with time. In order to apply initial velocity on the system, all elements and nodes have to be selected. Basic bumper model have two different zones which are bumper beam and rails. Mass of the car is also modelled by using solid elements and they are located just the end of each rail. At the end of each rail, 700 kg lumped mass is added. The model is symmetric from the mid-point; therefore the centre of gravity of the car is in the same axis with the mid-point of the model. Total mass of the empty car is 1100 kg and 4 occupants weighing 70 kg are also considered with their 20 kg luggage mass in the car. That makes the total mass of the car 1400 kg. If just bumper and chassis system hits to the wall, there will be a significant bounce back due to its low weight. Lumped mass of the car and the occupants prevent this bounce back action during the crash, resulting in a more realistic crash scenario.

There are two different versions of bumper and chassis system. Difference between those versions is not related with geometry, type of elements or material. It is directly related with the simplified masses of car. Difference is in the dimensions of simplified mass zone. Version one is just used in sensitivity analysis as sensitivity analysis does not depend on those simplified mass. Figure 22 shows the model that

is used in the dynamic analysis of this research. In order to investigate difference between both quasi-static and dynamic analysis, same model is used.

During the analysis stage, many different parameters affect the result of the system. Total load case time, number of steps, iterative procedure, contact type, non-linear procedure, buckle solution method, dynamic transient operator, and matrix solver type are the parameters that directly affect the solution of contact problem. Those parameters are independent from the initial modelling conditions such as geometry of the system, material type or initial velocity. Selected parameters are clarified in detail on solution parameters section. However, many different model type and solution parameters combinations are tried and all results are investigated one by one to find best solution method and geometry of the system. Those trials are tabulated in Table 3 with the selected parameters. Green filled ones perfectly work and the red ones give an unsuccessful solution.

Table 3 Different trials and related parameters

	Trial 1	Trial 2	Trial 3	Trial 4	Trial 5
<b>Element Type</b>	Shell	Shell	Shell	Shell	Shell
<b>Number of Elements</b>	11920	11840	11920	11920	11920
<b>Shell Thickness</b>	8	8	8	9	8
<b>Total Loadcase Time</b>	0.1	0.1	0.1	0.1	0.1
<b># Steps</b>	700	800	700	700	700
<b>Initial Condition Application Area:</b>	All	Back	All	All	All
<b>Deformation Type</b>	Small	Small	Small	Small	Small
<b>Material Type</b>	Steel	Steel	Steel	Steel	Steel
<b>Dynamic Implicit Type</b>	Generalized Alpha (S=0)	Generalized Alpha (S=0)	Generalized Alpha (S=0)	Generalized Alpha (S=0)	Generalized Alpha (S=0)
<b>Buckling Mode</b>	Inverse Power Sweep	Inverse Power Sweep	Inverse Power Sweep	Lancoz	Inverse Power Sweep
<b>Matrix Solver</b>	Multifrontal Sparse	Multifrontal Sparse	Multifrontal Sparse	Multifrontal Sparse	Multifrontal Sparse
<b>Iterative Procedure</b>	N-R with strain correction	N-R with strain correction	N-R with strain correction	N-R with strain correction	N-R with strain correction
<b>Car Weight Element Type</b>	Solid	Shell	Solid	Solid	Solid
<b>Contact Type</b>	Node to Segment	Node to Segment	Node to Segment	Node to Segment	Node to Segment
<b>Friction Type</b>	Coulomb Stick Slip	Coulomb Stick Slip	Coulomb Stick Slip	Coulomb Stick Slip	Coulomb Stick Slip
<b>Initial Velocity</b>	100	50	60	60	60
<b>Initial Contact</b>	Open (2 areas)	Open (1 areas)	Open (2 areas)	Open (2 areas)	Open (2 areas)
<b># Dynamic Modes</b>	20	20	20	20	20
<b># Buckle Modes</b>	20	20	20	20	20
<b># Pos. Buckle Modes</b>	15	15	15	15	15
<b>Complex Damping</b>	Close	Close	Close	Close	Open
<b>Mass Density</b>	0.00000298		0.00000298	0.00000298	0.00000298

Table 4 Different trials and related parameters (Table 3 continue)

	Trial 6	Trial 7	Trial 8	Trial 9	Trial 10
<b>Element Type</b>	Shell	Shell	Shell	Shell	Shell
<b>Number of Elements</b>	11920	11920	23840	23840	23840
<b>Shell Thickness</b>	8	9	7	7	7
<b>Total Loadcase Time</b>	0.1	0.1	0.1	0.1	0.1
<b># Steps</b>	700	700	700	700	700
<b>Initial Condition Application Area:</b>	All	All	All	Back	All
<b>Deformation Type</b>	Large(updated)	Large(updated)	Small	Small	Small
<b>Material Type</b>	Steel	Steel	Steel	Steel	Steel
<b>Implicit Type</b>	Generalized Alpha (S=0)	Generalized Alpha (S=0)	Single Step Houbout	Single Step Houbout	Single Step Houbout
<b>Buckling Mode</b>	Inverse Power Sweep	Inverse Power Sweep	Lancoz	Lancoz	Lancoz
<b>Matrix Solver</b>	Multifrontal Sparse	Multifrontal Sparse	Multifrontal Sparse	Multifrontal Sparse	Pardiso Sparse
<b>Iterative Procedure</b>	N-R with strain correction	N-R with strain correction	N-R with strain correction	N-R with strain correction	N-R with strain correction
<b>Car Weight Element Type</b>	Solid	Solid	Solid	Solid	Shell
<b>Contact Type</b>	Node to Segment	Node to Segment	Node to Segment	Node to Segment	Node to Segment
<b>Friction Type</b>	Coulomb Stick Slip	Coulomb Stick Slip	arctangent(0.1,nodal stress)	Coulomb Stick Slip	arctangent(0.1,nodal stress)
<b>Initial Velocity</b>	60	60	60	60	60
<b>Initial Contact</b>	Open (2 areas)	Open (2 areas)	Open (2 areas)	Open (2 areas)	Open (2 areas)
<b># Dynamic Modes</b>	20	20	20	20	20
<b># Buckle Modes</b>	20	20	20	20	20
<b># Pos. Buckle Modes</b>	15	15	15	15	15
<b>Complex Damping</b>	Close	Close	Close	Close	Close
<b>Mass Density</b>	0.00000298	0.00000298	0.000003		0.000003

### 3.5 Solution Parameters

Dynamic type of analysis significantly depends on time. Therefore, analysis time and number of steps directly affect solution and response of the system. As mentioned before, duration of low velocity crash varies between 0.04 to 0.1 seconds. The total load case time is selected as 0.1 s.

In Marc Mentat 2013™, three different iterative procedures are available. Full Newton-Raphson (N-R) method is selected by the software by default. Our model is created by shell elements except simplified car masses (solid elements). According to Marc Mentat 2013™ User Manual, N-R with strain correction iterative procedure is the best method in order to analyse shell elements.

There are two main types of contact available in Marc Mentat 2013™. Rigid surface does not have any mesh on it and bumper and chassis system is fully meshed so it has nodes and elements across the contact area. Then, contact type is selected as node to segment. Friction method is selected as Coulomb stick-slip. In this method, some parameters of slip to stick transition region, friction coefficient multiplier, and friction force tolerances are default in the software. Other important issue about contact is to define contact areas on the model. This procedure decreases

computing time. There are two different contact areas which are created separately. First one is between bumper beam and rigid surface. The other one occurs between solid car mass elements and the end of each rail.

There are two different non-linear procedure options in the Marc Mentat 2013™ which depend on the scale of deformation or strain that occurs during the analysis. In a car crash scenario large deformations occur in real life. The mesh of the simplified model is “fine”; in other words, numerous quadrilateral shell elements are created, and each element deformation occurs in the scale of  $10^{-4}$  m. Then, it is considered to take each elements’ strain into consideration instead of whole bumper and chassis system when selecting non-linear procedure type. Constant dilatation option is recommended for this type of models. Another important issue is to observe bending on the rails. Assumed strain is an option that improves pure bending behaviour of a system however this adversely increases computational time.

One of the main differences of dynamic analysis from quasi-static is the mass of the model, which is also taken into consideration. Lumped mass option is switched on in order to include diagonal mass matrix as an input variable. Mass of the system is calculated by the software. Using the density value that is entered by the user and the volume of model, Marc Mentat 2013™ directly calculates the mass value. Another parameter that depends on the mass is moment of inertia. For shell elements in dynamic mode, moment of inertia terms have to be included into analysis to have more realistic output.

Buckling can be observed in slender rectangular thin walled profiles when one side is fixed and the other side is compressed. Rails are in the shape of rectangular profile and compression action is applied from both of the ends. Buckling behaviour has to be observed in the simplified model. In quasi-static analysis, it is possible to activate buckling but it is not available for dynamic transient one. Inverse power sweep is default in Marc Mentat 2013™. However, for non-linear and large scale

problems Lancos method gives better buckling behaviour. In addition, total number of possible buckling modes can be changed by the user.

Single and Multi-step Houbolt, Generalized alpha, Newmark-beta, and Modal superposition are options of dynamic implicit operators. Modal superposition operator is better for dynamic modal analysis instead of dynamic transient analysis. Numerical damping effects are not taken into consideration in Newmark-beta operator, so system may result a resonance response and gives an undesired solution. On the other hand, buckling or bending behaviours can be clearly observed. Single and Multi-step Houbolt operators are generally used for contact problems. Generalized alpha is an operator that is modified for both contact and non-contact behaviour by changing its spectral radius from 0 to 1. Generalized alpha analysis system is the same as the single-step Houbolt for spectral radius of 0 (specified for contact analysis). Their numerical damping value is higher with respect to the other operators and it is hard to observe buckling, bending, or any other type of distortion on the system. In order to reduce this high numerical damping, number of increments should be lowered as much as possible. High number of increment values gives a higher numerical damping to the system. In Marc Mentat 2013™, arranging number of increments has a significant importance. Stabilization analysis was done in order to find proper number of steps and gather the best output from the model.

In Marc Mentat 2013™ software the analysis time can be divided into number of increments so each millisecond of the crash can be visualized easily. If number of increment increases, more computing time will be needed and result in a high numerical damping. In order to achieve successful and realistic results, number of increments is one of the most important criteria. Error analysis is done on the number of 100, 200, 300, 400, 500 and 600 increments. Results of this analysis are given in the Results and Discussion part of this thesis.

Matrix solvers are popular methods for linear equation systems. They are divided into two groups as symmetric and non-symmetric solutions. Multifrontal sparse and

direct sparse are the ones that are generally preferred. After 2013, Marc introduces a new matrix solver which solves equations as in Multifrontal and direct sparse in a much lower computational time. It is called Pardiso sparse. Matrix solvers primarily affect computational cost. In order to reduce it other actions can be taken such as dividing the whole body into sub-groups with respect to element base and solve each group separately.

### **3.6 Sensitivity Analysis**

In finite element analysis, mesh type and number of elements in mesh possess potential to significantly affect the results. Before starting the analysis, number of elements should be arranged at a proper value. In this research, quadrilateral 4 node elements are used, which might cause difficulty in visualising deformation at some points and areas. In order to get a realistic result, number of elements in mesh has a vital role. Another important aspect is the computational time of simulation. Greater number of elements needs higher computational time. After some determined higher number of elements, model gives the same or very similar responses even when the element number is increased more. Therefore, the main aim is to optimize both computational time and number of elements by finding a critical point. From rough to fine mesh, element number is increasing. However, other parameters like dimensions stay still. Numbers of elements are changed in some specific areas of the model. In this research, buckling and other major deformations occur in the rails of the system. Hence, the numbers of elements in the chassis rails are modified. Bumper beam and simplified car masses are not taken into consideration for this analysis. Two red lines represent the border point of the rails. In other words, numbers of elements are changed between those two red lines (Figure 23). Different numbers of elements are given in Table 5.

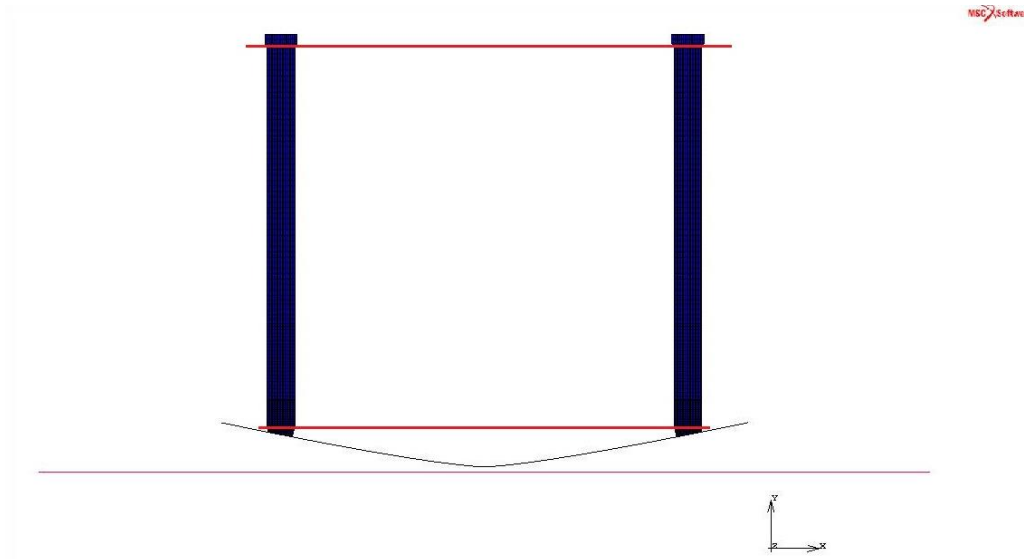


Figure 23 Element number changing areas

Table 5 Different number of elements of the bumper beam system

	m-1	m-2	m-3	m-4
Number of Elements	12800	17600	23840	73600

### 3.7 Material Properties

Conventional materials like steel and aluminium are used in the structure of vehicles in automobile industry. Although they have relatively high energy absorption capacity, they significantly add to the mass of the whole system. As a result, more fuel and energy are needed to move vehicle. In this research composite, recycled, and low-weight materials are compared with the conventional ones to identify whether they have better crashworthiness performance or not.

### 3.7.1 Mild Steel

Due to its high strength and toughness, steel is mainly preferred in the structure of today's vehicles. In this research, steel is a base material so all calculations and analysis are compared with respect to the steel material. Young's modulus, Poisson's ratio, and yield stress as a flow curve are needed to characterise the elastic-plastic behaviour of an isotropic material. Material of the impact wall is assumed as concrete. Therefore, concrete to steel contact friction is another important parameter to be introduced into the system. As a base material, mild steel is selected. Thickness effect, velocity analysis, stability analysis, and effects of number of elements are investigated by using mild steel. Necessary information about the material is given in the Table 6 and Figure 24.

Table 6 Mechanical properties of mild steel (Zein et al. 2013)

	Mild Steel
Modulus of Elasticity (MPa)	210000
Poisson's Ratio	0.3
Density (kg/m <sup>3</sup> )	8000
Friction Coefficient	0.4

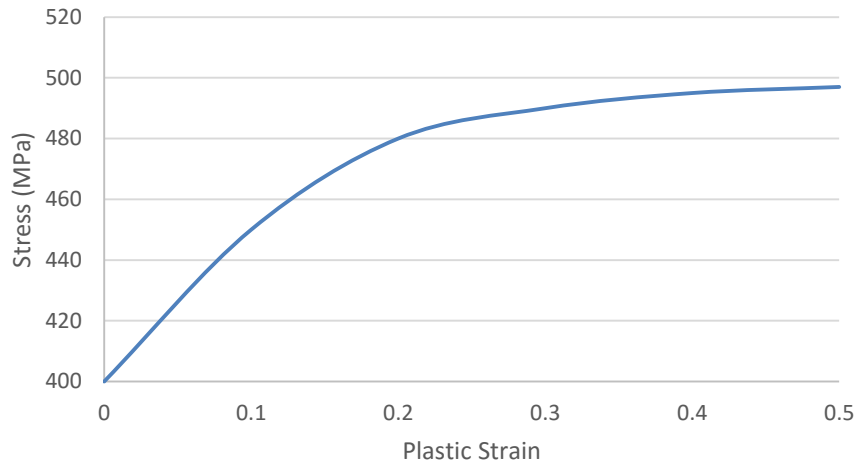


Figure 24 Flow curve of mild steel (Zein et al. 2013)

### 3.7.2 Dual Phase Steel

Generally steels show high strength and energy absorption capability. However, their weights are also high. As a new technology, dual phase steels are used in vehicles' chassis and other parts because of their high strength and relatively low density. This kind of steel is composed from ferritic matrix which has hard martensitic portions in it as a second phase. Microstructure representation of Dual Phase (DP) steels are given in Figure 25. 4 different kinds of DP steels are commonly used in the automotive industry, which are DP 500, DP 600, DP 800 and DP 900. DP 800 and 900 are widely used in aerospace industry. In this research DP-500 material's crash behaviour is investigated. A necessary mechanical property of DP-500 is given in Figure 26 and Table 7. Young Modulus and Poisson's ratio are exactly the same as mild steel. On the other hand, after elastic region, flow curve of DP-500 seems different than the mild one.

### Ferrite-Martensite DP

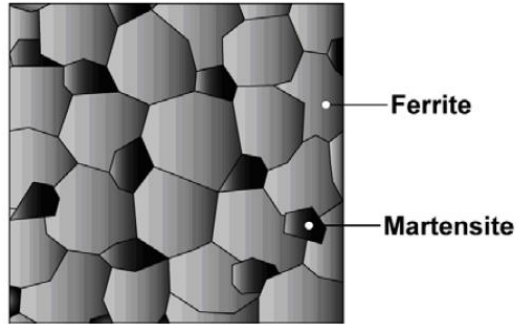


Figure 25 Dual Phase Steel microstructural representation (Steel Market Development 2015a)

Table 7 Mechanical properties of DP-500 Steel (Steel Market Development 2015b)

DP-500 Steel	
Modulus of Elasticity (MPa)	210000
Poisson's Ratio	0.3
Density (kg/m <sup>3</sup> )	7850

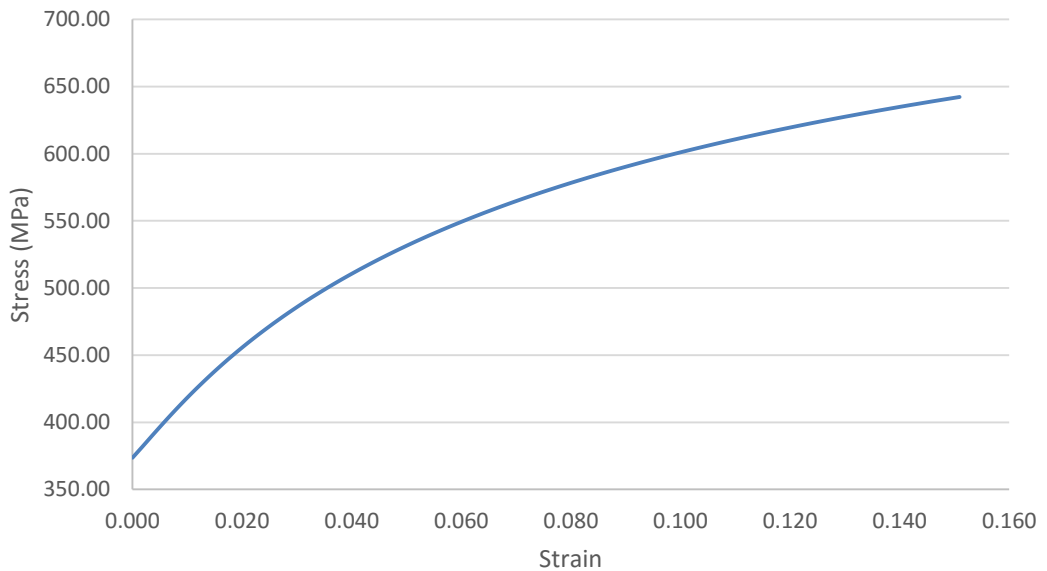


Figure 26 Flow curve of DP-500 steel (Steel Market Development 2015b)

### 3.7.3 AA 5182 Aluminium Alloy

Due to its low weight, aluminium is preferred by the automotive manufacturers as a production material for most of modern vehicles' parts. Space frame chassis which is made fully from aluminium alloy reduce 40% of total mass of a vehicle (Smerd et al. 2005). However, stiffness and toughness of aluminium are lower than most of the steels. Therefore, it does not showing a good performance at energy absorption during car crashes which may result in a fatality or serious injury on occupants. Generally, aluminium shows high sensitivity response in low strain rate values; but this statement is not valid for AA 5182 aluminium alloy. In high strain rates folding response of AA 5182 is like steel Smerd et al. (2005). Necessary mechanical properties and flow curve of AA 5182 is given in Table 8 and Figure 27.

Table 8 Mechanical properties of AA-5182 (Smerd et al. 2005)

	AA-5182
Modulus of Elasticity (MPa)	70000
Poisson's Ratio	0.33
Density (kg/m <sup>3</sup> )	2700

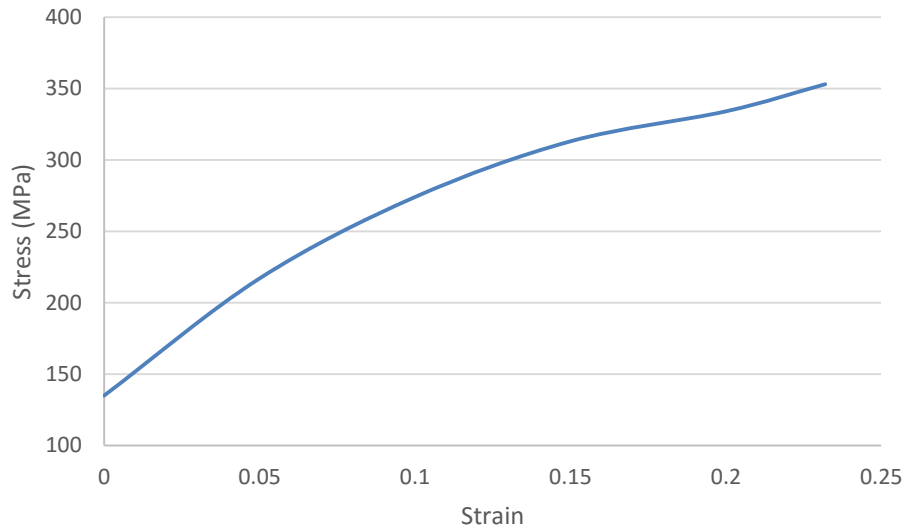


Figure 27 Flow curve of AA 5182 (Smerd et al. 2005)

### 3.7.4 Recycled AA-7175 Chips

Aluminium is a material that is widely used in different industries like aerospace and automotive as a base material of products. Due to their light weight, they are also used in aerospace industry. At the end of the manufacturing stage of many components, scraps are produced. Generally, those scraps are dumped without recycling which may add up to a considerable amount in a factory which adopts mass production. From chip to base material recycling needs another process which spends capital and energy. Pantke et al. (2013) introduce a three stage production method to convert chips of AA-7175 material to a base one. First stage is compacting chips by using high pressure. This pressure application can be achieved by using hydraulic presses. Then, compacted products are heated in furnaces. In the melt down temperature stage, gaps between the atoms are closed and stronger bonds are created. Last stage is the extrusion at the end of which AA-7175 profile tubes are created. According to Pantke et al. (2013) this recycling technique is used without losing much material. 95% efficiency is achieved through this technique. Another important aspect is that the mechanical properties of material are not

changed significantly. Mechanical properties of AA-7175 recycled chips and flow curve is given in Table 9 and Figure 28.

Table 9 Mechanical properties of AA 7175 recycled chips (Pantke et al. 2013)

AA-7175 recycled chips	
Modulus of Elasticity (MPa)	68500
Poisson's Ratio	0.33
Density (kg/m <sup>3</sup> )	2700

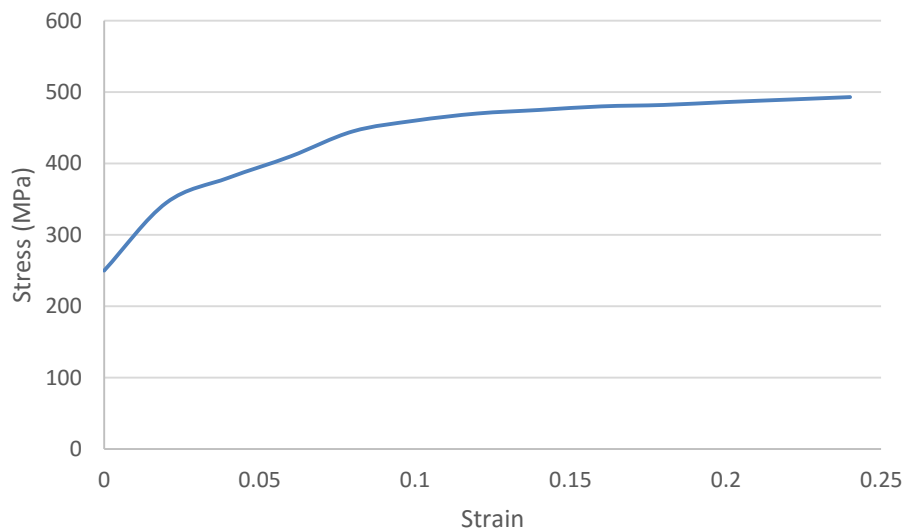


Figure 28 Flow curve of AA 7175 recycled chips (Pantke et al. 2013)

### 3.7.5 Aluminium with Carbon Nanotube Reinforcement

Carbon nanotubes (CNTs) have very high yield and ultimate tensile strengths. Their density is low (1300 kg/m<sup>3</sup>). On the other hand, aluminium is widely used in automotive industry due to its low weight. In this case, single wall carbon nanotubes are mixed with aluminium to increase strength. Al-CNT is widely used in automotive and aerospace industries. Production process of material is quite complicated. Firstly, powders of Al-CNT are filled into a copper can. Then, rolling and sintering methods are applied on this can. Lastly, copper cans are removed

from material Esawi & El Borady (2008). 0.5 wt % CNT is taken into consideration as pure aluminium has lower strength and higher CNT addition makes material brittle. A mechanical property of Al-CNT and flow curve is given in Table 10 and Figure 29.

Table 10 Mechanical properties of Al-CNT (Esawi & El Borady 2008)

	Al-CNT
Modulus of Elasticity (MPa)	60000
Poisson's Ratio	0.33
Density (kg/m <sup>3</sup> )	2654

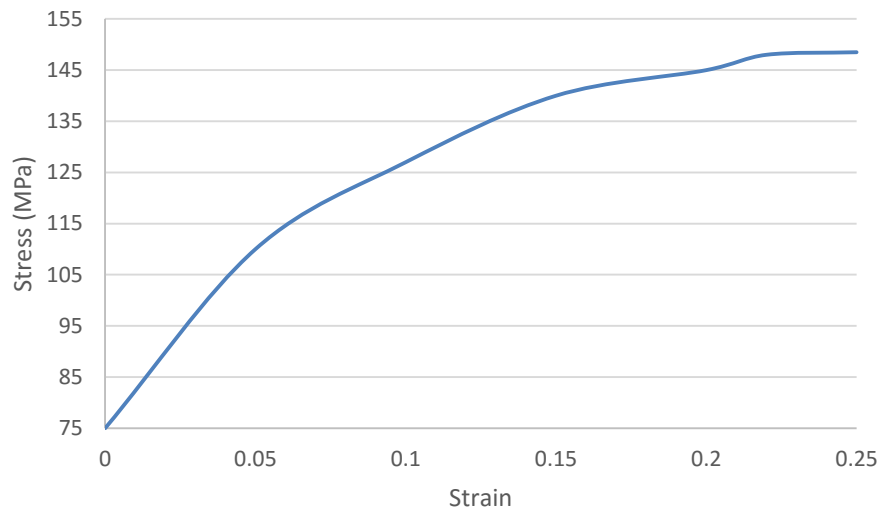


Figure 29 Flow curve of Al-CNT (Esawi & El Borady 2008)

### 3.7.5 Titanium Matrix Composite with Carbon Nanotube

#### Reinforcement

Due to its low weight and high strength, titanium is recently preferred in manufacturing the components of aerospace industry. It shows ductile behaviour which may create an opportunity to use this material on the structure of vehicle. Powder metallurgy method is used to produce the material. High strength multi-

walled carbon nanotubes are mixed with titanium to increase its strength. Mechanical properties of 35 wt % Multi-Walled CNT (MWNT) mixed with titanium Kondoh et al. (2009) are given in Table 11 and Figure 30.

Table 11 Mechanical properties of Titanium with MWCNT (Kondoh et al. 2009)

Titanium with MWCNT	
Modulus of Elasticity (MPa)	105000
Poisson's Ratio	0.31
Density (kg/m <sup>3</sup> )	4430

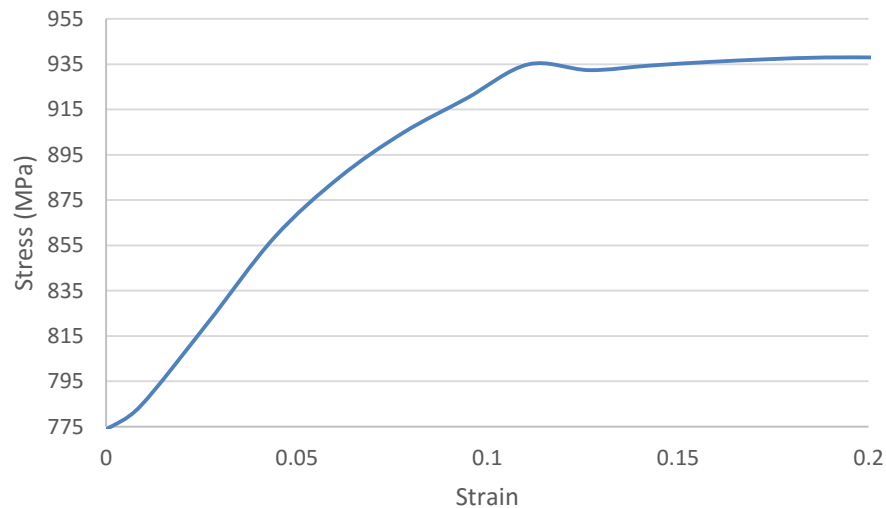


Figure 30 Flow curve of Titanium with MWCNT (Kondoh et al. 2009)

### 3.8 Profile Thickness Effect

All elements on the model is created as shell element type. Shell elements appear to be 2-D initially. However, thickness is input as an FEA parameter into the equations. This research seeks to find a proper thickness that have high energy absorption capacity. Two different parameters are taken into consideration in order to judge which thickness has better crash performance. Those parameters are crush force efficiency and specific total strain energy absorbed.

Crush force efficiency (CFE): is the ratio of the average force to the peak force value.

$$\eta = \frac{F_{average}}{F_{max}} \quad [2]$$

Specific energy absorbed (SEA) is the ratio of highest value of energy absorbed over total mass of the bumper beam and chassis system.

$$SEA = \frac{E_{max}}{m} \quad [3]$$

Total mass of vehicle is not taken into consideration in this research. Acar et al. (2011) analyse different shapes of chassis rails to find which one shows better crush performance. At that stage, optimization analysis was done by using parameters of SEA and CFE. Same optimization analysis is also done in this research and profile thickness of rectangular shape rails is one parameter that is modified.

Thicknesses of 7, 6, 5, 4 mm are applied on to the model even though other parameters and geometry of the model are kept unchanged. Dimensions of bumper and chassis system for 7 mm are given in Table 12 and 13 and different mass values for mild steel bumper and chassis system are given in Table 14.

Table 12 Dimensions of chassis rails for 7 mm thickness shell elements

	Right Rail	Left Rail
Thickness (mm)	7	7
Length (mm)	838.87	838.87
Width (mm)	60	60
Height (mm)	98	98

Table 13 Dimensions of bumper beam for 7 mm thickness shell elements

Bumper Beam	
Thickness (mm)	7
Outer Radius (mm)	572.36
Inner Radius (mm)	565.36
Height (mm)	100

Table 14 Total mass of bumper beam system for all thickness values

Thickness (mm)	Total Volume (m <sup>3</sup> )	Density (kg/m <sup>3</sup> )	Mass (kg)
7	0.0046	8000	37.07
6	0.0040	8000	32.10
5	0.0034	8000	27.03
4	0.0027	8000	21.84

### 3.9 Velocity Analysis

This study also investigates response of the bumper beam system for different velocity values. In real life, high velocity crash results in high damage and high risk of fatality to the occupants. This energy difference is visualized by showing results and the resultant shape of the bumper beam and chassis system. According to Euro-NCAP (2013) frontal impact protocol, all crash tests are conducted at 50 kph velocity. However, this study conducts all crash tests at 60 kph. In other words, a 1.2 safety factor is applied. 60 kph is base velocity but velocity of 80, 40, and 30 kph are also investigated and compared in Results and Discussion part. Response of bumper and chassis system is investigated for both high velocity (80 kph) and low velocity (30 kph) impacts.

### **3.10 Geometry Modifications**

Rectangular hollow rails and elliptical bumper beam is used as a base model in this research. Some modifications are carried out on the bumper beam system to search for an optimal design. Those modifications are removing some parts from the bumper beam, removing some parts from the rails, creating crash zone, changing the cross sectional shape of rails, creating runner zone, and creating a range hood crash zone. Response of the modifications is investigated and an optimization assessment is carried out to find which shape shows better crush performance.

#### **3.10.1 Removing Rectangular Parts from Bumper Beam**

Arbitrary rectangular parts are removed from the surface of bumper beam. This will lead to mass reduction. Expectation from the energy absorption characteristic is either somewhat reduction or staying constant. In the element removal stage, symmetry of both right and left side of system is considered. They are identically the same, so removed elements from one side are directly mirrored to the other side of bumper beam with respect to the mid-point of the whole system. Removed shape of the system is given in Figure 31 and the dimensions of the removed parts are given in Table 15. As it can be seen from the figure, three different areas are removed. Total mass of the system is reduced from 32.1 kg to 31.6 kg.

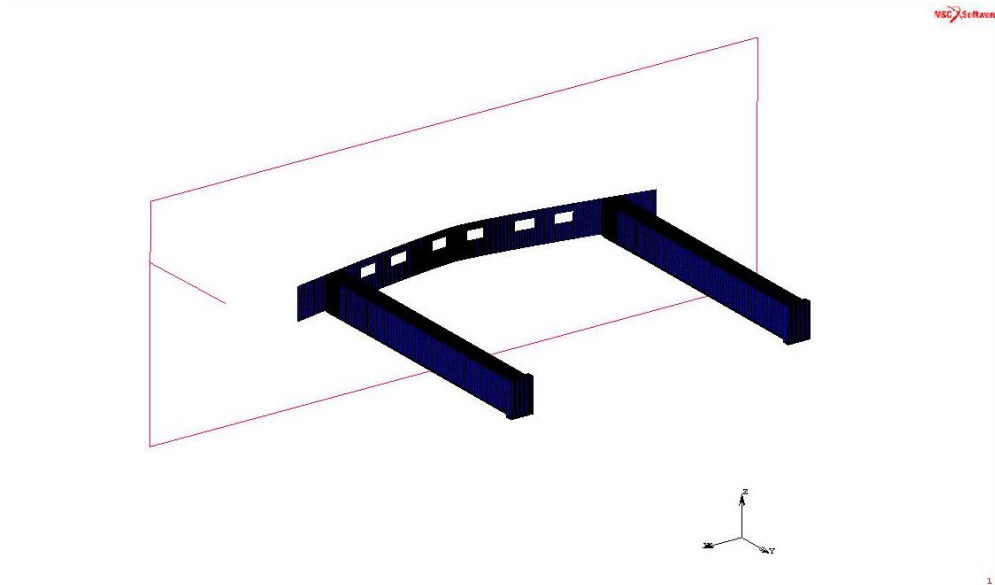


Figure 31 Modified bumper beam

Table 15 Dimensions of three different rectangular areas

	1	2	3
Thickness (mm)	6	6	6
Width (mm)	49.54	57.39	54.53
Height (mm)	30	30	30

### 3.10.2 Removing Rectangular Parts from Rails

Arbitrary rectangular parts are removed from the upper and lower surface of both rails. Rails are the main energy absorbing elements of the chassis for frontal crash. In the element removal stage, symmetry is observed. Removed shape of the system is given in Figure 32 and the dimensions of the removed parts are given in Table 16. As it can be seen from the figure, four different areas are removed. Total mass of the system is reduced from 32.1 kg to 30.9 kg. In this case more mass is removed than the previous one.

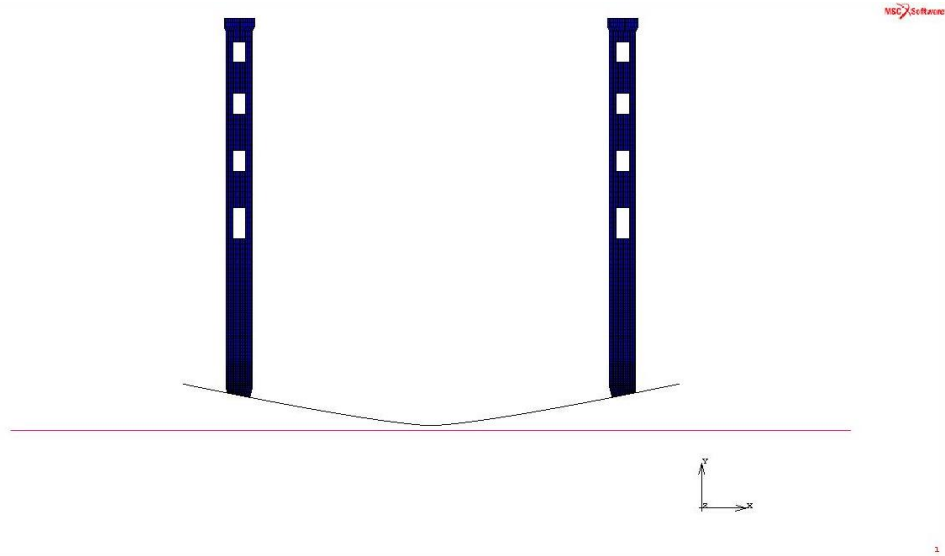


Figure 32 Removed parts from rails

Table 16 Dimensions of four different rectangular areas

	1	2	3	4
Thickness (mm)	6	6	6	6
Width (mm)	30	30	30	30
Height (mm)	47.76	47.76	47.76	71.64

### 3.10.3 Crash Zone Generation

Name of the crash zone comes from its high energy absorption characteristic. Its shape is like the musical instrument accordion so that it allows buckling and decreases energy that is transferred to the occupants. Total length and thickness of rectangular profile of rails are not changed. Crash zone is located at the start of both rails. Each tapered zone is created with 5 mm offset and 45° tapered angle is selected. There are 21 tapered areas that are located in each rail. Bumper beam and rail joining area is untouched. New bumper beam system with crash zone is given in Figure 33, detailed view is given in Figure 34 and the dimensions are given in Table 17. Total mass of the system is reduced from 32.1 kg to 31.9 kg.

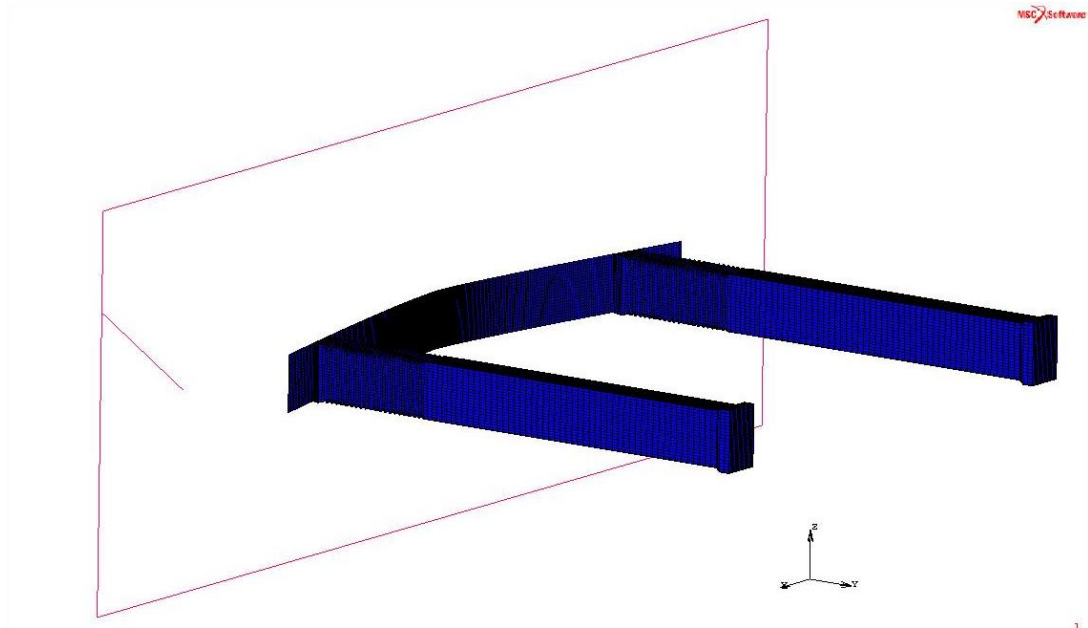


Figure 33 Bumper beam system with crash zone

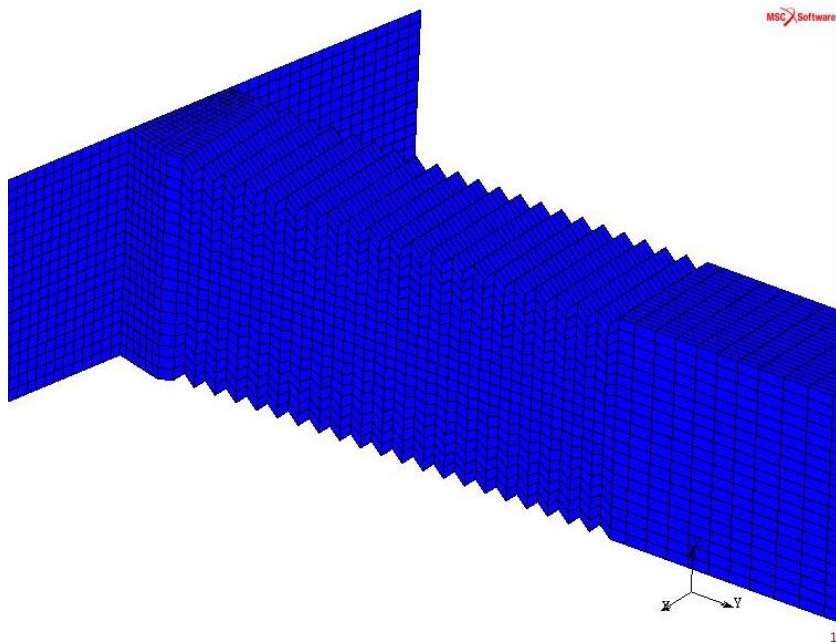


Figure 34 Detailed view of crash zone model

Table 17 Dimensions of new bumper beam system

	Right Crash Zone	Left Crash Zone	Right Rail	Left Rail
Thickness (mm)	6	6	6	6
Length (mm)	210	210	628.87	628.87
Width (mm)	60	60	60	60
Height (mm)	98	98	98	98

### 3.10.4 Hexagonal Cross-Section

Instead of rectangular cross-section, hexagonal cross-section with the same dimensions are applied to the system. Only the cross-section of the rails are changed. Expectation about crash energy absorption will be a higher value. However, this profile increases mass of the system. Production method of hexagonal shape profile needs more energy than rectangular shape profile. New bumper beam system with hexagonal shape is given in Figure 35 and the dimensions are given in Table 18. Total mass of the system is increased from 32.1 kg to 33.5 kg.

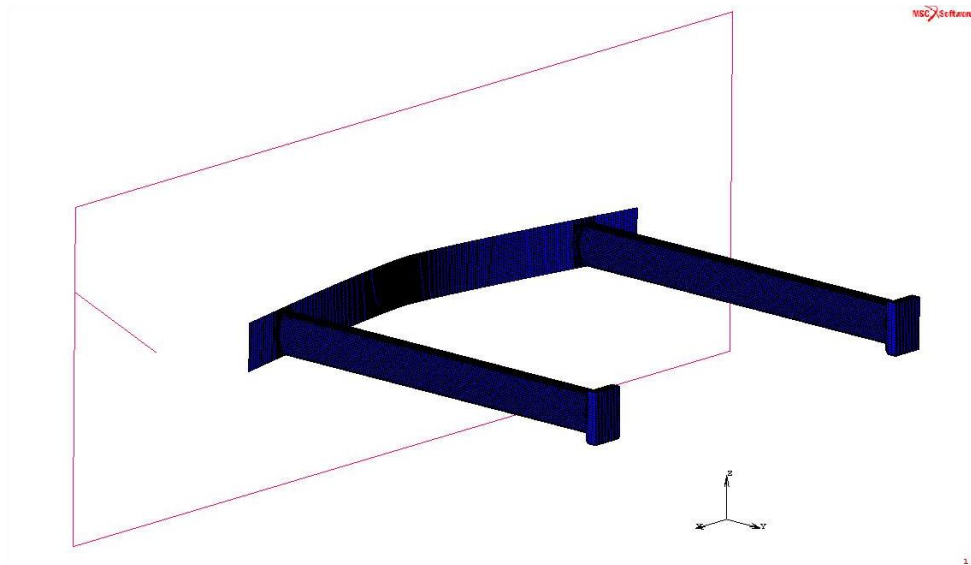


Figure 35 Bumper beam system with hexagonal cross-section

Table 18 Dimensions of new bumper beam system

	Right Rail	Left Rail
Thickness (mm)	6	6
Length (mm)	817	817
Width (mm)	60	60
Height (mm)	78.4	78.4

### 3.10.5 Runner

This modified model takes its name of runner from its behaviour during the crash. Around mid-point of both rails, runner area is created with 1 mm offset with respect to normal dimensions of rail. During impact, joints between runner area and rail break down and smaller runner area moves inside of rail. Smaller area tightly fits into rail profile and the friction between them slows down the system. Other positive effect of this special area is about displacement. Large displacement of rail is covered by this area so that this special area acts as a runner for the system. New bumper beam system with runner zone is given in Figure 36, detailed view is given in Figure 37 and the dimensions are given in Table 19. Total mass of the system is reduced from 32.1 kg to 32 kg.

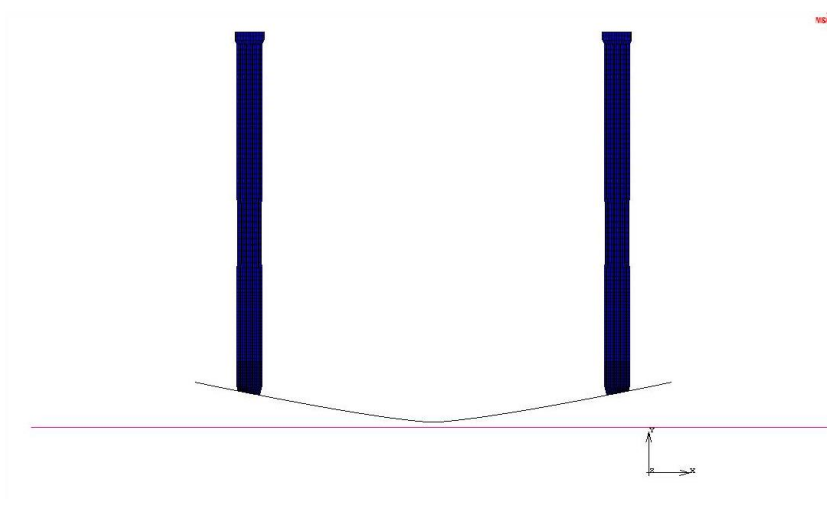


Figure 36 Bumper beam system with runner

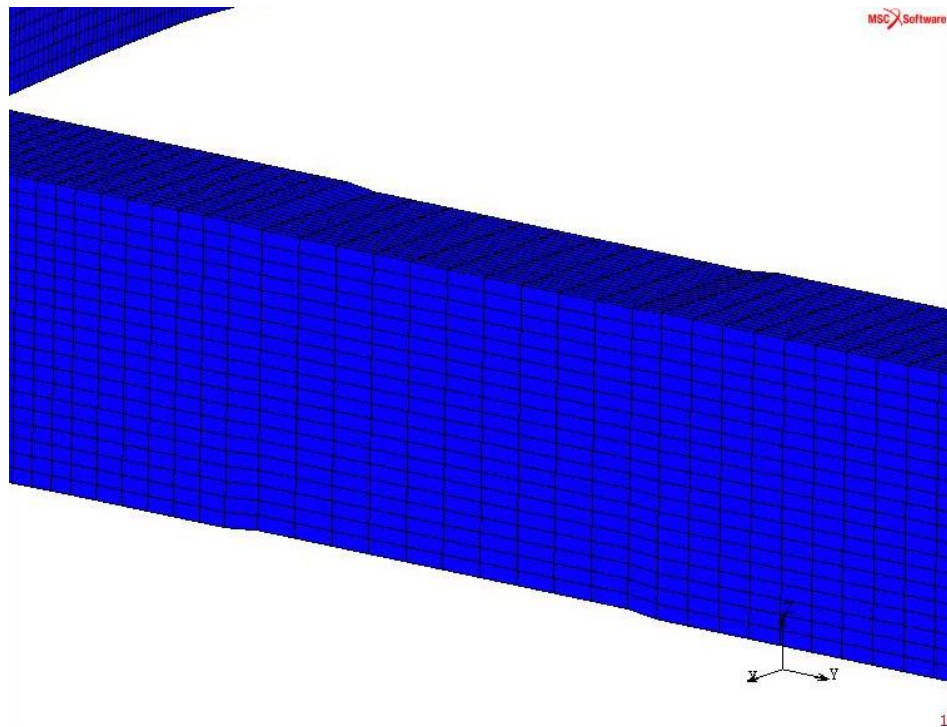


Figure 37 Detailed view of runner model

Table 19 Dimensions of new bumper beam system

	Right Runner	Left Runner	Right Rail	Left Rail
Thickness (mm)	6	6	6	6
Length (mm)	143.28	143.28	695.59	695.59
Width (mm)	58	58	60	60
Height (mm)	96	96	98	98

### 3.10.6 Range Hood

This geometry is created at the connection point of bumper beam and rail. It took its name from the geometrical shape. From rail side to bumper beam side area of this specific region is narrowed down and looks like a range hood that is generally seen in kitchens. In the base model, this section has same dimensions with rail. Mass of this model is less than the base model. During the impact, range hood section act as a damper for the system and expected to absorb more energy. New

bumper beam system with range hood zone is given in Figure 38, detailed view is given in Figure 39 and the dimensions are given in Table 20. Total mass of the system is reduced from 32.1 kg to 31.8 kg.

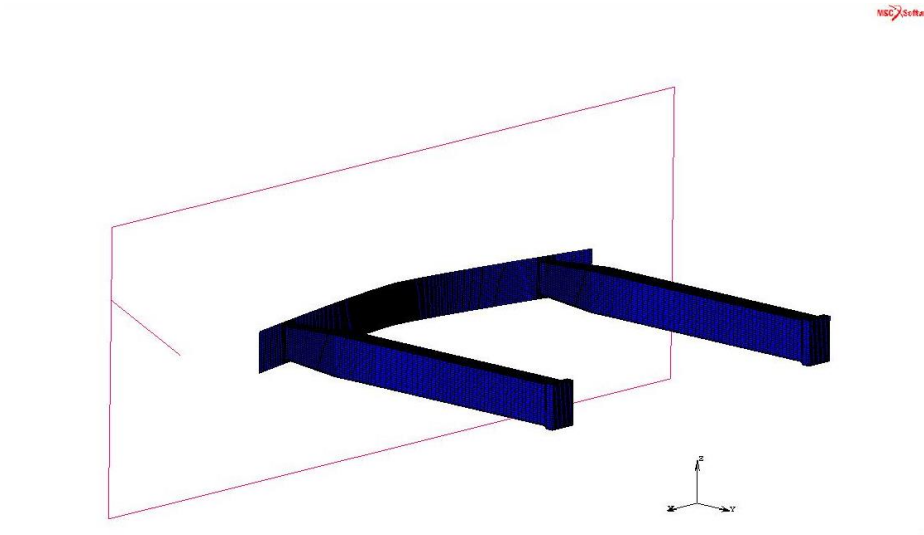


Figure 38 Bumper beam system with range hood

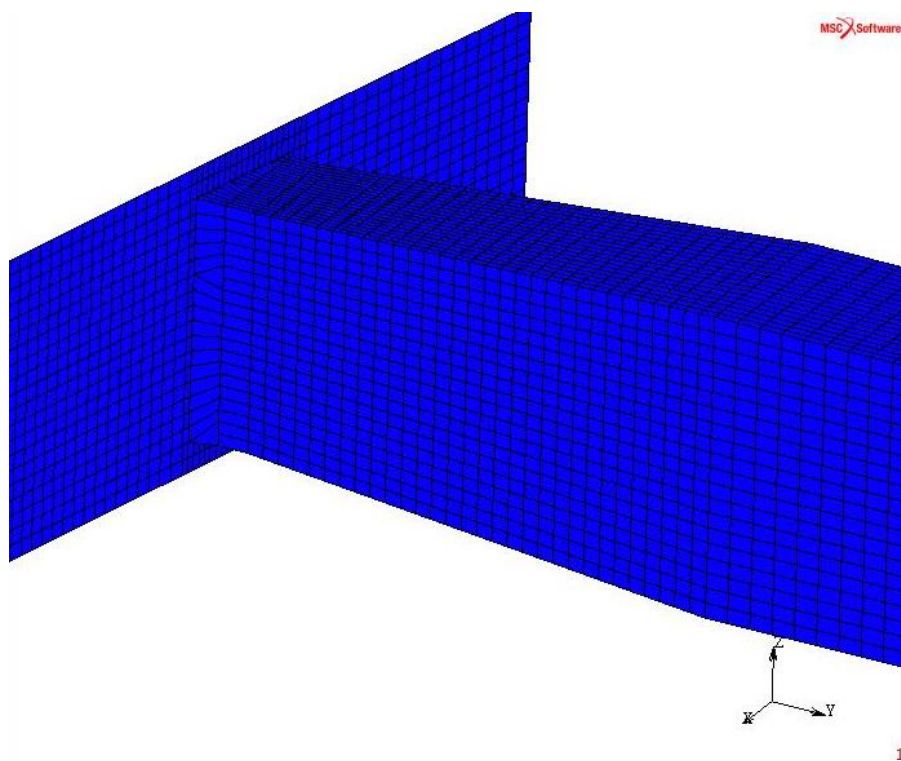


Figure 39 Detailed view of range hood model

Table 20 Dimensions of new bumper beam system

	Range Hood (Bumper Side)	Range Hood (Rail Side)	Right Rail	Left Rail
Thickness (mm)	6	6	6	6
Length (mm)	170		668.87	668.87
Width (mm)	40.33	60	60	60
Height (mm)	78.60	98	98	98

### 3.11 Hybrid Bumper and Chassis System

Hybrid terms are taken its name from the design of model. In this chapter modelling stage of four different hybrid systems is given. In three of them, different material combinations are used to improve crashworthiness and in the light of same purpose one of them is composed from different geometrical modifications. Materials were selected with respect to their mechanical properties. In other words, lightweight and strongest materials were selected. As a base geometrical modification crash zone model was taken into consideration.

#### 3.11.1 Hybrid Bumper and Chassis System with Different Material

##### Combination

Dimensions and geometry of the model is same with the crash zone model. However, both conventional and other type materials are used in different parts of model. Model is divided into three different sub-sections. DP-500, AA-5182, recycled AA-7175 chips, and titanium with MWCNT were used. Three different material combinations are given in Table 21.

Table 21 Three different hybrid model with used materials and related mass values

Model Name	Bumper Beam	Crash Zone	Rails	Mass (kg)
H-1	DP-500	AA-5182	Recycled AA-7175	16.28
H-2	AA-5182	DP-500	Recycled AA-7175	14.38
H-3	AA-5182	Titanium with MWCNT	Recycled AA-7175	11.97

### 3.11.2 Hybrid Bumper and Chassis System with Different Geometrical

#### Modifications

Runner and crash zone are two special regions that are designed to dissipate impact energy by displacement. In this hybrid model (H-4), both runner and crash zone is applied. Mild steel is used as a base material again and other parameters like initial velocity and thickness of shell elements are stay still. Aim is to improve crashworthiness of system as using combination of those two geometric modifications. Hybrid model is given in Figure 40, and the dimensions are given in Table 22.

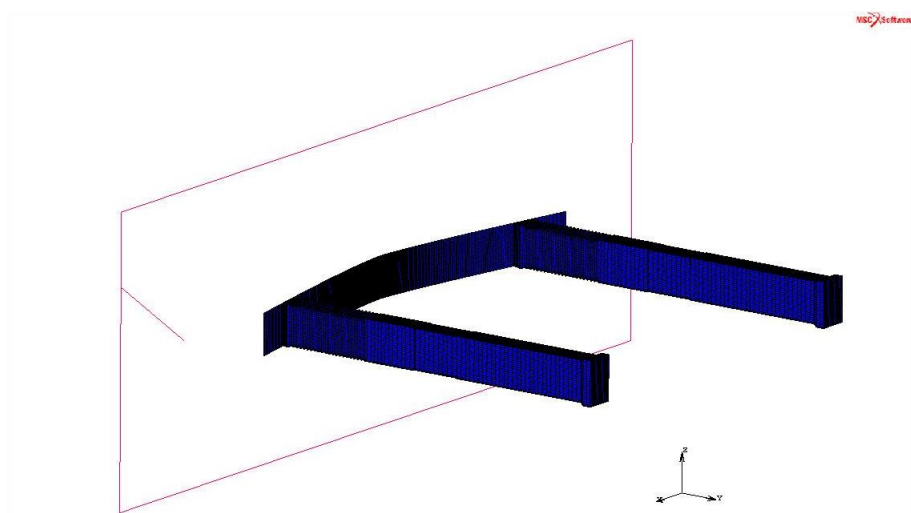


Figure 40 Hybrid bumper and chassis system

Table 22 Dimensions of geometrically hybrid system

	Right Crash Zone	Left Crash Zone	Right Rail	Left Rail	Runner
Thickness (mm)	6	6	6	6	6
Length (mm)	210	210	628.87	628.87	115.4
Width (mm)	60	60	60	60	58
Height (mm)	98	98	98	98	96

## **4. RESULTS AND DISCUSSION**

Data that are gathered from Marc Mentat 2013™ with various models are discussed. In modelling section many combinations are given in a detailed way. Generally, base model with a profile thickness of 6 mm and impact velocity of 60 kph impact velocity is used to compare both material and geometric modifications that are done on the bumper and chassis system. Comparison of alternatives played a key role in determining the best model which is good at impact energy absorption and light weight. Investigated parameters and modification alternatives are thickness of profile, impact velocity, material of system, and geometrical changes.

### **4.1 Sensitivity and Error Analysis**

#### **4.1.1 Sensitivity Analysis**

Before starting to make analysis on model this part has a crucial role on determining proper number of the elements. As it is mentioned before; number of elements effects the response of the system. In order to determine where system become stable, data of maximum energy absorbed by bumper and chassis system are gathered and investigated. Graph of sensitivity analysis is given in Figure 41. Maximum absorbed energy value is just a base response of system. It is selected as a base parameter because energy absorption graph becomes constant at its maximum value and easy to gather data.

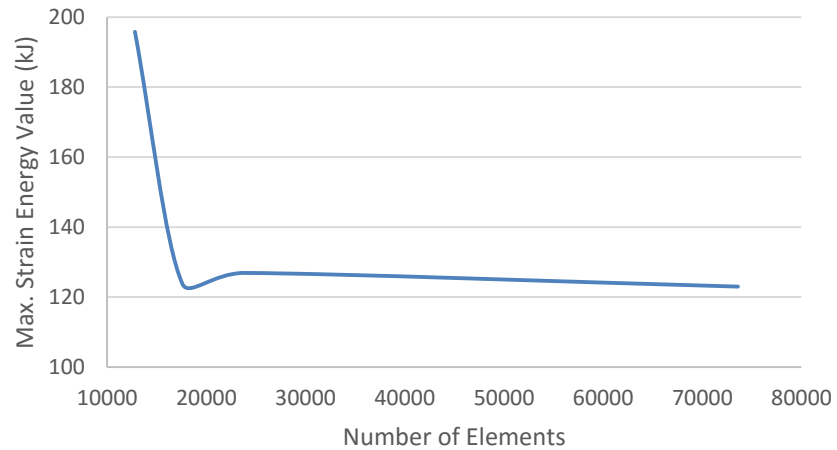


Figure 41 Maximum strain energy vs number of elements

After element number of 23840 point; response of system become stable and give the same result. There is a direct proportion between number of elements and computational time so it is not efficient to select the finest mesh. Relation between computational time and number of element is given in Figure 42. According to graph computational time rise linearly with respect to increasing element number. Critical point for bumper model is 3<sup>rd</sup> point on the graph. Before that point system does not capable to give buckling behaviour. That can be the main reason why energy absorption value is so high. After that critical point system gives same response so element number of 23840 is selected and it takes around four hours to complete analysis.

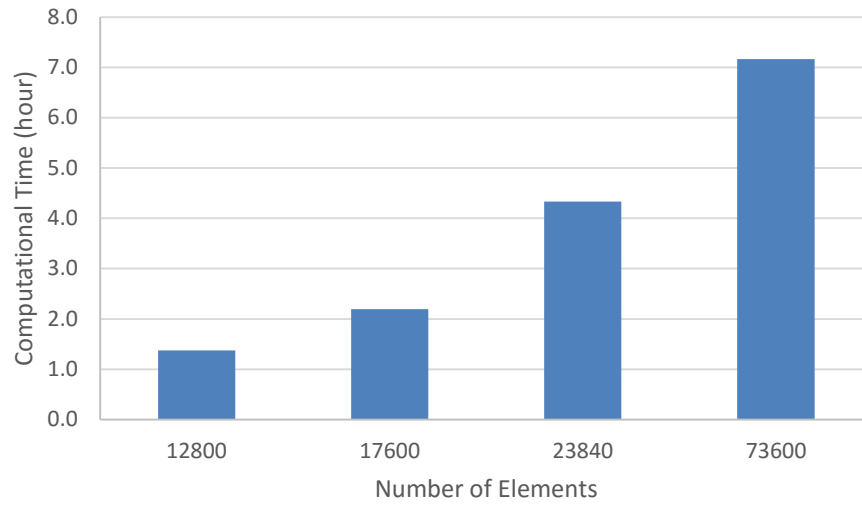


Figure 42 Computational time vs number of elements

#### 4.1.2 Error Analysis

Error analysis aims to find increment value in which peak resistive force value is given. Besides, this analysis helps to understand error margins of obtained result from software. For different increment values (from 100 to 600), related error bars are given in Figure 43. However, total analysis time and other parameters were kept stable. Highest resistive peak force value ( $3146 \pm 300$  kN) is observed in increment number of 200.

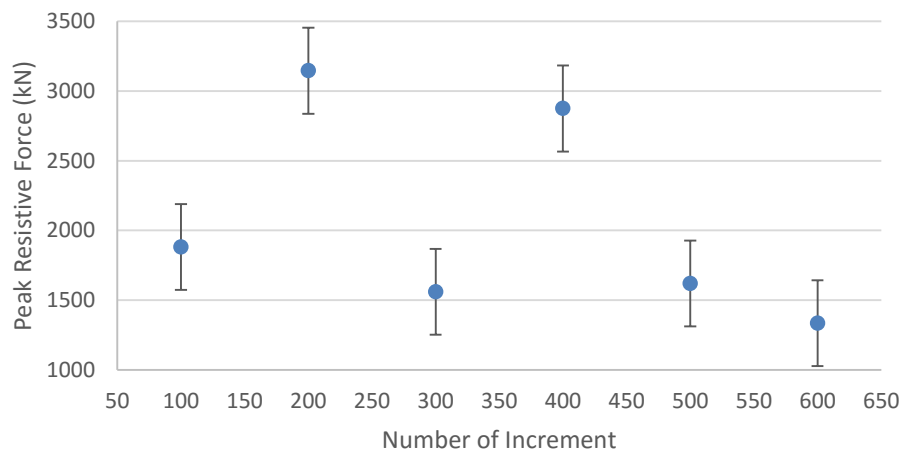


Figure 43 Computational time vs number of elements

## 4.2 Quasi-static Analysis vs Dynamic Transient Analysis

Impact characteristics of both quasi-static and dynamic transient analysis are different from each other. In quasi-static analysis, bumper beam was fixed from ends of each rail and wall moved towards to the model with a known displacement value and then analysis was done. Resistive force results of quasi-static analysis are lower than dynamic transient ones in Figure 44. Although their numerical values are different from each other, both analysis shows the same force pattern.

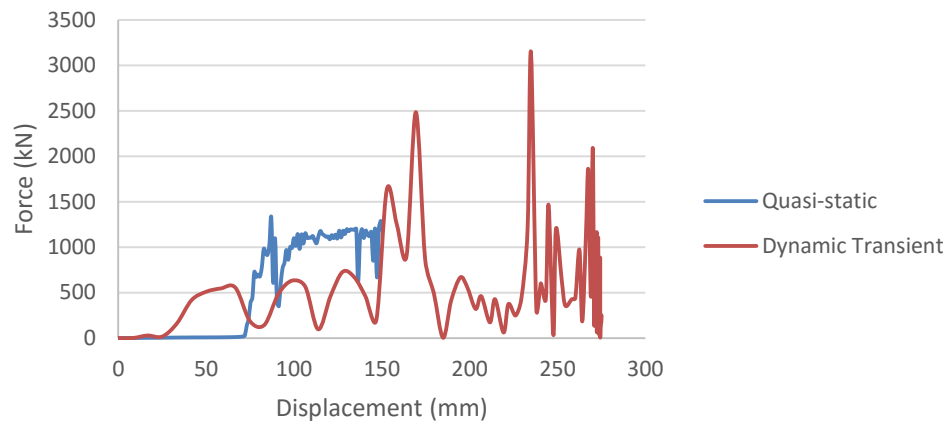


Figure 44 Crush force vs displacement graph for both quasi-static and dynamic transient analysis

On the other hand, impact energy patterns show different behaviour in Figure 45. After contact starts impact energy trend line of quasi-static analysis is linearly increasing. In dynamic transient analysis vehicle bounces back the rigid wall after crash done. Plateau on dynamic transient analysis represents that crash is over. It can be concluded that, quasi-static analysis is not realistic and applicable to represent crashworthiness of vehicle in simulation. Besides, deformed shape of quasi-static analysis is given in Figure 46.

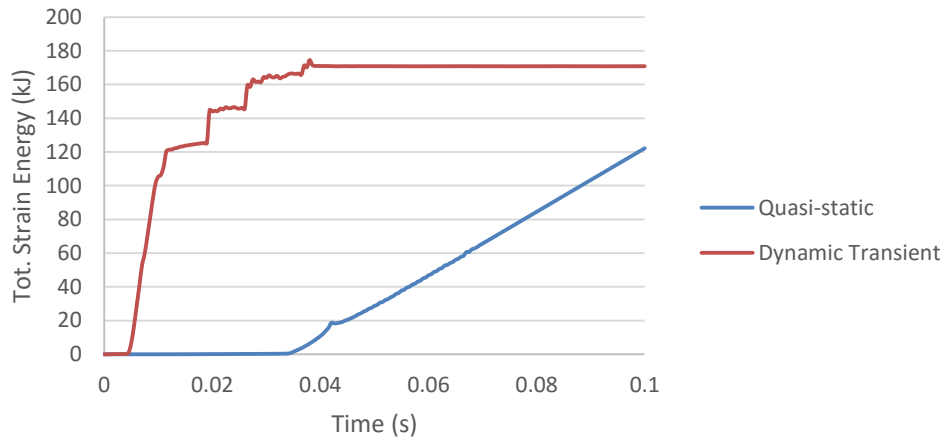


Figure 45 Total strain energy vs time graph for both quasi-static and dynamic transient analysis

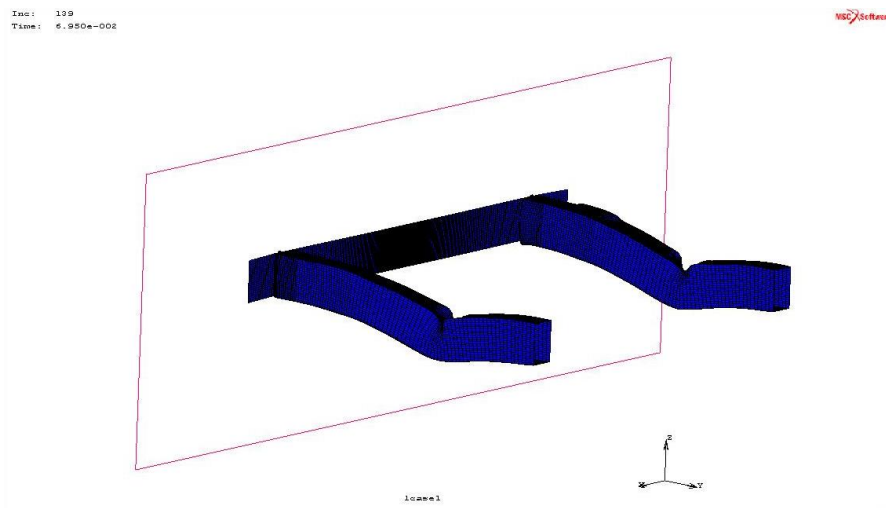


Figure 46 Deformed auxiliary view of quasi-static analysis

### 4.3 Profile Thickness Effect

Lowering mass can be achieved by lowering thickness of rectangular profiles and bumper beam. Mass of the system significantly decreases when thickness becomes slimmer. In Table 23, mass of the system ranges between 37.1 kg to 21.8 kg. At that point the main question is crash energy absorption performance of the slim bumper and the chassis system stay still or not?

Table 23 Mass values for each thickness

Thickness (mm)	Total Volume (m <sup>3</sup> )	Density (kg/m <sup>3</sup> )	Mass (kg)
7	0.0046	8000	37.07
6	0.0040	8000	32.10
5	0.0034	8000	27.03
4	0.0027	8000	21.84

Crush force is the type of force that is created on system during crush. Higher crush force is good for system. In other words, most of the crash energy is absorbed in the region of bumper beam system. Because absorbed crash energy is the total area under the graph of force vs displacement. Figure 47 gives an idea about both force and energy absorbed characteristics of specified thickness values.

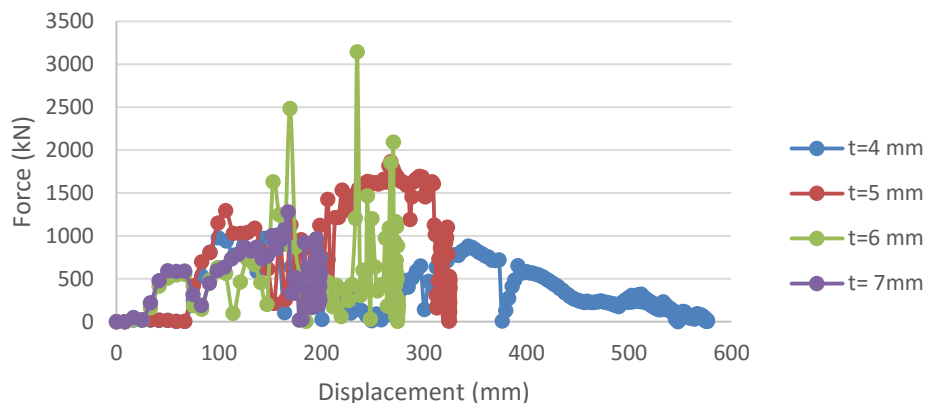


Figure 47 Crush force vs displacement graph for different thickness values

Crush performance of system directly depends on parameters of both contact time and mass of the system. Although analysis time of system is the same for all models, contact time shows variation. Smaller thickness means lighter model. Light models' contact time and displacement is higher than the heavier one. End point of rails is used as a reference for displacement measurement. Displacement is 577 mm in the model of 4 mm profile thickness. On the other hand, displacement of 7 mm profile thickness is 200 mm.

Reason of fluctuations in force is buckling behaviour. Crush force is increasing when system resist. Buckling starts when this resistance is broken and force suddenly drops. Base model has two different contact surfaces and this may lead desultoriness in a graph of crush force and displacement. First contact is occurred between rigid wall and bumper beam. Second contact is occurred between rails and simplified masses of vehicle. Another important situation is the initial distance between rigid wall and bumper and chassis system. Due to profile thickness change, contact start time may vary.

Resistance force behaviour of profile thickness of 6 and 7 mm similar to each other and same similarity can also be seen in profile thickness of 4 and 5 mm. Profile thickness of 6 and 7 mm starts to resist earlier than profile thickness of 4 and 5 mm and their trend lines are nearly the same at the starting point. Before peak force value, bumper beam resists to the impact action and related force values are lower than the peak force value. It can be said that bumper beam has little effect on energy absorption. Majority of crush energy is absorbed by rails of the system. Contact starts when the displacement of system is around 25 mm. However, resistance force is not formed in the thinner models at that time. For thinner models, resistance force is formed when rails starts to contact with rigid wall. Rails undergo a high magnitude of forces which means resistance force reaches its peak value. Then buckling starts and force value drops suddenly. For each model peak force value does not correspond to same displacement.

Although desultoriness is observed in the crush peak force values, expected energy absorption characteristic is obtained. Although their peak values are different from each other, all trend lines show the same characteristic in Figure 48. The heaviest model reaches its peak values in a shorter time period than the other models. According to Figure 48, higher profile thickness shows the best energy absorption performance than other models. Lowering mass of the vehicle has lots of positive effects on our earth however it is not effectively protects occupants and crash may result with casualties. Energy absorption difference between lighter and heavier

model is 80 kJ and this difference cannot be acceptable because priority of this research is not only focusing on the reduction of carbon emission but also addressing the life security of occupants of vehicle. In order to decide which thickness satisfies both criteria, crush force efficiency and specific energy absorption parameters are calculated and tabulated in both Tables 24 and 25.

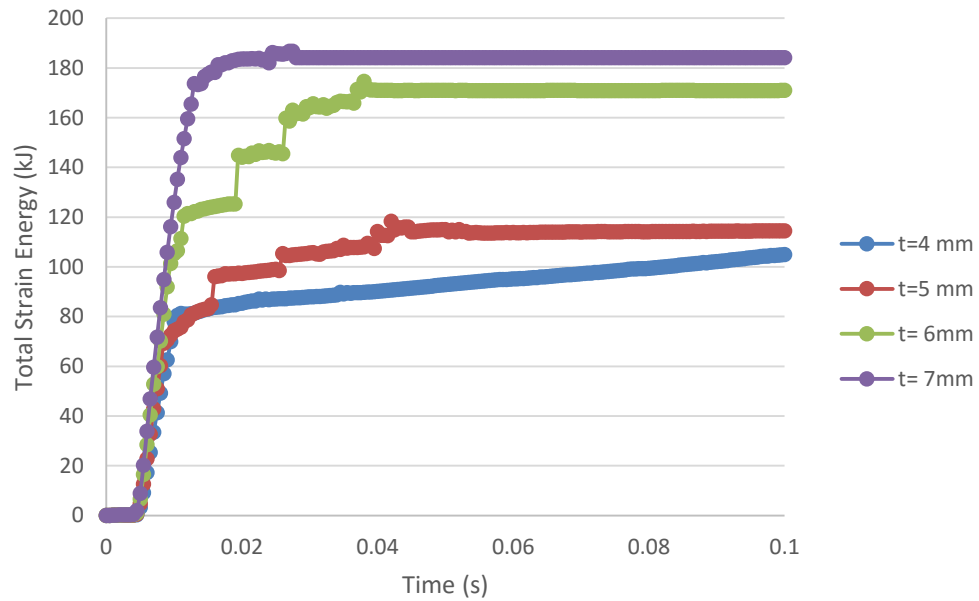


Figure 48 Total strain energy vs crash time graph for different thickness values

In order to check absorbed energy results with theoretical ones, theoretic initial kinetic energy was calculated using equation 4.

$$E = \frac{1}{2} * m * v^2 \quad [4]$$

For 7 mm profile thickness, total mass of the vehicle is 1400 kg and initial velocity is 60 kph ( $16.67 \text{ ms}^{-1}$ ).

$$E = \frac{1}{2} * 1400 * 16.67^2 = 194.5 \text{ kJ}$$

Initial kinetic energy and total absorbed impact energy were compared. There is a 10.5 kJ (5.4%) difference between them. This difference occurred due to bounce back behaviour.

As it is mentioned in the modelling section, crush force is the ratio of average force to the peak one. For an ideal case, crush force efficiency should be equal to 1. So the model with the highest efficiencies resists more and transmits less impact energy to the occupants. From the results, the most resistive bumper and chassis system profile thickness is 5 mm and then 7 mm. Another important parameter to justify results is the SEA. SEA gives a better idea about models crash performance. Although mass of the model changes with respect to thickness, maximum strain absorbed energy also changes. From the results, higher thickness has characteristics of absorbing more impact energy. According to Table 25, model that has highest energy absorption per unit mass is 6 mm profile thickness.

Table 24 Crush force efficiency for different thickness values

Thickness (mm)	Average Force (kN)	Peak Force (kN)	Crush Force Efficiency
4	297.14	1012.56	0.29
5	831.50	1863.87	0.45
6	564.67	3145.73	0.18
7	524.66	1278.80	0.41

Table 25 Specific energy absorption for different thickness values

Thickness (mm)	Mass (kg)	Max. Strain Energy (kJ)	Specific Energy Absorption (kJ/kg)
4	21.84	104.92	4.80
5	27.03	114.40	4.23
6	32.10	170.88	5.32
7	37.07	184.03	4.96

Deformed shapes of different profile thickness verify that thicker models have higher strength during impact (Figure 49-52). More deformation is observed in thinner models and bounce back phenomena occurs in thicker models. Because higher strength cause a higher resistive force on the rails and model deflected from the wall. According to all those after impact figures, it looks like 7 mm profile thickness is the safest model. On the other hand, specific energy absorbed value shows that the safest model which has 6 mm profile thickness. In fact 5 mm thickness is the critical point in this study. After that all thickness values are safe enough for occupants. However, profile thickness of 7 mm model increases total mass of the system by 5kg when compared to 6mm one. For that reason, 6 mm profile thickness is a better choice to use as a base model for further analyses. Other views of all deformed models are given in Appendix section.

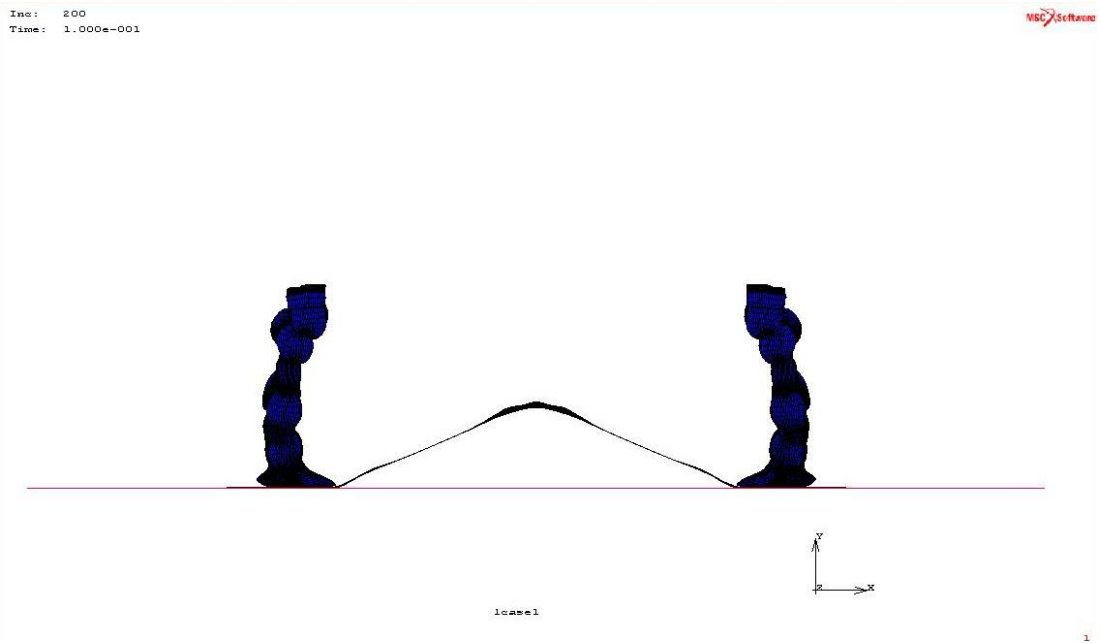


Figure 49 Deformed shape of 4 mm thick profile

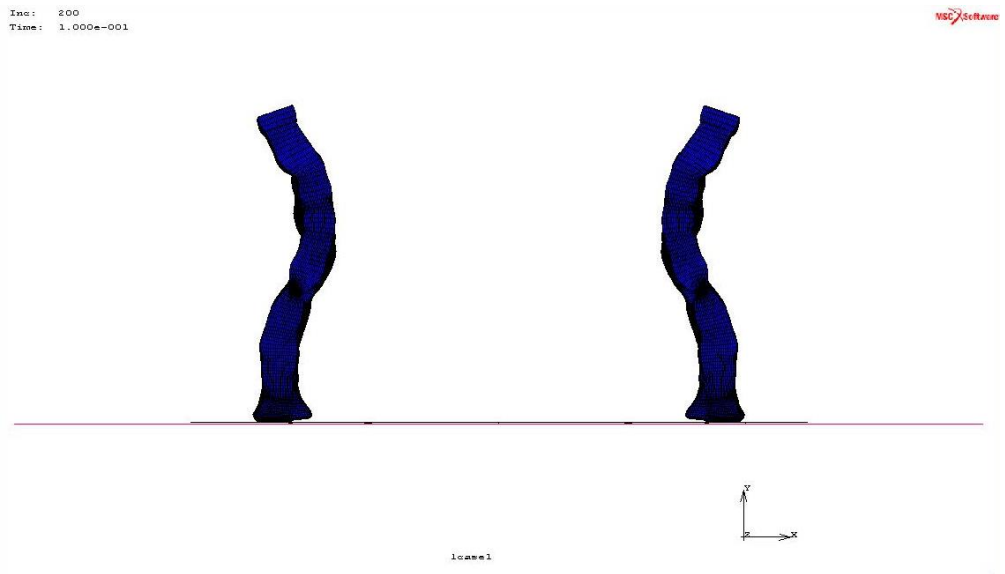


Figure 50 Deformed shape of 5 mm thick profile

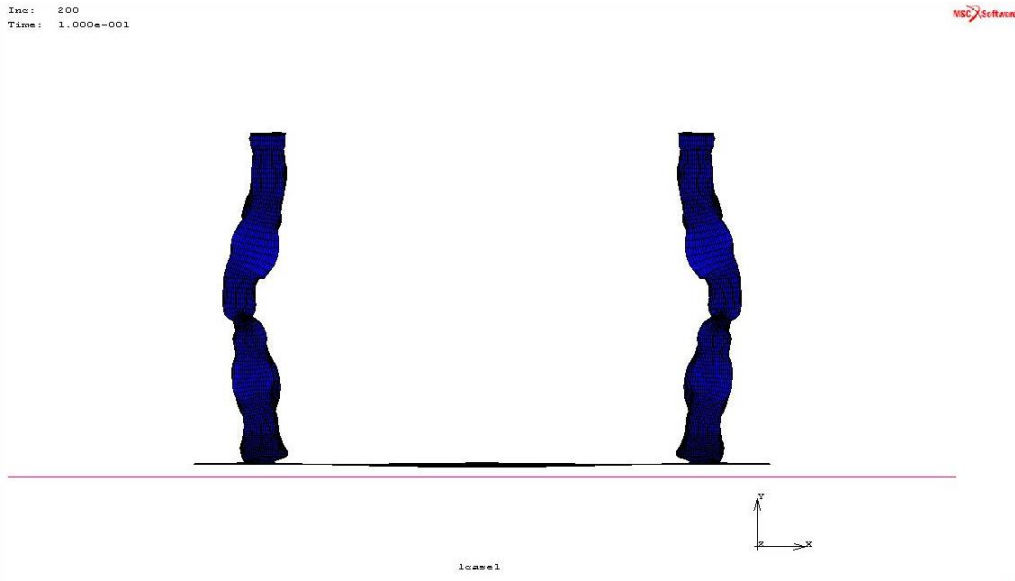


Figure 51 Deformed shape of 6 mm thick profile

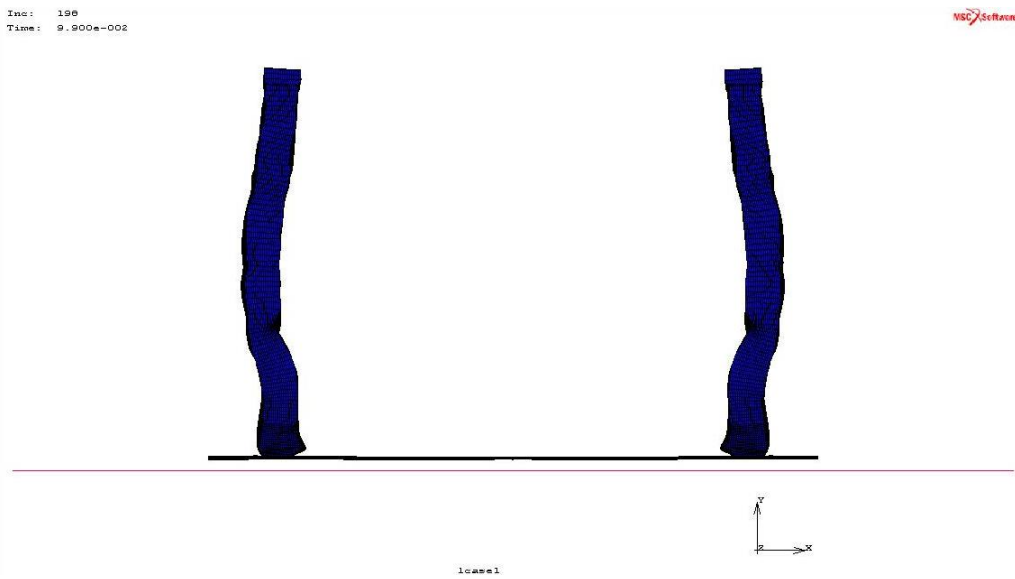


Figure 52 Deformed shape of 7 mm thick profile

#### 4.4 Velocity Analysis

Reason to analysis different crash velocities is to show effect of velocity on crash. As it is mentioned before, EuroNCAP investigates crashworthiness of vehicles by applying 50 kph. In real life, generally, drivers use their vehicles over this safe velocity and crashes result with casualties. In much country, highway speed limitations are also around 120 kph. In fact, low velocity crash is 30 kph and over that velocity all crashes are in the region of high velocity crash. In this research, base velocity is 60 kph. In order to prove negative effects of velocity and compare each case with others, this analysis is done with different velocities of 30, 40, 60, and 80 kph.

According to Figure 53, there is a direct proportion between velocity and displacement of bumper beam system. Displacement ranges from 113 mm to 329 mm. That means higher forces and higher energies created in the higher velocities. Force trend of 60 and 80 kph velocities are similar to each other. Peak forces occur at the same displacement values. Due to more displacement higher energy is formed. In 30 kph velocity case maximum energy is around 55 kJ. On the other hand, it is around 260 kJ in 80 kph case. Although velocity change is not much, its effects on the impact energy difference are high. For example, from 60 to 80 kph energy difference is 90 kJ which nearly equals to the impact energy that in the case of 40 kph.

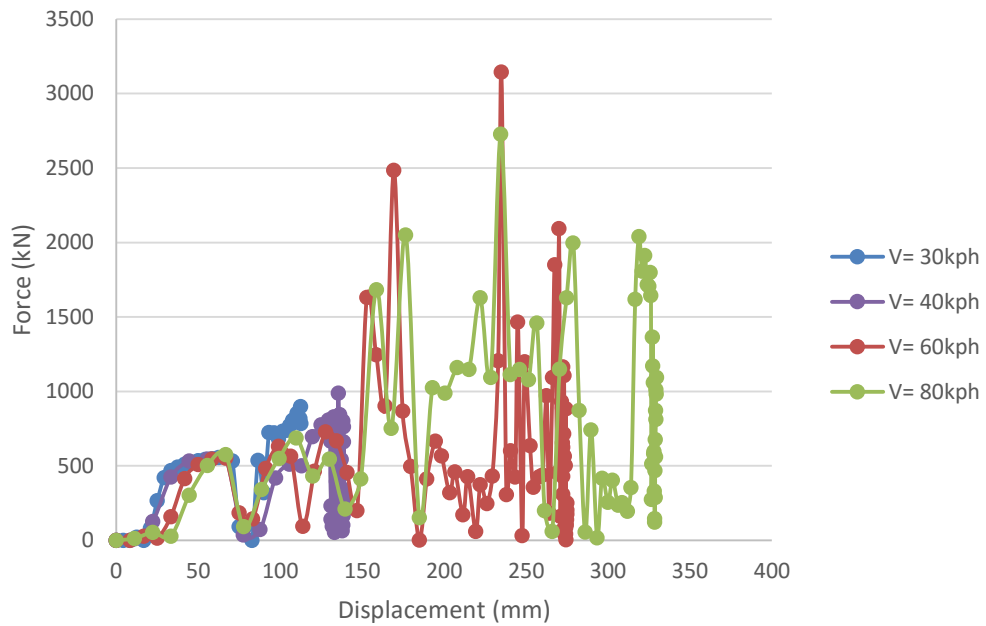


Figure 53 Crush force vs displacement graph for different velocity values

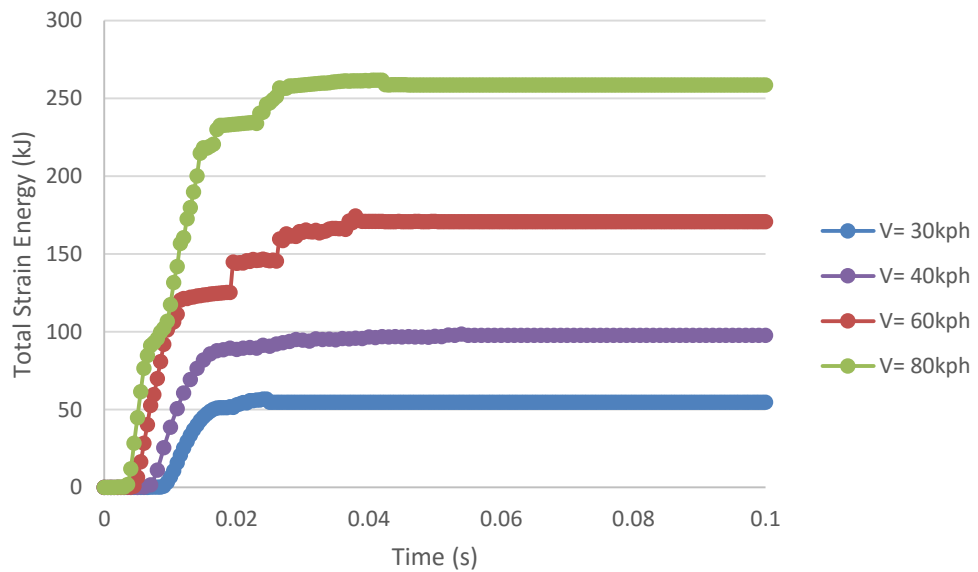


Figure 54 Total strain energy vs crash time graph for different velocity values

After impact figures prove that speed cause fatality or seriously injury of occupants. Deformation of bumper beam increases with increasing initial speed and bumper and chassis system is exposed to higher impact energy (Figure 55-58). For 40 kph, just one point on the rails buckled. Number of buckling region increases for further

speed values. At 80 kph system reaches its maximum buckling and bends around bumper beam. Besides, deformations that occur on the case of both 60 and 80 kph initial velocity; can be irreparable. However, same statement is not valid for further speed values. It can be concluded that 40 kph is the limit speed to avoid fatalities or serious injuries. Other views of all deformed models are given in Appendix section.

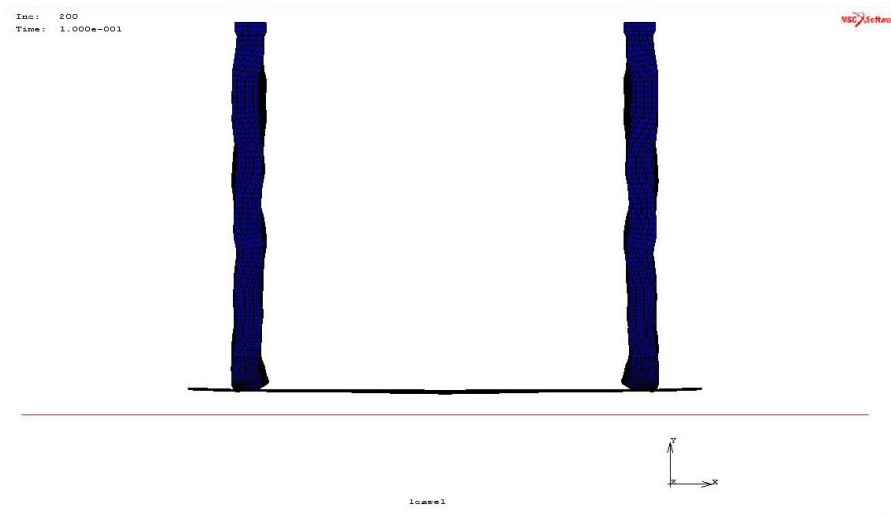


Figure 55 Deformed shape of 30 kph initial velocity model

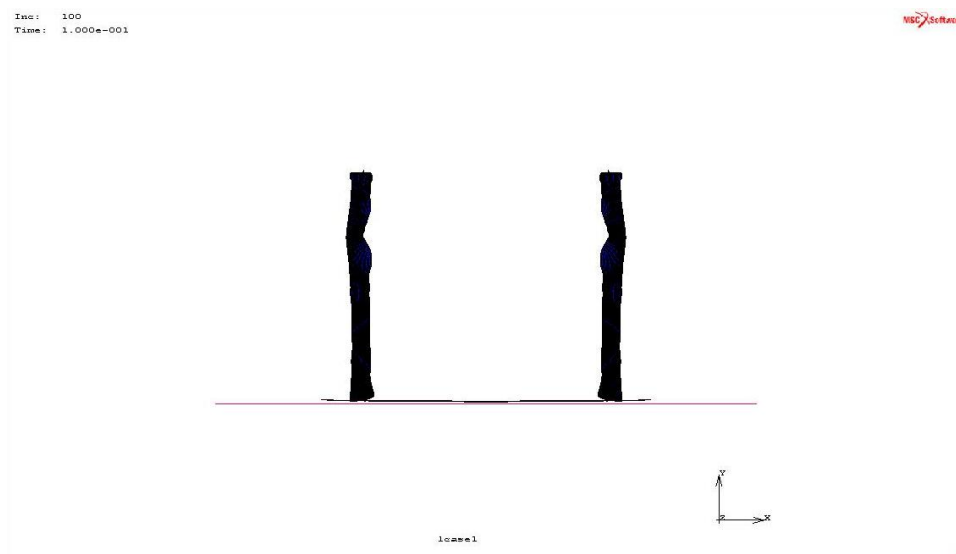


Figure 56 Deformed shape of 40 kph initial velocity model

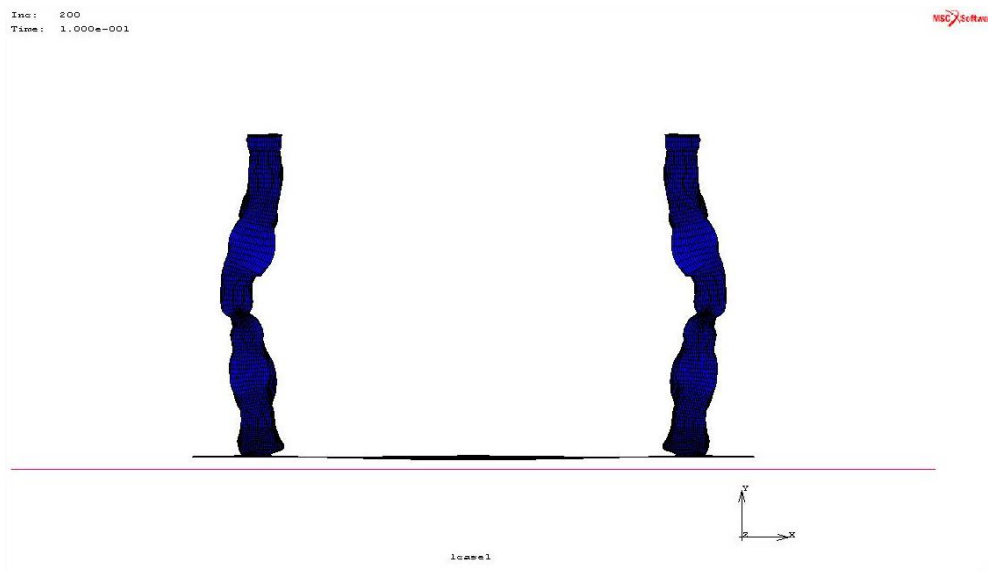


Figure 57 Deformed shape of 60 kph initial velocity model

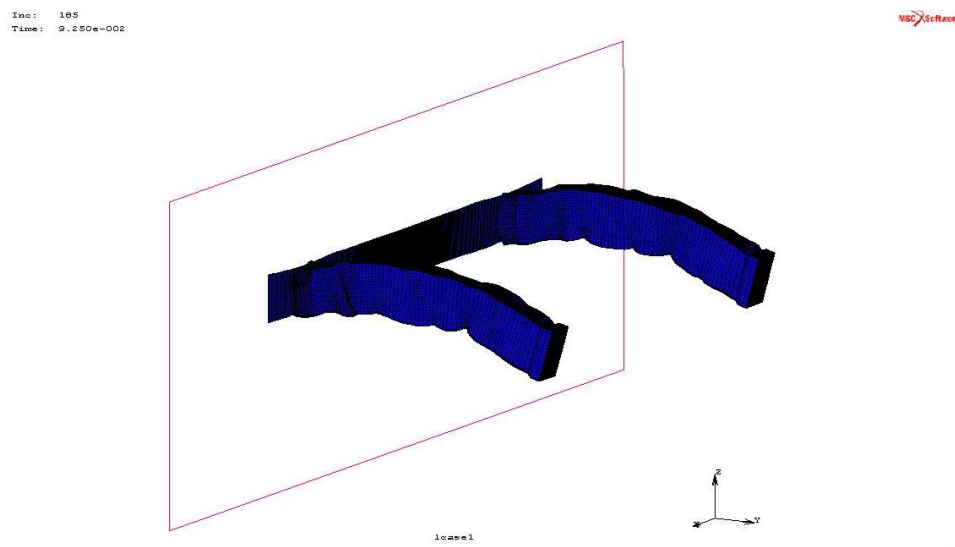


Figure 58 Deformed auxiliary view of 80 kph initial velocity model

## 4.5 Geometrical Modifications

Geometry of bumper beam system (base model) directly originates from the well-known automotive brand Toyota Yaris. In this section, some geometrical modifications are done on the system in order to improve crashworthiness

performance. Energy absorption characteristics and crush force values of geometrically modified models are compared with base model. Figure 59 seems complicated to distinguish trend lines individually. In fact, important points are clearly seen from the graph and each model is discussed individually to understand effect of its geometry on crashworthiness and then all of them compared.

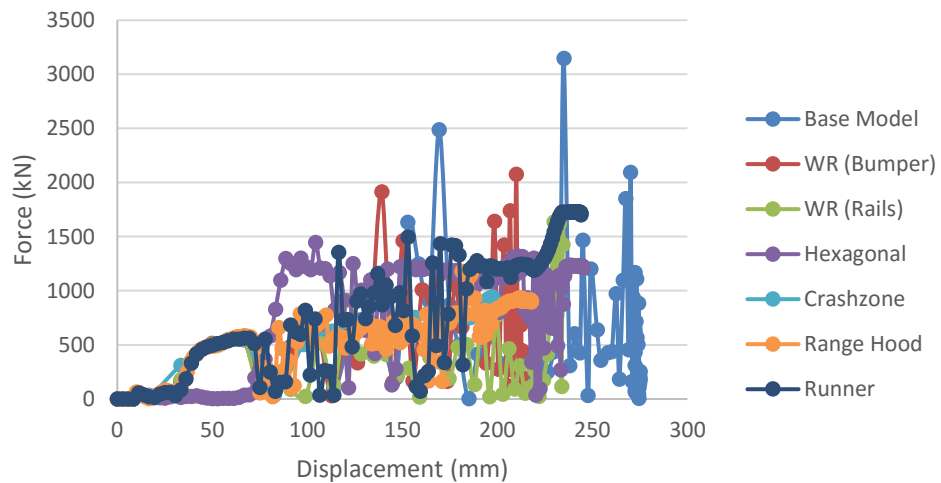


Figure 59 Crush force vs displacement graph for different geometrical shape

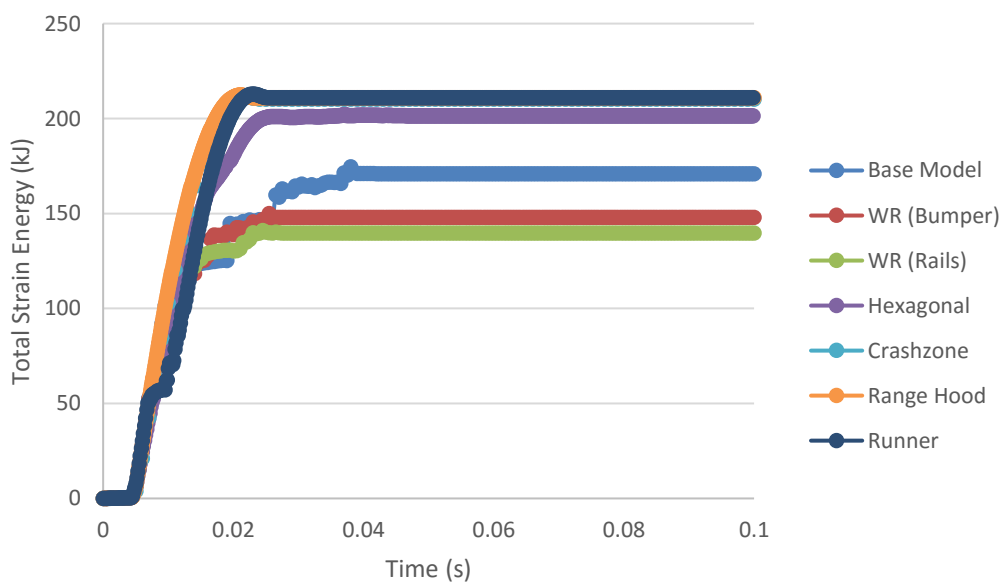


Figure 60 Total strain energy vs crash time graph for different geometrical shapes

In both weight reduction (WR) models geometrical modifications are the same. Some materials are taken from bumper beam or rails to reduce mass of vehicle. Instead of bumper beam, rails are better in energy absorption role. Another issue is related with the mass reduction. More mass reduction causes a strength loss into the system. Peak resistive crush force of WR (bumper) model (2076 kN) is higher than one that is on WR (rails) model (1726 kN) in Figure 60. Besides, maximum impact energy absorption values are showing a little difference. It is 148 kJ for WR (bumper) model and 140 kJ for WR (rails) model. Although mass reduction achieved, strength of those two models is lower than base one. Maximum absorbed energy decreases from 171 kJ to 148 kJ.

Instead of rectangular profile rails hexagonal shape can be better idea to absorb more impact energy. It has the highest displacement value with respect to other models. Peak force is reached at the contact beginning point of rails. Then, reaction force tread line keeps itself on the same line. This may cause a higher average force value which is closest to peak force. Energy absorption also shows better performance with respect to three models that are discussed before. Different from other modifications hexagonal model increase total mass of system. Although crush force efficiency characteristic is pretty high, higher mass value decreases specific energy absorption characteristic. However, it is still a better model with respect to the base one.

Crash zone, runner and range hood models are created in order to maximize impact energy absorption performance of system. This purpose is achieved by dissipating energy on displacement. Detailed information about their modelling stage was given in modelling section. Due to its design purpose highest displacement is done by runner model among the three models. During impact, connections between smaller size region and rail are broke down and get inside of rails. This specific region tightly fit into the space of rails and slows down system. On the other hand, both resistive crush force and energy absorption characteristics of crash zone and range hood models are nearly the same. Crash zone creates a bounce back and

slower system. Same principle is also acceptable for range hood model. Although slight differences can be observed on those three models, their energy absorption performances are higher than all other models and similar to each other. Among those three models the best impact performance is observed in crash zone model. Crush force efficiency value is nearly 1 and due to its low weight and high impact energy absorption value specific energy absorption is also the highest. It can be easily said that aim of this research is achieved by modifying bumper and chassis system to crash zone one.

Table 26 Crush force efficiency for different geometrical shapes

Model	Average Force (kN)	Peak Force (kN)	Crush Force Efficiency
Base Model	546.67	3145.73	0.17
WR (Bumper)	629.51	2076.01	0.30
WR (Rails)	445.39	1718.43	0.26
Hexagonal	857.39	1446.13	0.59
Crash zone	629.61	941.35	0.67
Range Hood	629.16	1177.53	0.53
Runner	962.79	1728.77	0.56

Table 27 Specific energy absorption for different geometrical shapes

Model	Mass (kg)	Max. Strain Energy (kJ)	Specific Energy Absorption (kJ/kg)
Base Model	32.10	170.88	5.32
WR (Bumper)	31.64	147.87	4.67
WR (Rails)	30.86	139.63	4.52
Hexagonal	33.50	201.39	6.01
Crash zone	31.85	210.09	6.60
Range Hood	31.78	210.93	6.64
Runner	32.00	211.03	6.59

As it was mentioned before range hood, crash zone, and runner models increase energy absorption performance of system by increasing displacement of system. This statement is proved by looking deformed shape of those models. According to Figure 61-63, range hood and crash zone deformed in the same manner. Buckling occurs just at these specific zones. Majority of impact energy is absorbed on those regions as well. As a result, rails are protected from deformation and buckling. On the other hand, runner region is also created by using same displacement principle. However, region is short and remaining part of rails covers this region in a very short time period. Hence, deformations start on the surface of rails.

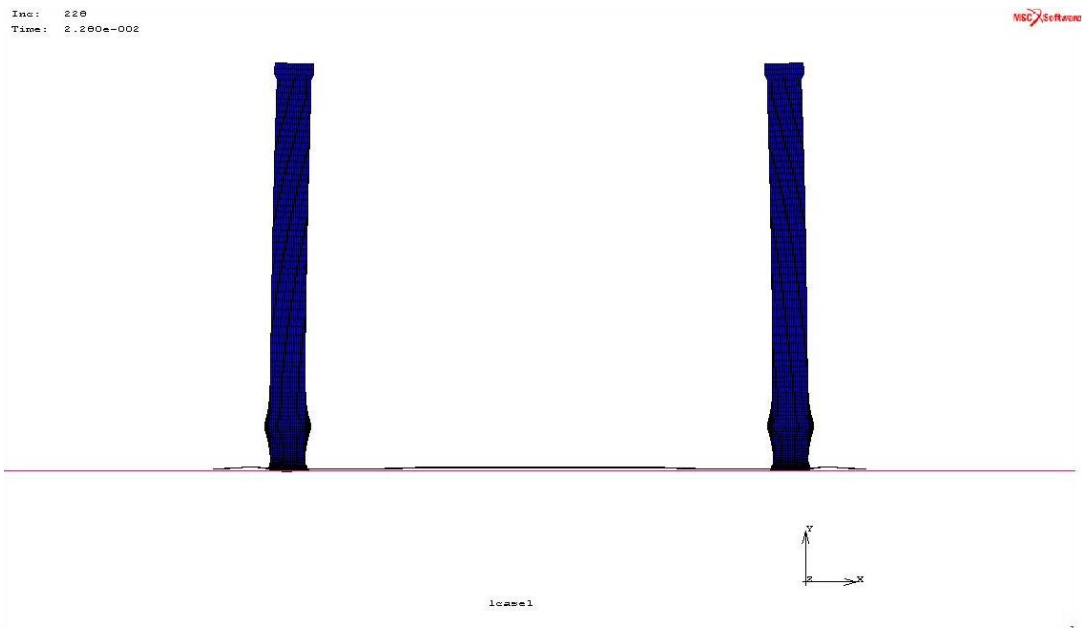


Figure 61 Deformed shape of range hood model

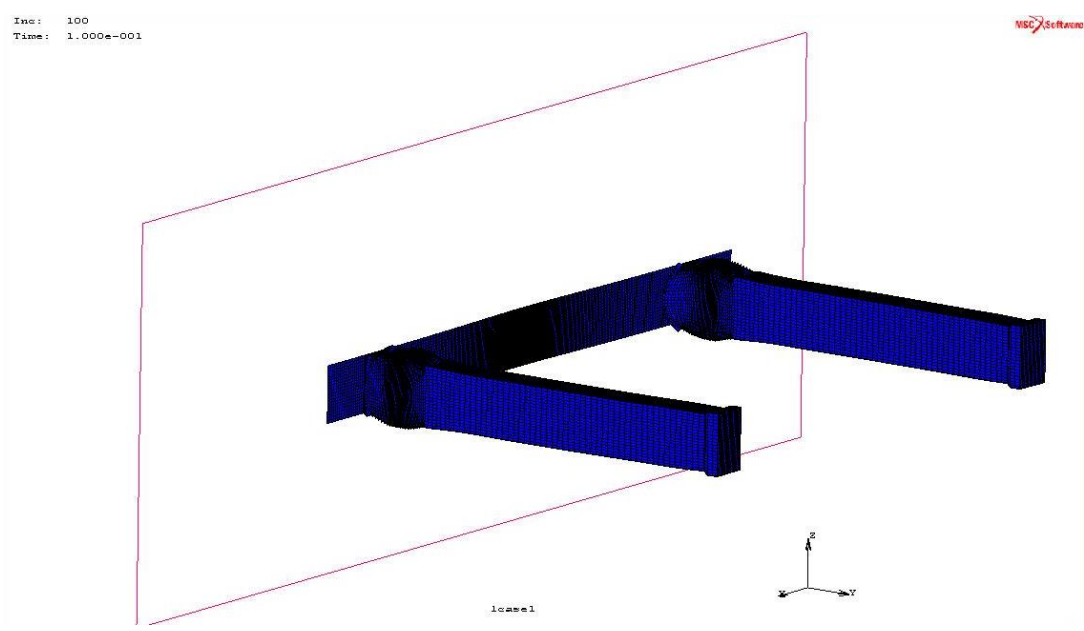


Figure 62 Deformed auxiliary view of crash zone model

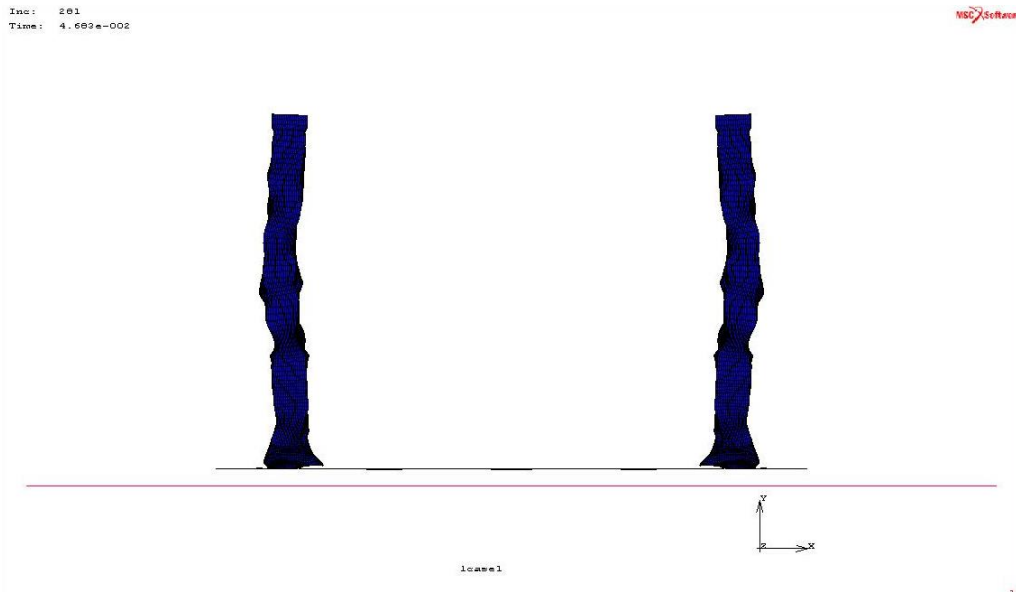


Figure 63 Deformed shape of runner model

WR models are mainly aim to reduce mass of system even though impact energy characteristic stay still. This purpose is not achieved by looking their deformed shapes (Figure 64-65) and resultant data. Deformation is more on the WR (rail) model. Because, rails are responsible for resisting impact force. It can be concluded that, both model failed due to their poor impact energy absorption performance.

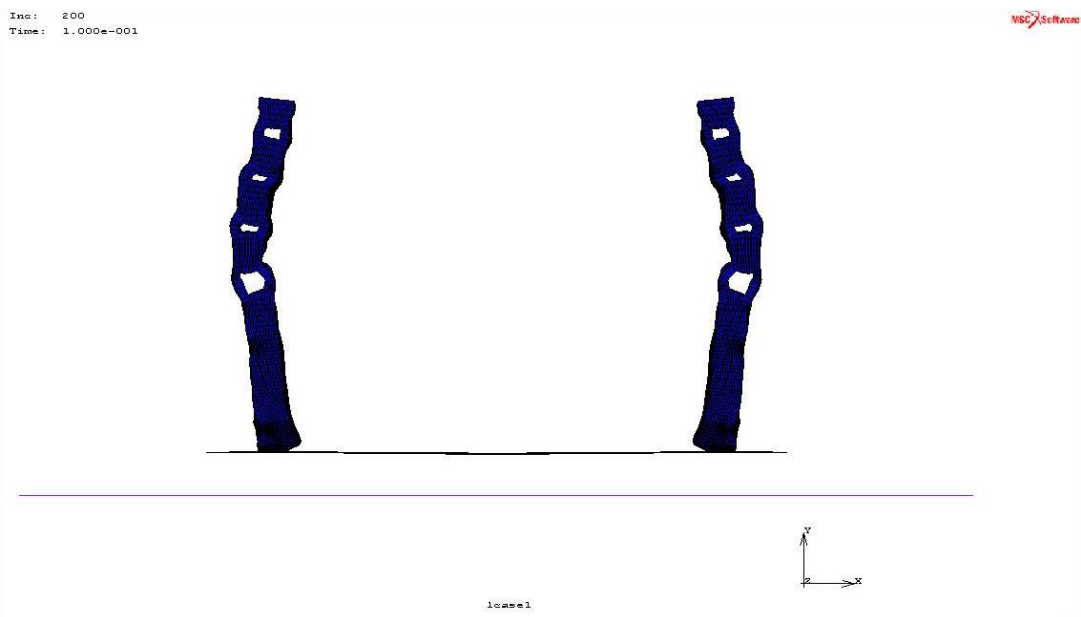


Figure 64 Deformed shape of WR (rails) model

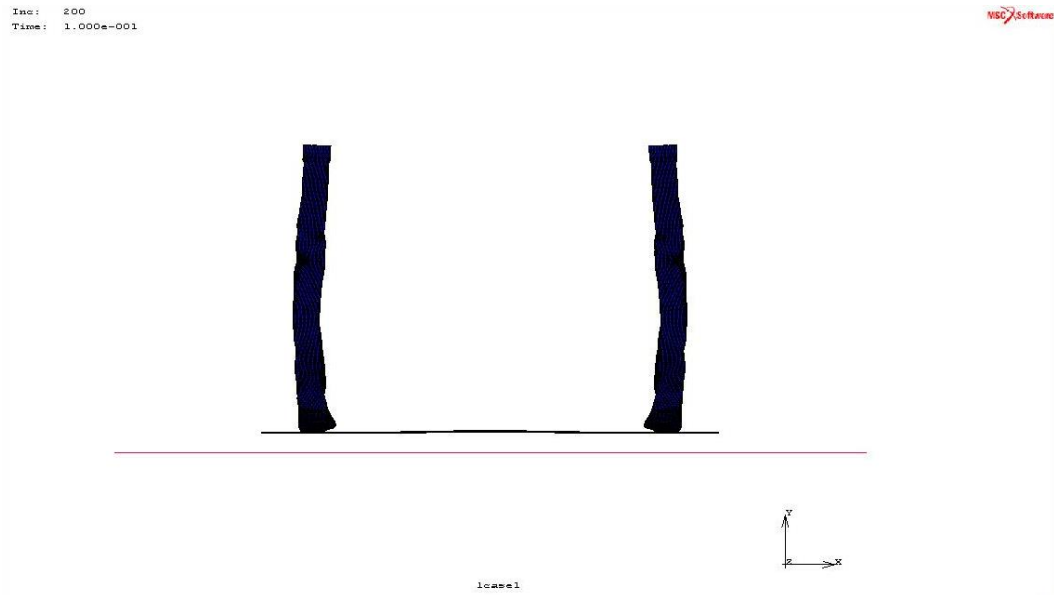


Figure 65 Deformed shape of WR (bumper) model

Different from rectangular cross-section, hexagonal shape shows better performance (Figure 66). However it does not give a symmetric response on rails. On the other hand, mathematical results shows that hexagonal cross-section shows better performance than standard one. Other views of all deformed models are given in Appendix section.

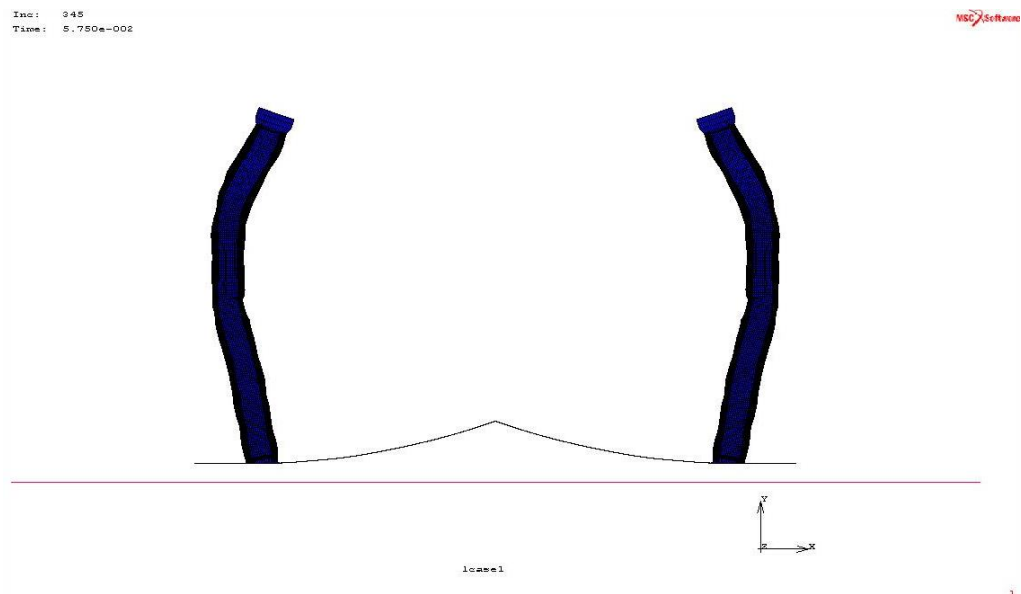


Figure 66 Deformed shape of hexagonal cross-section model

## 4.6 Material Analysis

Six different materials were analysed in this research and their response to the impact was investigated. Although material of the model was changed, other parameters like initial velocity, thickness of elements, and geometry of system remains same. As a base material mild steel is used. In this research one recycled, two composite and two recently preferred materials are investigated.

Firstly, it is important to understand materials' mechanical behaviour. Figure 67 represents flow curves of all materials. All materials have ductility and this make them eligible to use in the bumper beam system. Sometimes vehicle may hit the wall with very low speed and a brittle material is easily broken down into pieces so it is important to select ductile materials instead.

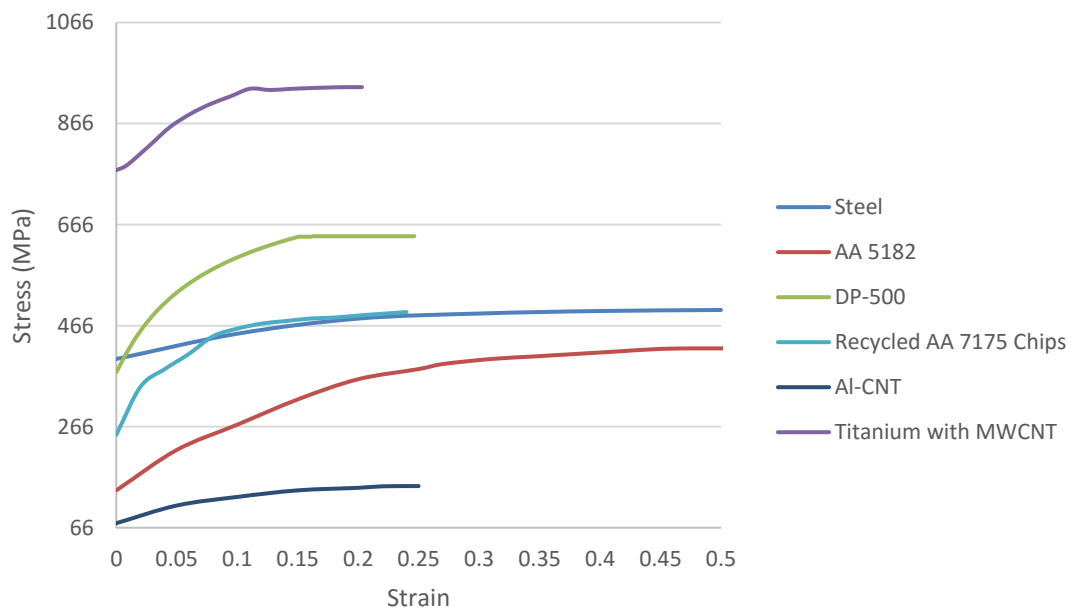


Figure 67 Flow curve of different material types

According to their deformation in Figure 68 the most deformed model is Al-CNT. Due to its relatively weak mechanical properties, it is an expected result. In fact all aluminium type materials showing same response. Another important point is related with their peak resistive force. Aluminium type materials have relatively

small peak force value. Due to its production method, recycled aluminium 7175 material has the best resistance due to its low displacement and high peak force. On the other hand, AA-5182 absorbs highest impact energy during crash. Aluminium makes system lighter and because of that SEA values of all aluminium type materials have the highest value. AA-5182 is recently used in automotive industry. It is good at both mass reduction and impact energy absorption. However, scope of this research is to seek a new type of material that is recycled or composite. Then, recycled 7175 aluminium is the best alternative among three choices.

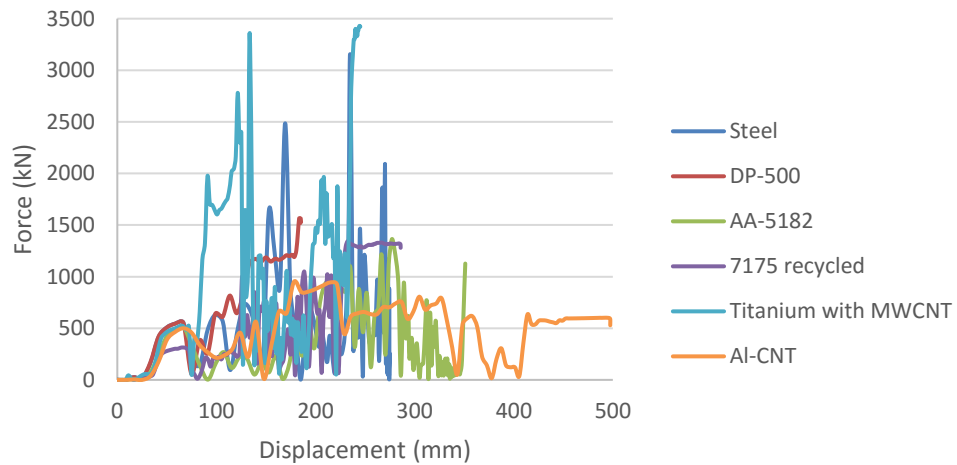


Figure 68 Crush force vs displacement graph for different material types

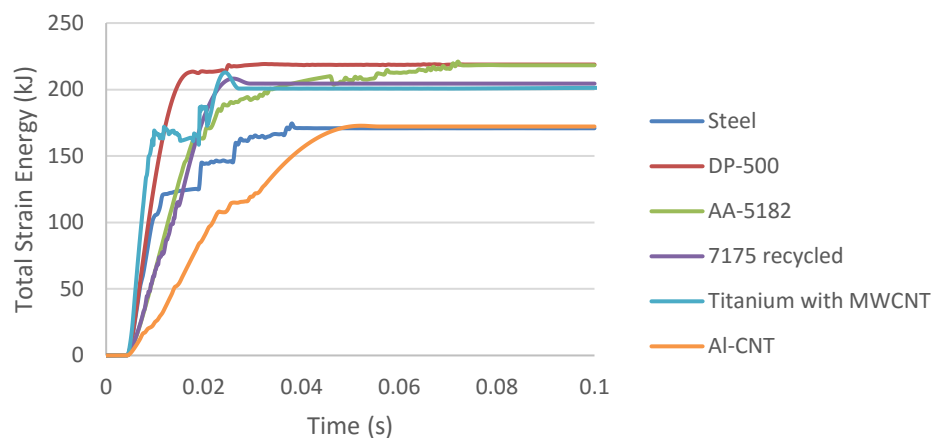


Figure 69 Total strain energy vs crash time graph for different material types

Steel is widely used in many components of vehicle. However, it makes vehicle heavier. They are strong enough to resist impact forces. The lowest displacement value is seen in DP-500 model. Due to its high strength it is an expected result. On the other hand, base model is failed from impact test. Because it shows the worst performance on both CFE and SEA (Table 28-29). This model is heavy and weak with respect to other models. However, displacement value is still lower than aluminium type models. Mild steel is simply eliminated from material selection. Although it is pretty dense, DP-500 is a good candidate due to its high impact energy absorption characteristic.

For comparison purposes, analyses conducted by other researchers are investigated. Zaouk et al. (1996) analysed full frontal crash of pick-up truck with 1800 kg, and 56 kph initial velocity. Although type of vehicle is different from this study, geometry of bumper beam and chassis system, and total mass of the vehicle is similar to the current work. DP-500 is used as the chassis material. Results show that 214 kJ impact energy is absorbed by the vehicle as a result of the impact. In this study, 218.8 kJ of impact energy is absorbed when DP-500 material is used. Results seem to be in good agreement in similar analysis conditions.

Titanium and MWCNT makes a good combination due to its high plastic behaviour and resistive force. Besides, it lowers mass of the system. Displacement value is less with respect to base model so it shows a good resistance to impact. Among composite material alternatives Titanium with MWCNT is the best alternative. However, recycled aluminium is still better than composites.

Table 28 Crush force efficiency for different material types

Material	Average Force (kN)	Peak Force (kN)	Crush Force Efficiency
Mild Steel	564.67	3145.73	0.18
DP-500	841.92	1565.35	0.54
AA-5182	361.61	1362.24	0.27
7175 recycled	746.55	1342.36	0.56
Al-CNT	513.11	602.32	0.85
Titanium with MWCNT	1221.39	3430.44	0.36

Table 29 Specific energy absorption for different material types

Material	Mass (kg)	Max. Strain Energy (kJ)	Specific Energy Absorption (kJ/kg)
Mild Steel	32.1	170.88	5.32
DP-500	31.5	218.81	6.95
AA-5182	10.63	218.24	20.53
7175 recycled	10.63	204.45	19.23
Al-CNT	10.65	172.19	16.17
Titanium with MWCNT	17.78	201.60	11.34

In order to decide which material is the best; deformed shapes should also be investigated. Many different buckling regions created after impact on rails. However, initial length of steel type models is nearly same as the final length. Deformations on the DP-500 model are generally created at the backside of rails. Due to simplified masses of vehicle, critical stresses occur at that point.

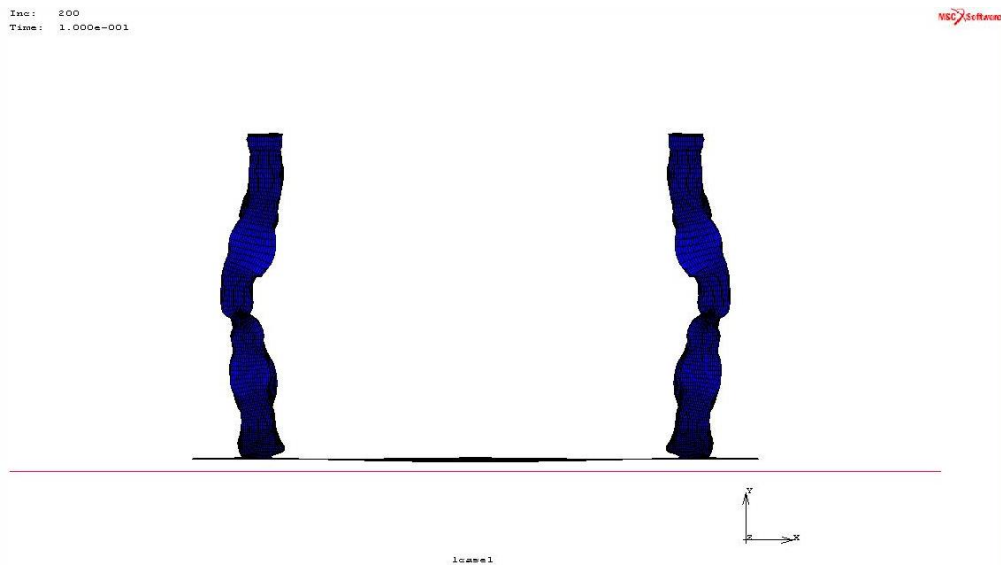


Figure 70 Deformed shape of mild steel model

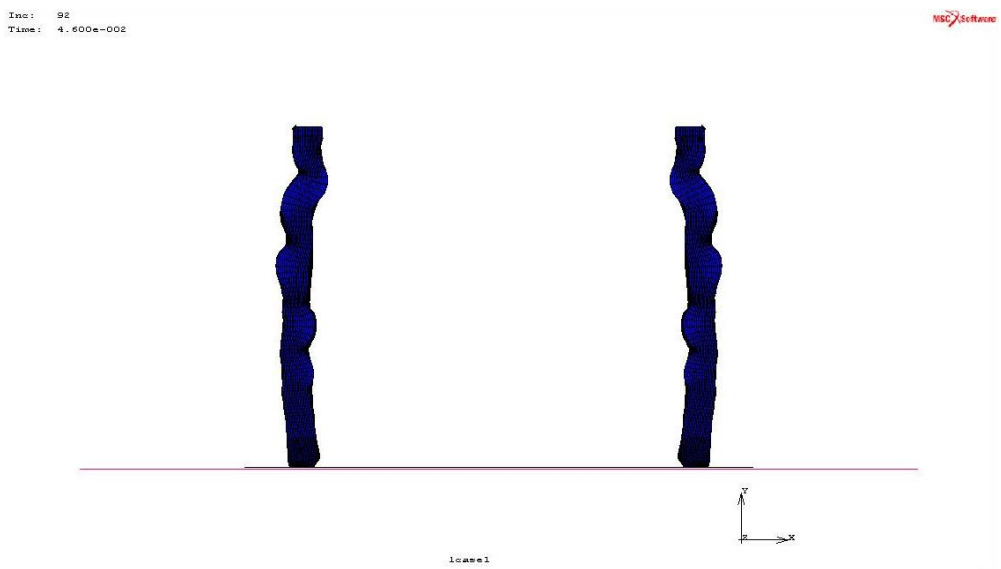


Figure 71 Deformed shape of DP-500 model

As it is seen from Figure 72-74 deformations and length change is more in aluminium type models, especially in Al-CNT one. It can be said that Al-CNT is not a proper model to use in bumper beam system. Rails become weaker and gather around bumper beam in AA-5182 model. Irreparable deformation occurs on the chassis of the vehicle. Recycled aluminium stands still after impact. Not so much deformation occurs on the rails.

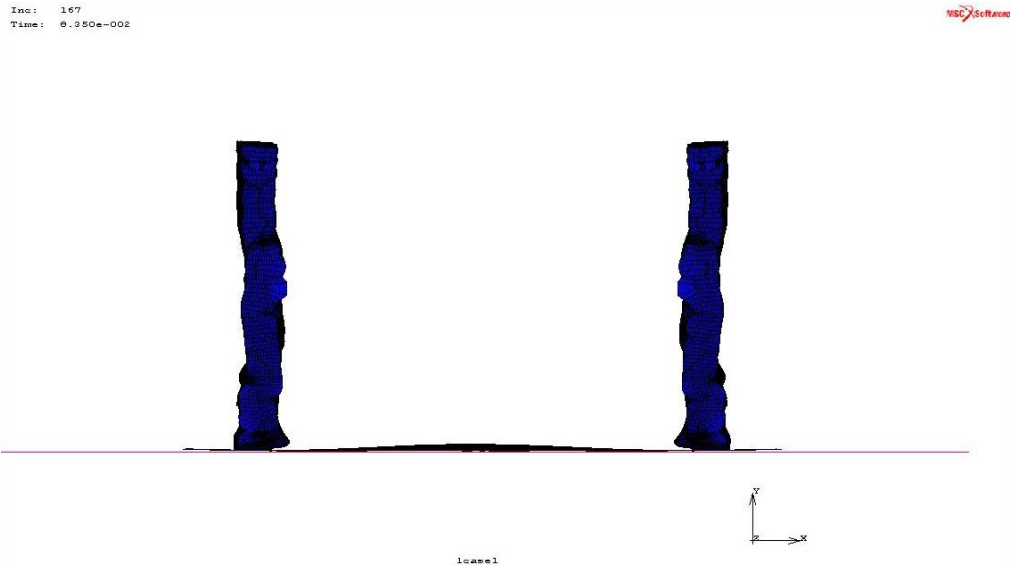


Figure 72 Deformed shape of AA-5182 model

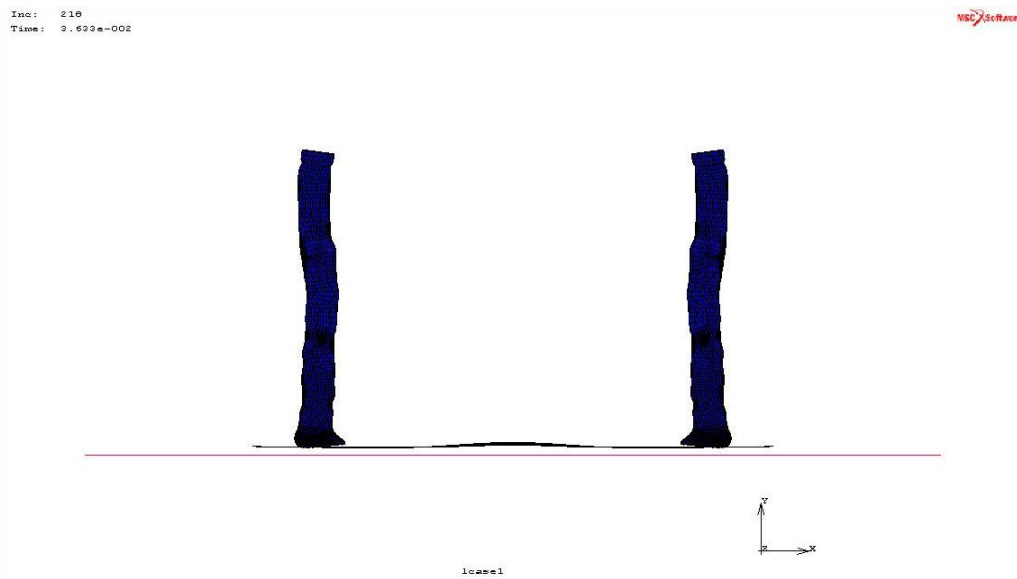


Figure 73 Deformed shape of 7175 recycled model

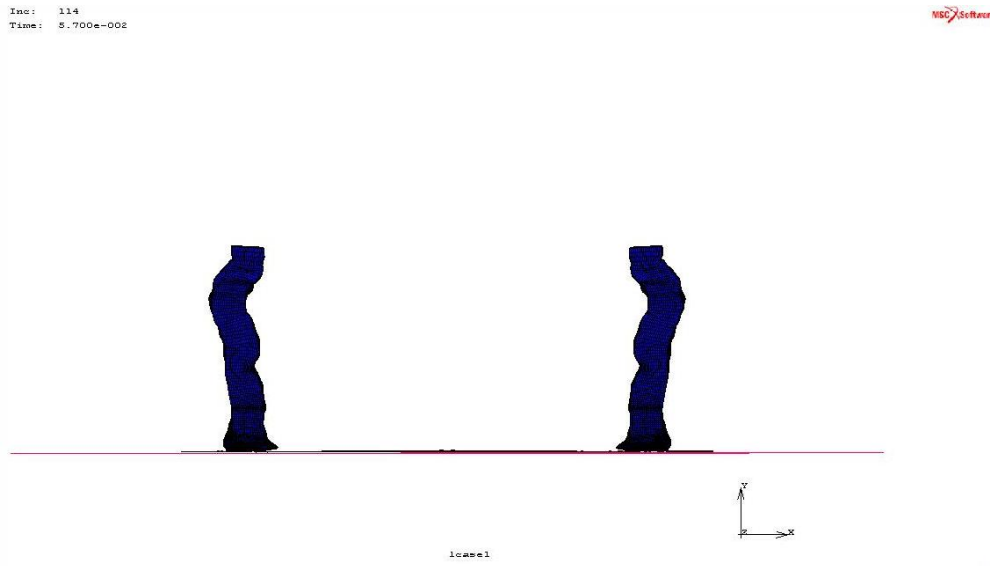


Figure 74 Deformed shape of Al-CNT model

Lastly, titanium model deformed asymmetrically (Figure 75). A right rail is deformed more than left one. Due to stress that are created from lumped masses backside of rails are deformed more than bumper beam side. However, it is still good enough to use in model because majority of system remains undeformed. Other views of all deformed models are given in Appendix section.

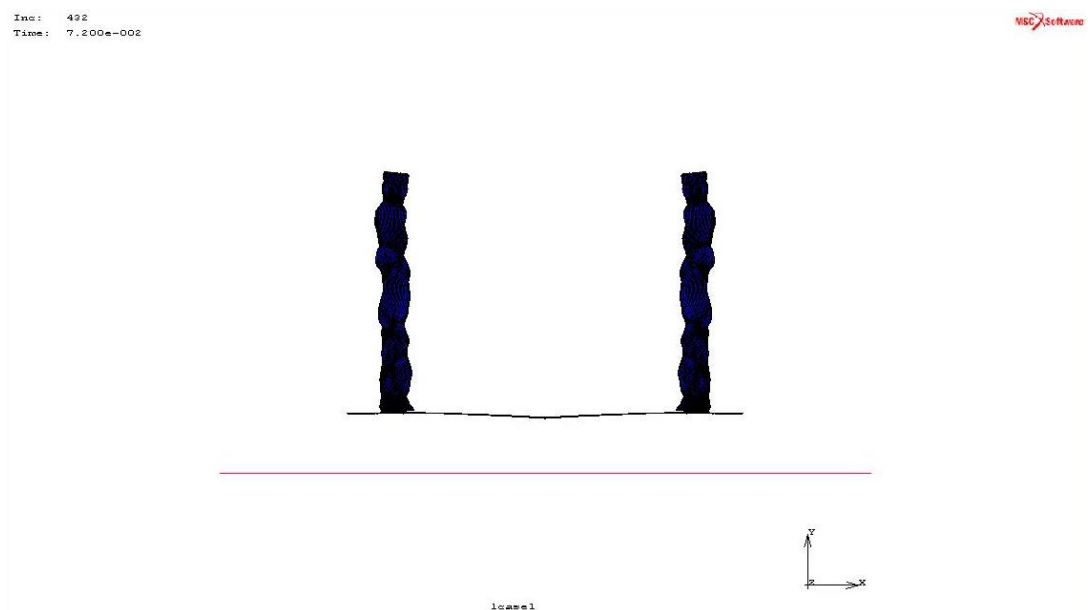


Figure 75 Deformed shape of Titanium with MWCNT model

To sum up, among all material alternatives recycled 7175 aluminium material shows best performance due to its good impact energy absorption and high resistance to deformation.

#### 4.7 Hybrid Bumper and Chassis System

Hybrid models are aimed to maximize impact energy absorption as high as possible. Previous analyses show that crash zone model performs good crashworthiness behaviour. Besides, crashworthiness performance of materials that were applied to hybrid systems has high energy absorption capacity.

Each model has its own peak when rails contact with rigid wall (Figure 76). It occurs just after the bumper beam was crushed. However, bumper beam has resisted till the first peak and later on it was crushed and resistive force suddenly dropped. Rails are designed to resist more. Because of that higher peak is obtained when rails are contact with rigid wall.

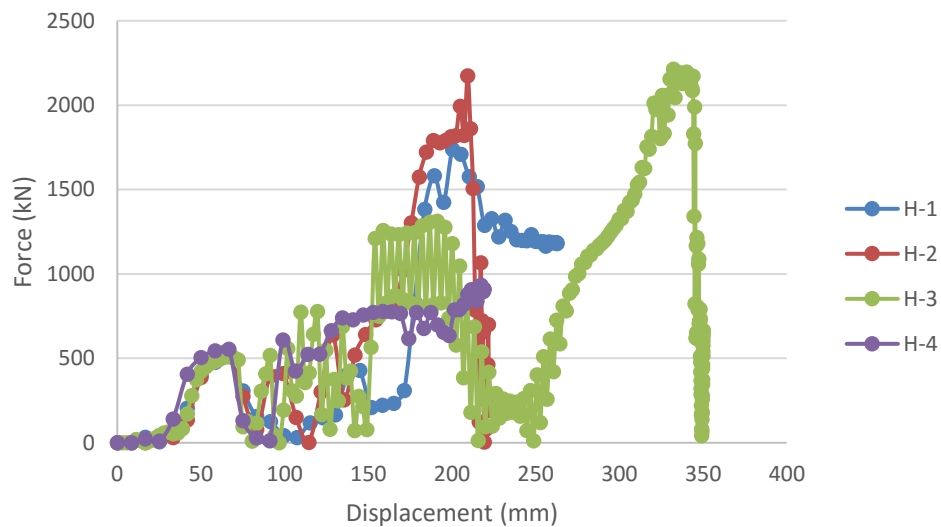


Figure 76 Crush force vs displacement graph for different material types

Although each model shows same force pattern, their displacement values are different from each other. Highest displacement is observed in H-3 model. Reason

is to use titanium with MWCNT material in crash zone. As a result, crashworthiness performance of model is the best one due to its high energy absorption and impact force resistance. Besides, composite and recycled materials make model lightweight and specific energy absorption of all H-1, 2, and 3 models are very high with respect to previous alternatives (Figure 77).

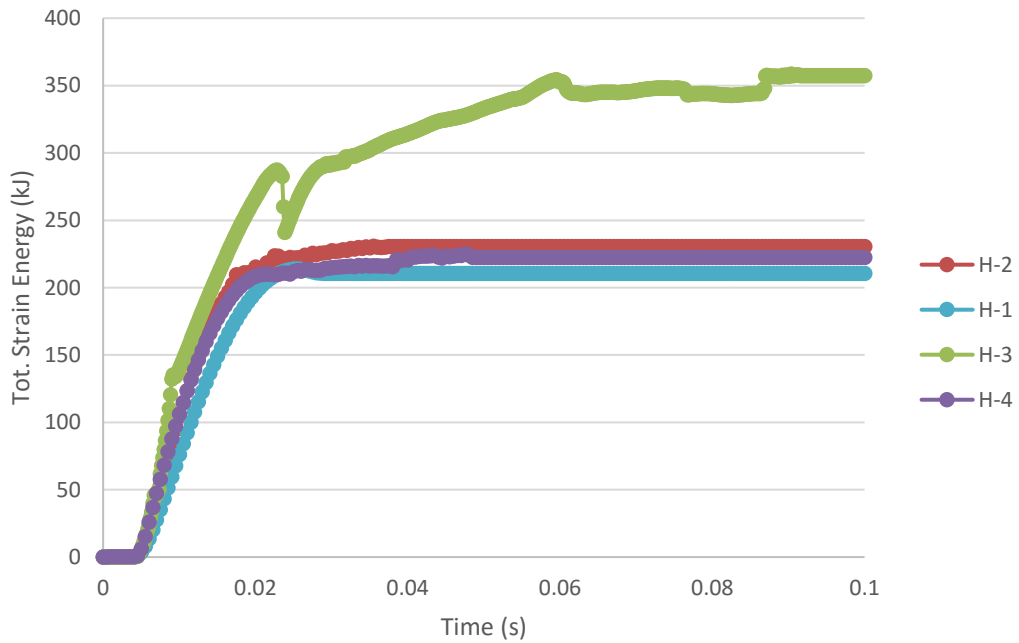


Figure 77 Total strain energy vs crash time graph for different material types

Weakest model is H-1 due to the material that was used in crash zone. Compared to recycled aluminium and DP-500 steel, AA-5182 is weaker and crash zone is deformed easily. On the other hand, geometrical hybridization is not effective to absorb impact energy as expected. However, peak crush force and average one is closer to each other. So, CFE value of H-4 model has the highest value.

Table 30 Crush force efficiency for hybrid systems

Model	Average Force (kN)	Peak Force (kN)	Crush Force Efficiency
H-1	803.97	1736.54	0.46
H-2	727.04	2173.71	0.33
H-3	828.07	2195.54	0.38
H-4	605.20	932.81	0.65

Table 31 Specific energy absorption for hybrid systems

Model	Mass (kg)	Max. Strain Energy (kJ)	Specific Energy Absorption (kJ/kg)
H-1	16.28	210.39	12.92
H-2	14.38	230.33	16.02
H-3	11.97	357.25	29.85
H-4	31.76	222.32	7.00

Lastly, deformed shape of all models are given (Figure 78-81). As it is mentioned before, using AA-5182 material in crash zone make H-1 model to absorb less impact energy. In Figure 78, just crash zone is buckled and remaining parts stay still.

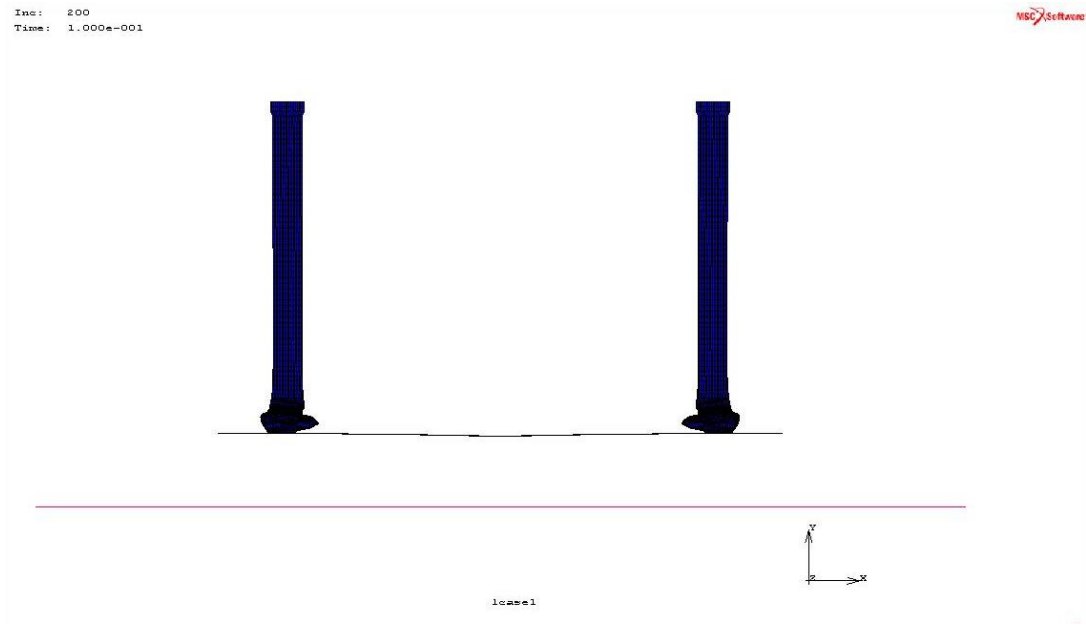


Figure 78 Deformed shape of H-1 model

Bumper beam is not designed to absorb all impact energy so AA-5182 was applied to this section. Stiffer materials were applied to critical regions like rails and crash zone. For that reason, both rails and crash zone was buckled in H-2 model and more energy absorbed in this case (Figure 79).

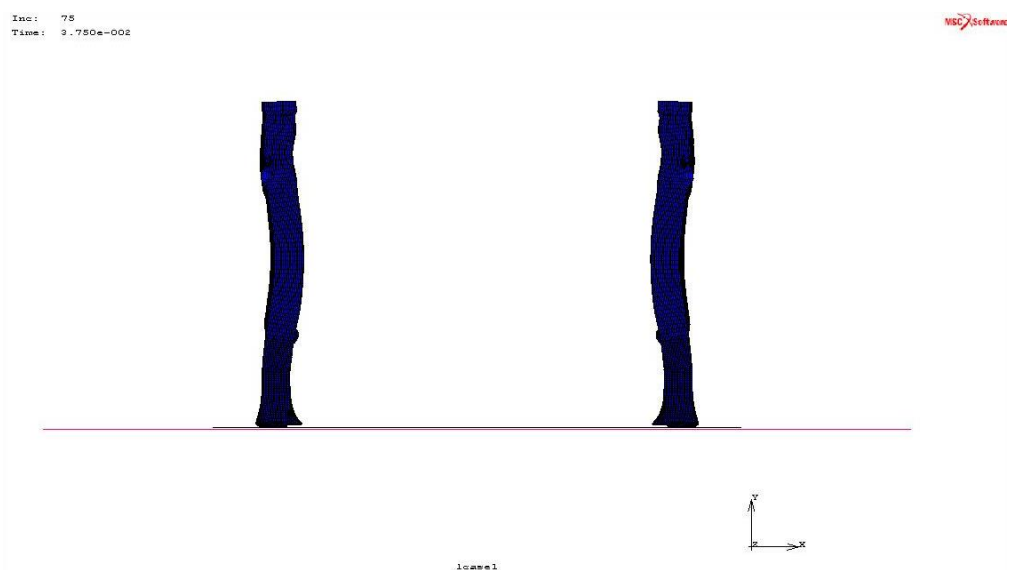


Figure 79 Deformed shape of H-2 model

H-3 model is designed by using both recycled and composite materials so its mass is reduced. Main aim of this research is achieved by doing this modification. Buckling and deformation is more due to its low weight (Figure 80). All impact energy can be absorbed by the bumper beam and chassis system.

As a base material mild steel is used in geometrical hybrid system but response to the impact does not seem good. System starts to buckle on the runner region and this eliminates the majority of energy absorption characteristic. Besides, duty of crash zone was not totally performed. Other views of all deformed models are given in Appendix section. According to all models, H-3 one is the best due to its low weight and high energy absorption characteristic.

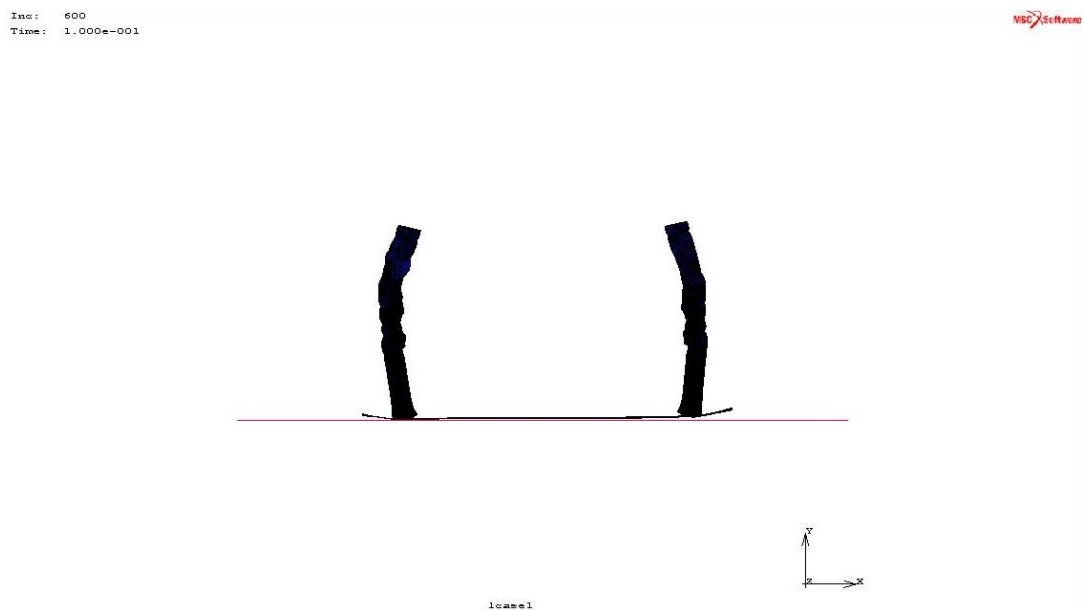


Figure 80 Deformed shape of H-3 model

Iter: 200  
Time: 1.000e-001

ANSYS Software

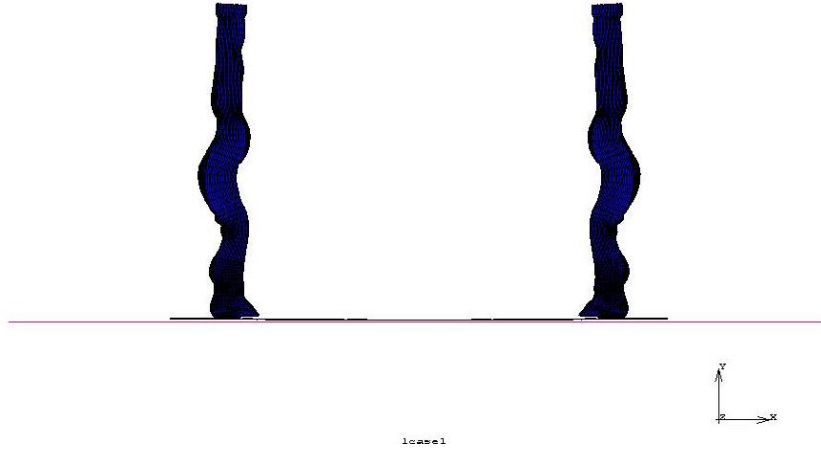


Figure 81 Deformed shape of H-4 model

## 5. CONCLUSION

This study focuses on bumper beam system that is made from stronger and lightweight or recycled material. First of all, conventional bumper beam systems are investigated from literature. Results shows that conventional systems are made from heavy material to absorb as many impact energy as possible. Toyota Yaris bumper beam system is used as a base model. Base model have an important role for this research in order to compare results of other models. Widespread usage and simple geometry make Toyota Yaris bumper beam system as an eligible candidate. Mild steel is used and the geometry of system is simple. Advantages and disadvantages of whole system is investigated and research is done in the light of these information.

Secondly, literature review is done to find proper lightweight or recycled material and geometry of the system. In the light of those purposes, carbon and glass fibres, nano carbon composites, metallic fibres, dual phase steels, recycled aluminium chips, lightweight aluminium alloys, and carbon nanotube reinforced composites are analysed. Besides, different impact techniques and their applications investigated. Although it is not analysed in this study, effects of dissimilar material joining is also investigated.

In modelling section, Toyota Yaris bumper beam system carefully disassembled from other parts of vehicle and simplified model is created by using same dimensions as a base model. It is time wasting operation to generate 3D model of vehicle, finding 3D model from literature is the most crucial part of the study. It is also not easy to find meshed 3D model of vehicle from literature. Another problem is faced with while searching composite or recycled material. All necessary mechanical properties of materials are not available in the same source. Besides, tension tests of composite materials are just covered for very small strain values. For that reason, literature review is done on a detailed way and extrapolation is done on the stress vs strain graphs of some material types. Once all problems were solved, finite element analysing stage starts. However finite element analysis takes

so much times and for that reason sensitivity analysis is done. As a suggestion, computer with good processor and memory should be used to compile Marc Mentat 2013™ analyses in a shorter time period.

Lastly, result of thickness effect, velocity analysis, geometric modifications, and material selection is analysed. As a result of this analysis, it was observed that some of the geometrical modifications have improved crash performance of bumper beam system. In other words, they aim to reduce mass and absorb as much energy as possible. Among all geometrical modifications best choice is to apply crash zone to the system.

Material selection is also vital to achieve the aim of this research. Many different materials are investigated and compared with conventional ones. Results shows that recycled and composite materials are safe enough to use in vehicles' chassis. Among all material alternatives best alternative is recycled 7175 aluminium due to its lightweight and pretty high impact energy absorption performance.

Hybrid systems are designed to maximize both mass reduction and impact energy absorption performance. All hybrid models achieve this mission. Among all four alternative model, H-3 model shows the best crashworthiness performance and absorbs two times higher impact energy than base model. Besides, mass of the total model is reduced from 32.10 kg to 11.97 kg.

Although joining effects and manufacturing effects are discussed in the literature review section of this research, their effects on crashworthiness are not taken into consideration. According to literature, welding can be used where rails and bumper beam joining and there is not so much difference between welded model and without welded one during crash scenario.

As a future work, effects of residual stresses that are occurred after manufacturing stage can be investigated so energy absorption performance of system can be improved by finding new production methods. Moreover, it is not easy to join composite material to another type of material so new joining methods and their

effects on the crash scenario will be investigated. Besides, hybrid system which has different materials on different sections of model can be modelled.

## REFERENCES

- Acar, E. et al., 2011. Multi-objective crashworthiness optimization of tapered thin-walled tubes with axisymmetric indentations. *Thin-Walled Structures*, 49(1), pp.94–105.
- Anon, World Health Organization. Available at: [http://www.who.int/gho/road\\_safety/mortality/traffic\\_deaths\\_number/en/](http://www.who.int/gho/road_safety/mortality/traffic_deaths_number/en/) [Accessed June 18, 2016].
- Balle, F., Wagner, G. & Eifler, D., 2009. Ultrasonic metal welding of aluminium sheets to carbon fibre reinforced thermoplastic composites. *Advanced Engineering Materials*, 11(1-2), pp.35–39.
- Belingardi, G. et al., 2015. Alternative lightweight materials and component manufacturing technologies for vehicle frontal bumper beam. *Composite Structures*, 120, pp.483–495. Available at: <http://dx.doi.org/10.1016/j.compstruct.2014.10.007>.
- Belingardi, G., Beyene, A.T. & Koricho, E.G., 2013. Geometrical optimization of bumper beam profile made of pultruded composite by numerical simulation. *Composite Structures*, 102, pp.217–225. Available at: <http://dx.doi.org/10.1016/j.compstruct.2013.02.013>.
- Besant, T., Davies, G.A.O. & Hitchings, D., 2001. Finite element modelling of low velocity impact of composite sandwich panels. *Composites - Part A: Applied Science and Manufacturing*, 32(9), pp.1189–1196.
- Beyene, A.T. et al., 2014. Design and manufacturing issues in the development of lightweight solution for a vehicle frontal bumper. *Procedia Engineering*, 88, pp.77–84. Available at: <http://dx.doi.org/10.1016/j.proeng.2014.11.129>.
- Cheon, S.S., Choi, J.H. & Lee, D.G., 1995. Development of the composite bumper beam for passenger cars. *Composite Structures*, 32(1-4), pp.491–499.
- Cole, G.S. & Sherman, a. M., 1995. Light weight materials for automotive applications. *Materials Characterization*, 35(1), pp.3–9.
- Conner, R.D., Dandliker, R.B. & Johnson, W.L., 1998. Mechanical properties of tungsten and steel fiber reinforced Zr<sub>41.25</sub>Ti<sub>13.75</sub>Cu<sub>12.5</sub>Ni<sub>10</sub>Be<sub>22.5</sub> metallic glass matrix composites. *Acta Materialia*, 46(17), pp.6089–6102. Available at: <http://www.sciencedirect.com/science/article/pii/S1359645498002754>.
- Davoodi, M.M. et al., 2010. Mechanical properties of hybrid kenaf/glass reinforced epoxy composite for passenger car bumper beam. *Materials and Design*, 31(10), pp.4927–4932. Available at: <http://dx.doi.org/10.1016/j.matdes.2010.05.021>.
- Davoodi, M.M., Sapuan, S.M. & Yunus, R., 2008. Conceptual design of a polymer composite automotive bumper energy absorber. *Materials and Design*, 29(7),

pp.1447–1452.

- Esawi, A.M.K. & El Borady, M.A., 2008. Carbon nanotube-reinforced aluminium strips. *Composites Science and Technology*, 68(2), pp.486–492.
- Euro-NCAP, 2013. EUROPEAN NEW CAR ASSESSMENT PROGRAMME ( Euro NCAP ) FRONTAL IMPACT. , (October), p.52. Available at: <http://www.euroncap.com/files/Euro-NCAP-Frontal-Protocol-Version-6.0.2---0-0ba7731f-4866-40c8-8dc5-31db64d92f8d.pdf>.
- Grimmer, C.S. & Dharan, C.K.H., 2008. High-cycle fatigue of hybrid carbon nanotube/glass fiber/polymer composites. *Journal of Materials Science*, 43(13), pp.4487–4492.
- Hosseinzadeh, R., Shokrieh, M.M. & Lessard, L.B., 2005. Parametric study of automotive composite bumper beams subjected to low-velocity impacts. *Composite Structures*, 68(4), pp.419–427.
- Jones, N. & Wierzbicki, T., 2010. *Structural Crashworthiness and Failure: Proceedings of the Third International Symposium on Structural Crashworthiness held at the University of Liverpool, England, 14-16 April 1993*, CRC Press.
- Kim, D.H., Kim, H.G. & Kim, H.S., 2015. Design optimization and manufacture of hybrid glass/carbon fiber reinforced composite bumper beam for automobile vehicle. *Composite Structures*, 131, pp.742–752. Available at: <http://dx.doi.org/10.1016/j.compstruct.2015.06.028>.
- Kondoh, K. et al., 2009. Characteristics of powder metallurgy pure titanium matrix composite reinforced with multi-wall carbon nanotubes. *Composites Science and Technology*, 69(7), pp.1077–1081.
- Luda, M.P. et al., 2003. Regenerative recycling of automotive polymer components: Poly(propylene) based car bumpers. *Macromolecular Materials and Engineering*, 288(8), pp.613–620.
- Martinsen, K., Hu, S.J. & Carlson, B.E., 2015. Joining of dissimilar materials. *CIRP Annals - Manufacturing Technology*, 64(2), pp.679–699.
- Moghaddam, A.R.M. & Ahmadian, M.T., 2011. Design and analysis of an automobile bumper with the capacity of energy release using GMT materials. *World Academy of Science, Engineering and Technology*, 52.
- OICA, 2015. International Organization of Motor Vehicle Manufacturers. Available at: <http://www.oica.net/> [Accessed June 19, 2016].
- Pantke, K. et al., 2013. Aluminum Scrap Recycling Without Melting. In *Future Trends in Production Engineering*. Springer, pp. 373–377.
- Qi, W., Jin, X.L. & Zhang, X.Y., 2006. Improvement of energy-absorbing structures of a commercial vehicle for crashworthiness using finite element method. *International Journal of Advanced Manufacturing Technology*, 30(11-12), pp.1001–1009.

- Saidpour, H., 2006. Lightweight high performance materials for car body structures.
- Shafiee, S. & Topal, E., 2009. When will fossil fuel reserves be diminished? *Energy policy*, 37(1), pp.181–189.
- Smerd, R. et al., 2005. High strain rate tensile testing of automotive aluminum alloy sheet. *International Journal of Impact Engineering*, 32(1), pp.541–560.
- Steel Market Development, 2015a. *Advance High Strength Steel Application Guidelines*, Available at: [www.autosteel.org](http://www.autosteel.org).
- Steel Market Development, 2015b. Dual Phase Steel. Available at: <http://www.autosteel.org/research/ahss-data-utilization/dp500.aspx> [Accessed May 20, 2016].
- The George Washington, 2015. Finite element model archive. Available at: <http://www.ncac.gwu.edu/vml/models.html> [Accessed October 15, 2015].
- UN FCCC, 2015. COP21 Draft December 5 2015. , (October), pp.1–34.
- Velmurugan, R. & Balaganesan, G., 2013. Energy absorption characteristics of glass/epoxy nano composite laminates by impact loading. *International Journal of Crashworthiness*, 18(June), pp.82–92. Available at: <http://www.tandfonline.com/doi/abs/10.1080/13588265.2012.745975>.
- WHOI, 2006. Woods Hole Oceanographic Institution. Available at: [http://polardiscovery.whoi.edu/poles/images/emission\\_graph-1g](http://polardiscovery.whoi.edu/poles/images/emission_graph-1g) [Accessed June 18, 2016].
- Zaouk, A.K. et al., 1996. Development and evaluation of a C-1500 pickup truck model for roadside hardware impact simulation. In *Proceedings of the FHWA Vehicle Crash Analysis Crash Conference, Mclean, VA*. pp. 1–31.
- Zein, H. et al., 2013. Effect of Die Design Parameters on Thinning of Sheet Metal in the Deep Drawing Process. *American Journal of Mechanical Engineering*, 1(2), pp.20–29. Available at: <http://pubs.sciepub.com/ajme/1/2/1/index.html>.

## APPENDIX

### Part A: Profile Thickness Effect

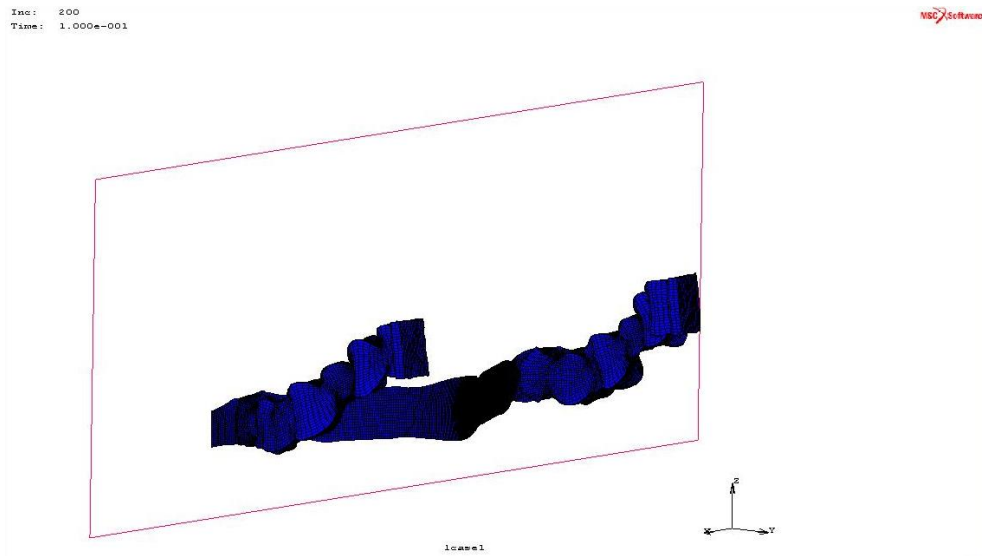


Figure 82 Deformed auxiliary view of 4 mm thick profile

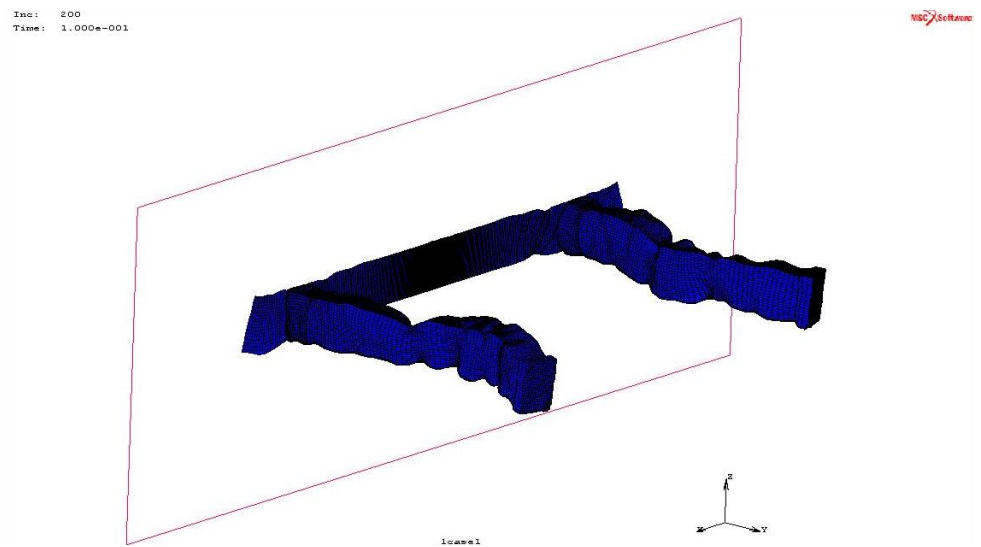


Figure 83 Deformed auxiliary view of 5 mm thick profile

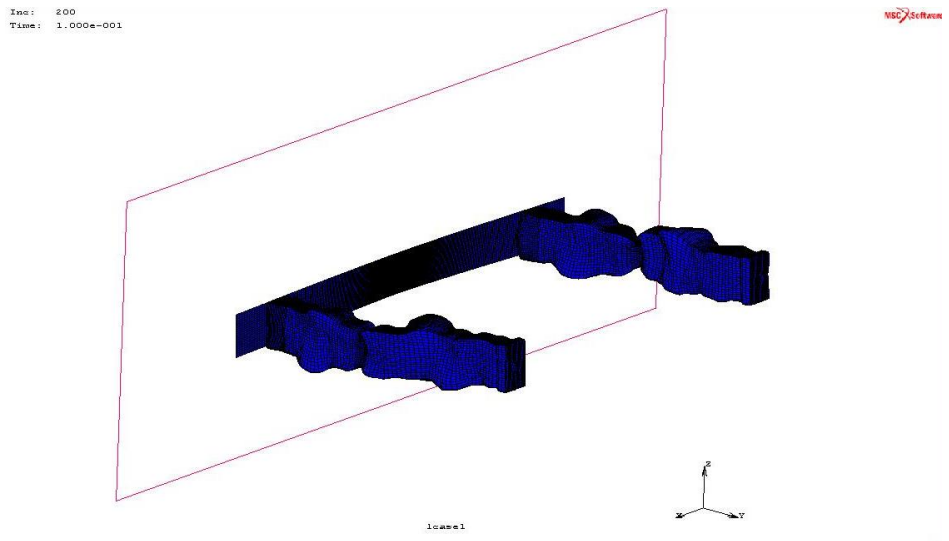


Figure 84 Deformed auxiliary view of 6 mm thick profile

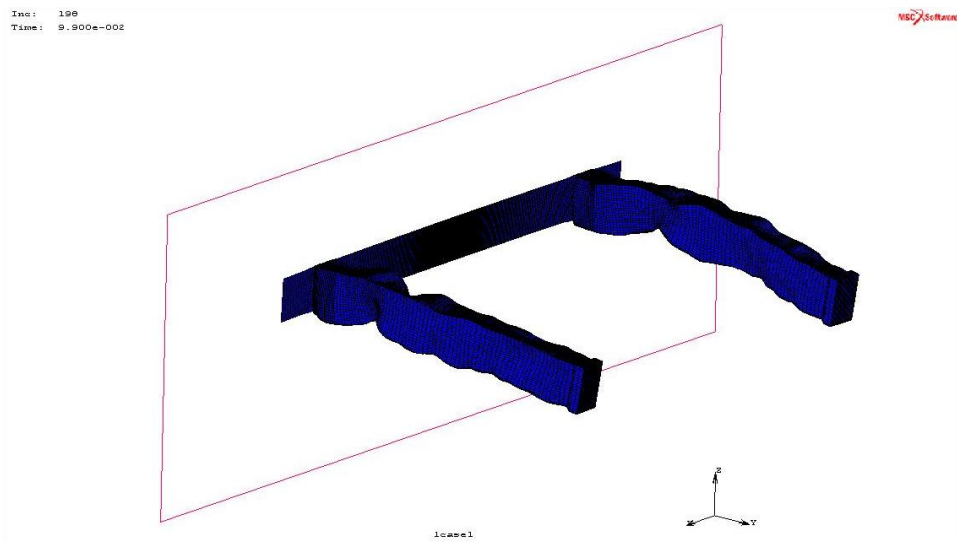


Figure 85 Deformed auxiliary view of 7 mm thick profile

## Part B: Velocity Analysis

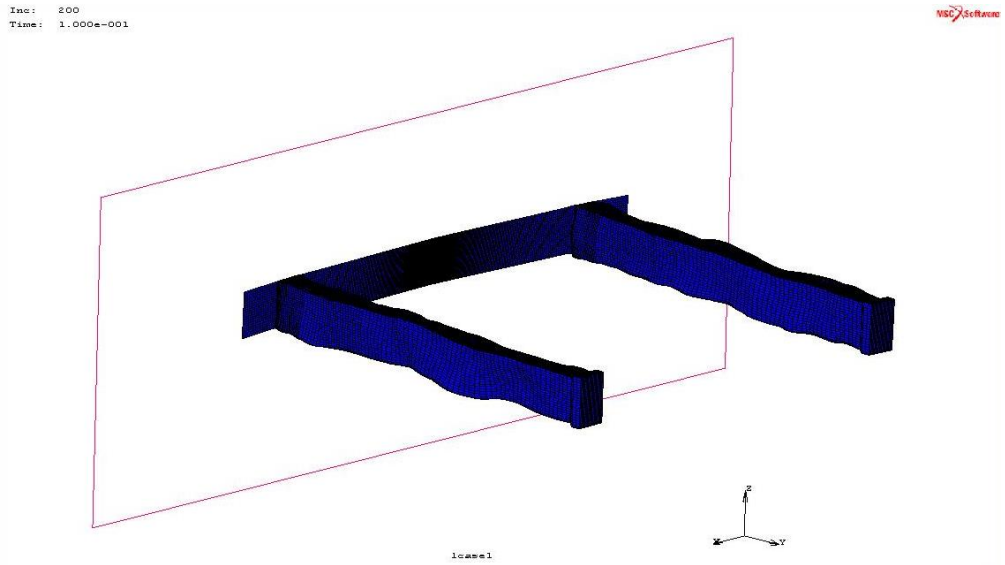


Figure 86 Deformed auxiliary view of 30 kph initial velocity model

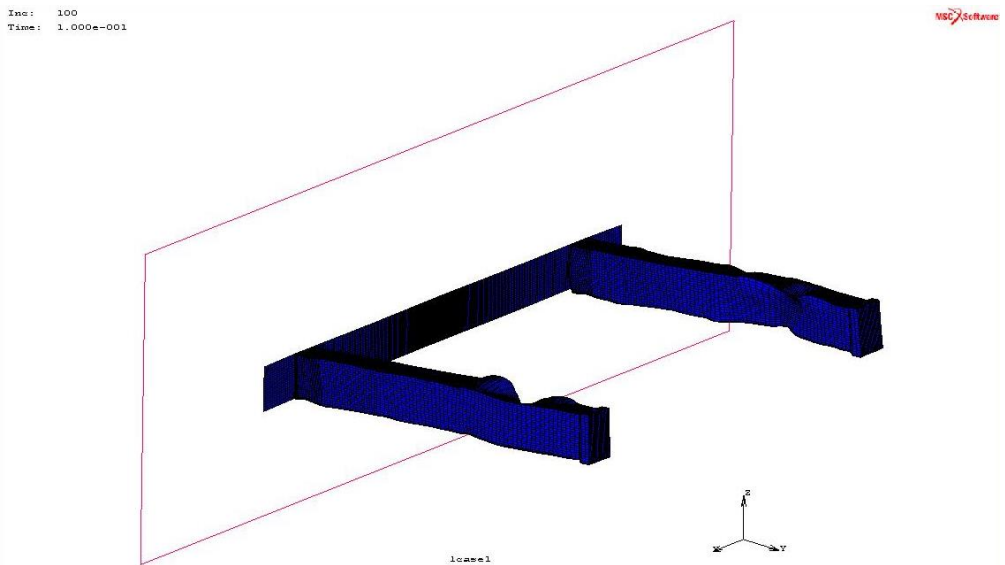


Figure 87 Deformed auxiliary view of 40 kph initial velocity model

## Part C: Geometrical Modifications

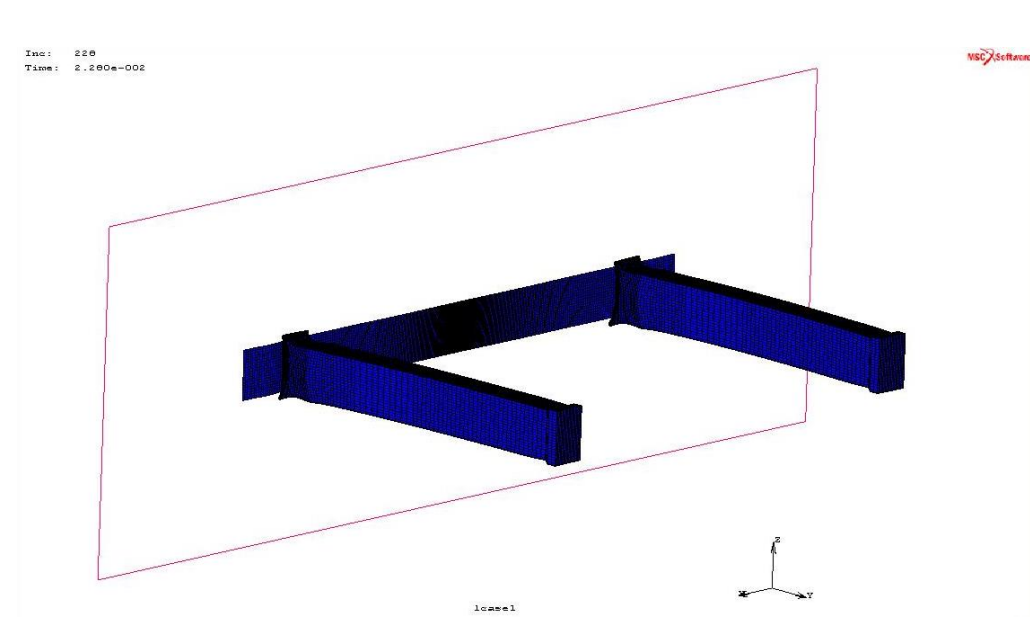


Figure 88 Deformed auxiliary view of range hood model

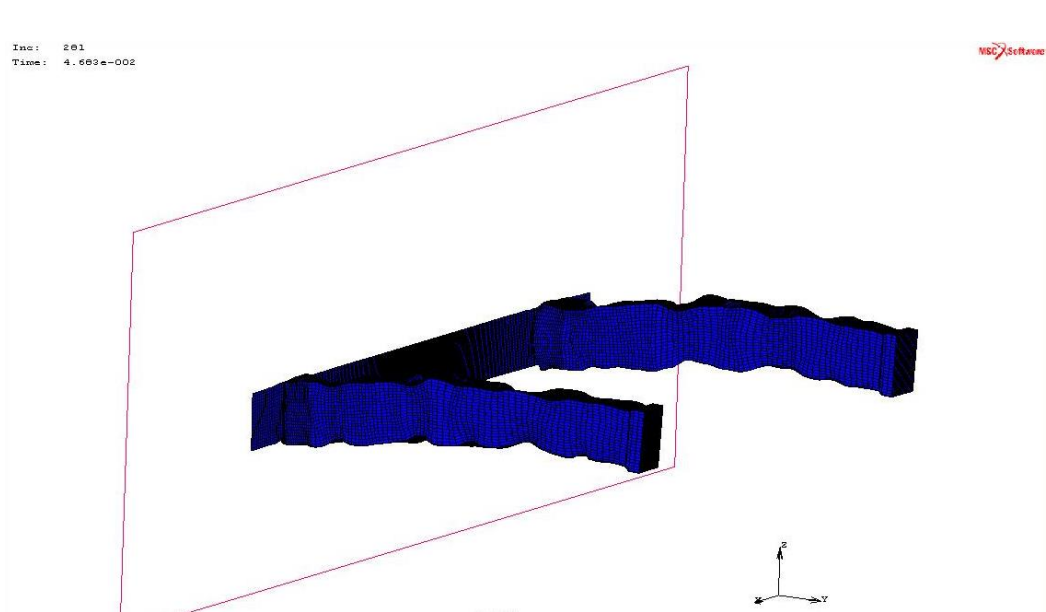


Figure 89 Deformed auxiliary view of runner model

Inc: 345  
Time: 5.750e-002

MSC Software

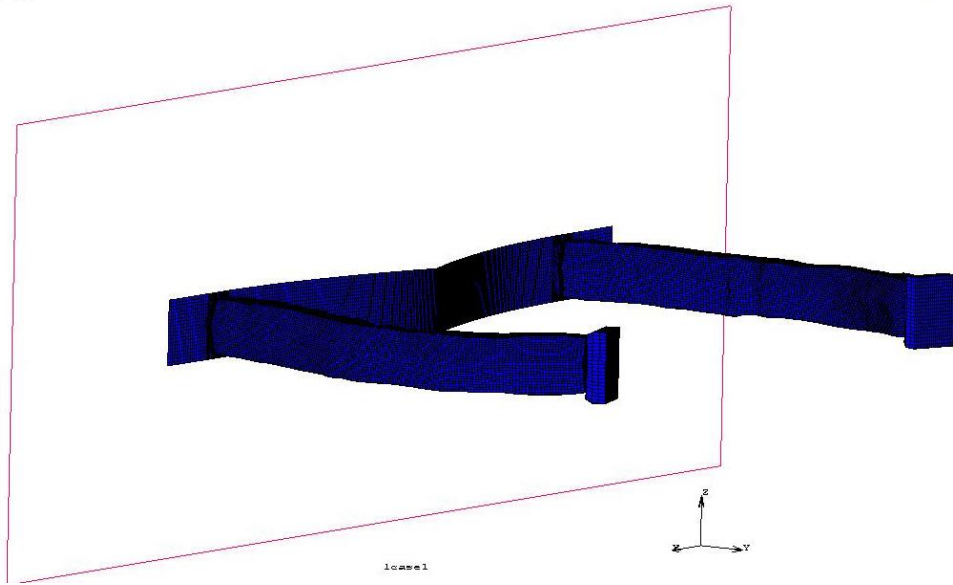


Figure 90 Deformed auxiliary view of hexagonal model

Inc: 92  
Time: 4.600e-002

MSC Software

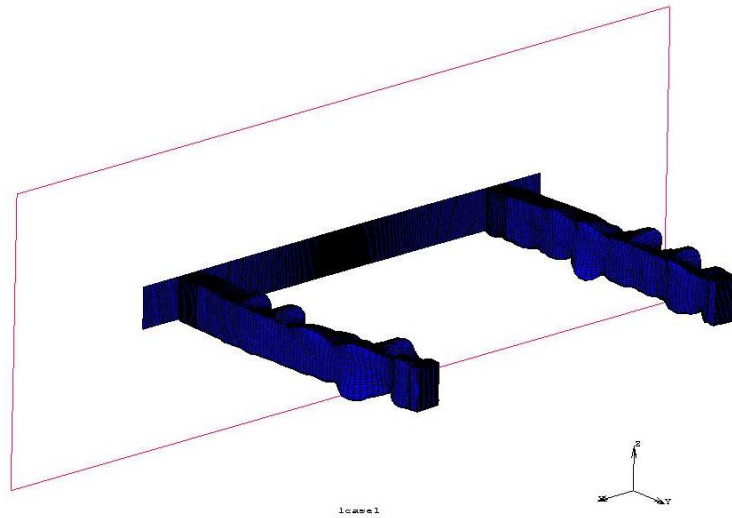


Figure 91 Deformed auxiliary view of DP-500 model

## Part D: Material Analysis

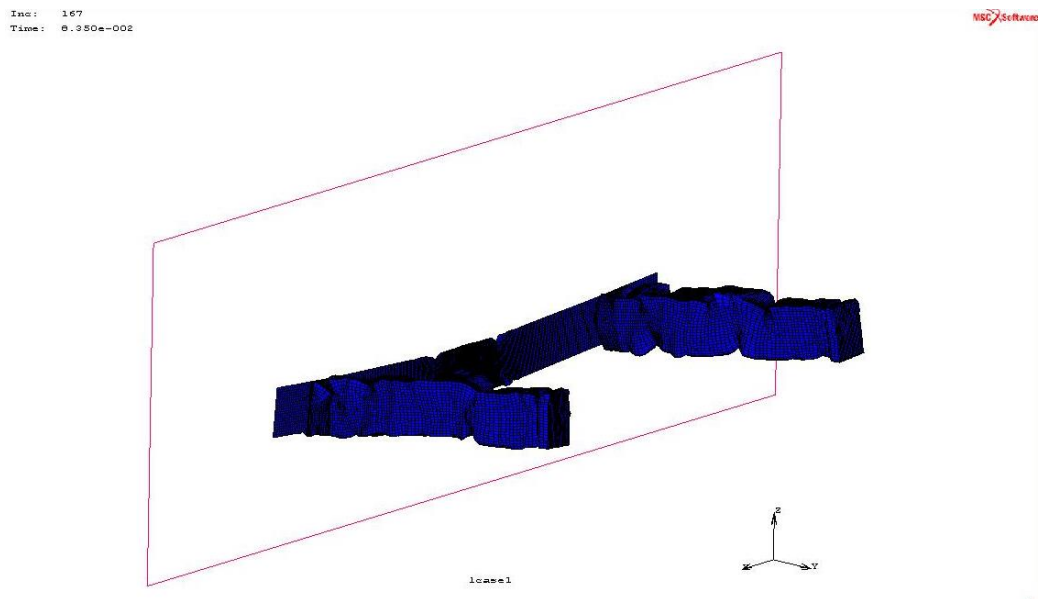


Figure 92 Deformed auxiliary view of AA-5182 model

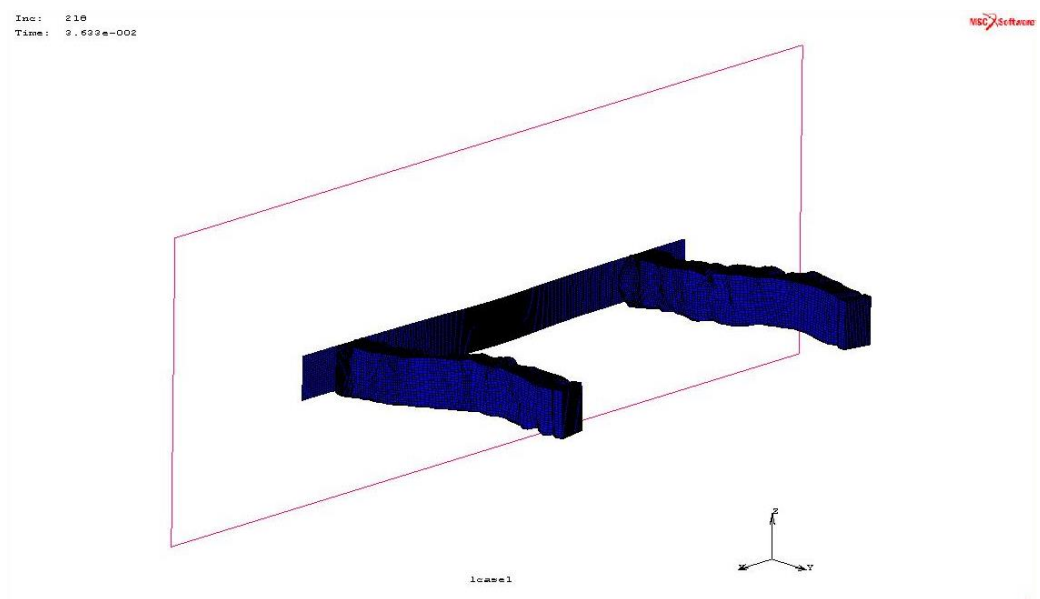


Figure 93 Deformed auxiliary view of 7175 recycled model

Inc: 210  
Time: 3.639e-002

MSC Software

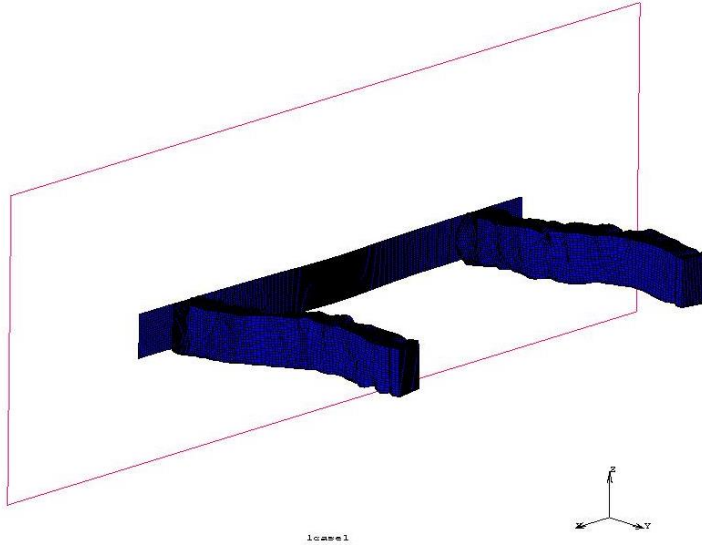


Figure 94 Deformed auxiliary view of Al-CNT model

Inc: 492  
Time: 7.200e-002

MSC Software

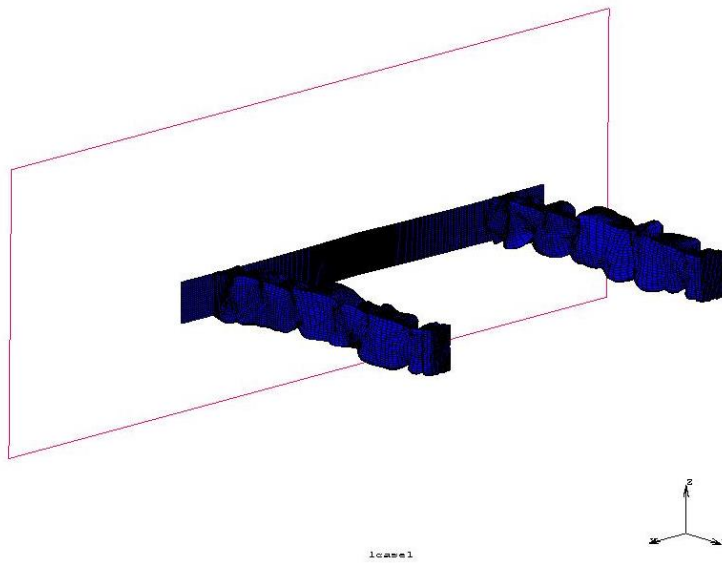


Figure 95 Deformed auxiliary view of Titanium with MWCNT model

## Part E: Hybrid Bumper Beam and Chassis System

Inc: 200  
Time: 1.000e-001

MSC Software

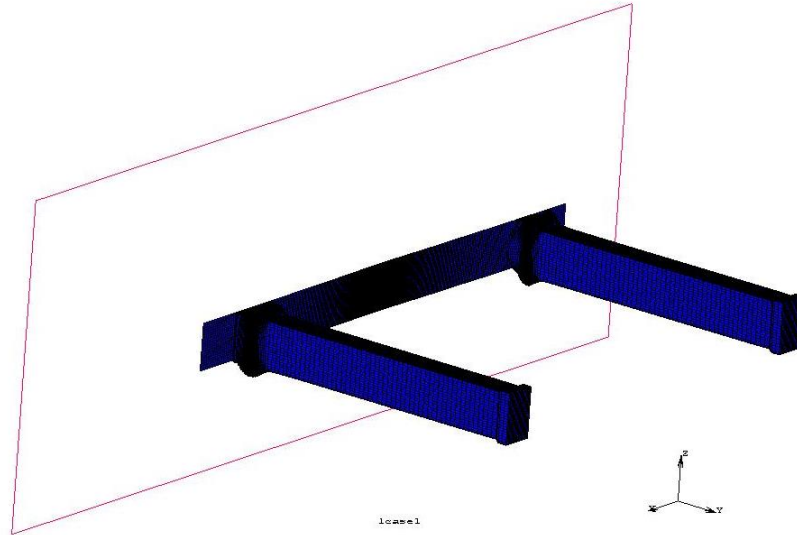


Figure 96 Deformed auxiliary view of H-1 model

Inc: 75  
Time: 9.750e-002

MSC Software

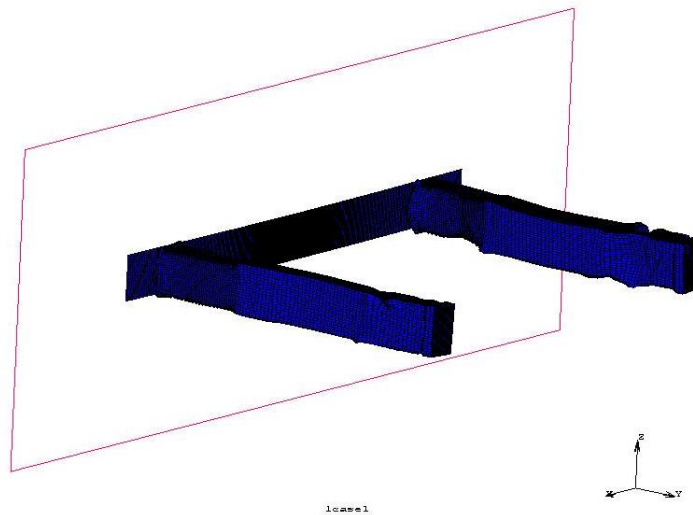


Figure 97 Deformed auxiliary view of H-2 model

Inc: 600  
Time: 1.000e-001

MSC Software

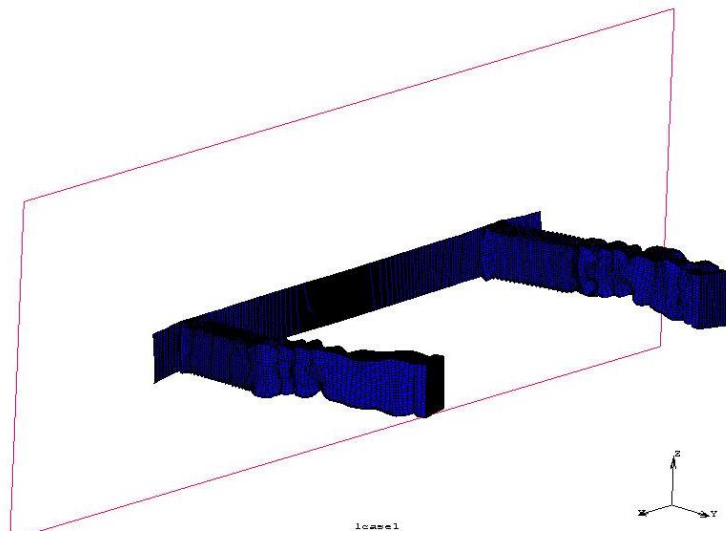


Figure 98 Deformed auxiliary view of H-3 model

Inc: 200  
Time: 1.000e-001

MSC Software

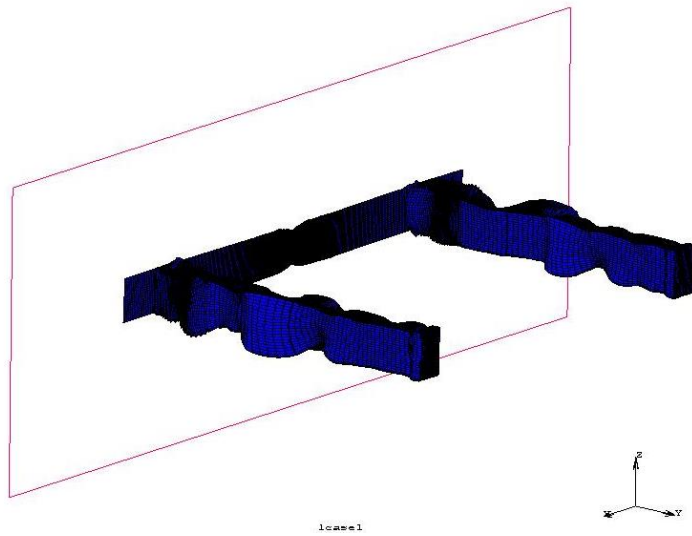


Figure 99 Deformed auxiliary view of H-4 model